UM-911 AENEAS

THE URBAN DISASTER RESPONSE SYSTEM

Alfred Gessow Rotorcraft Center
Department of Aerospace Engineering
University of Maryland, College Park

University of Maryland

Alfred Gessow Rotorcraft Center
Department of Aerospace Engineering
University of Maryland
College Park, Maryland 20742

UM–911 AENEAS

THE URBAN DISASTER RESPONSE SYSTEM

In response to the 2003 American Helicopter Society
Student Design Competition - Graduate Category
June 15, 2003

Shreyas Ananthan - Team Leader

Dr. Inderjit Chopra - Faculty Advisor

Jayasimha Atulasimha

Aubrey Goodman

Vinit Gupta

Wei Hu

Sudarshana Koushik

Anand Radhakrishnan

Maria Ribera

Celestine Wakha

Joseph Whitt

Acknowledgements

The design team would like to acknowledge the following people and thank them for their advice and assistance:

Dr. Vengalattore T. Nagaraj — Research Scientist, Dept. of Aerospace Engineering, University of Maryland, College Park. Co-advisor for the design course, for his valuable guidance throughout the design process.
Dr. Marat Tishchenko — Former Chief Designer, Mil Design Bureau, for his numerous comments and useful suggestions.
Dr. J. Gordon Leishman — Professor, Dept. of Aerospace Engineering, University of Maryland, College Park, for his valuable insightful comments during the design process and help with the final report.
Dr. Fred Schmitz — Professor, Dept. of Aerospace Engineering, University of Maryland, College Park.
Dr. Darryll Pines — Professor, Dept. of Aerospace Engineering, University of Maryland, College Park.
Dr. Vincent Brannigan — Professor, Dept. of Fire Protection Engineering, University of Maryland, College Park.
Matthew Tarascio, Shen Jinwei, Beerinder Singh, Jayanarayanan Sitaraman, Anubhav Datta, Jayant Sirohi, Ron Couch and Beatrice Roget — Graduate Students, Department of Aerospace Engineering, University of Maryland, College Park.
Gary Olson — Breeze Eastern, NJ.
Melissa Weese — Assistant Professor, School of Architecture, University of Maryland, College Park.
Bob Dingwell — Crossbow Technology Inc.
Diane Dowd — Private helicopter pilot, New York City.
Rudy Steur — Ifex Technologies, Germany.
George Schafer — Kaman Aerospace.
Matt Yarno — Simplex Manufacturing.
Mark Rager — Director of Maintenance, Glenwood Aviation LLC.
Steve Jones — Pilot/Training Captain, Glenwood Aviation LLC.

CONTENTS

LIST OF FIGURES

LIST OF TABLES

RFP Requirements and Compliance

RFP Requirement	Action Taken	Reference
Description of missions	Detailed mission strategy presented for all missions.	Ch. 3, Pg. 15
Transport minimum 1200 people/hour from rooftop	1200 people evacuated using four helicopters in one hour.	Sec. 3.6.1, Pg. 32
Rescue subsystem landing on congested rooftop	Underslung pod designed to land on congested rooftops.	Sec. 3.3.1, Pg. 19
Deploy teams of 15 firefighters in 2 minute cycles	Firefighters deployed using an underslung pod on the rooftop.	Sec. 3.6.1, Pg. 32
Safe hover within urban canyons	Autonomous flight control system implemented to enhance maneuver capabilities in urban canyons.	Sec. 5.2.2, Pg. 77
Precision hover	High-resolution inertial & position sensors coupled with FCS for attitude hold.	Sec. 5.1, Pg. 71
Penetration of windows at any floor	Different cable lengths provided.	Sec. 3.4, Pg. 23
Extraction of 800 people/hour from windows.	800 people rescued	Sec. 3.6.2, Pg. 33
Lift for 5” hose pumping 1500 gal/min to 100 stories	Lift provided for ground based water pumps.	Sec. 3.8.2, Pg. 39
Engagement of fires at any floor with water cannon	Enabled with both on board tank and ground based systems. Capable of pumping 2000 gal/min.	Sec. 3.8, Pg. 38
500 gal water tank refillable in under 1 min	800 gal tank refillable in 54 seconds	Sec. 3.7.1, Pg. 34
Command and control with min 4 personnel	Module designed with five personnel	Sec. 3.1, Pg. 17
Endurance 1 hr hover & 1 hr cruise at 60 kt	Designed for 1 hr. hover and 1 hr. cruise	Ch. 7, Pg. 86
Navigation system for accurate response	GPS system with DGPS enabled.	Sec. 5.1, Pg. 71
Sensors for thermal maps	Infrared sensors used.	Sec. 1.2.2, Pg. 9; Sec. 5.1.1, Pg. 71
Ease of operation – non-professional pilot	User-friendly operator interface and enhanced autopilot designed.	Sec. 5.3, Pg. 80
Transport minimum 5000 lbs external cargo	Helicopter capable of carrying 10,000 lb	Sec. 6, Pg. 83
Performance in hot day at Denver	Performance analysis done in Denver conditions.	Ch. 7, Pg. 86
Transportable on wide load flat bed truck	Subsystems designed to fit on a wide load flat bed truck.	Sec. 3.5, Pg. 23; Sec. 3.7, Pg. 34
Reconfigurable in under 20 mins	All modules reconfigurable	Ch. 3, Pg. 15
Capability of executing mission after 20 min deployment with minimum 1 hour endurance	Capable of 20 min deployment and 1 hr. endurance.	Ch. 3, Pg. 15; Ch. 7, Pg. 86

Executive Summary

"I, as Aeneas our great ancestor
Did from the flames of Troy upon his shoulder
The old Anchises bear, so from the waves of Tiber
Did I the tired Caesar."

Cassius in Shakespeare's Julius Caesar, Act I *Sc.* 2

The UM–911 Aeneas is a multi-role urban disaster rescue vehicle designed in response to the American Helicopter Society's Annual Student Design Competition. The Request For Proposals (RFP), sponsored by Sikorsky Aircraft and NASA, identified the need for a hovering aerial vehicle capable of evacuating people from high-rise buildings in the event of an emergency. Aeneas features a single-helicopter multiple-module design philosophy, enabling the same rotorcraft to perform different missions specified by the RFP when equipped with the appropriate mission module. Throughout the design of Aeneas, emphasis has been placed on maximizing the safety and controllability of the rescue system, even when operating in the most challenging emergency situations. The heavy lift capability, minimum reconfiguration time and unparalleled safety makes Aeneas the ideal choice for emergency rescue operations.

Mission Requirements and Design Objectives

The RFP specifies different mission requirements as part of the standard rescue vehicle package. Broadly speaking, the rescue operation consists of two main parts, evacuating victims trapped on the upper floors of a high-rise, and containment and suppression, if possible, of the fire (or other disaster situations). The primary goals specified by the RFP included the ability to evacuate at least 1,200 from rooftops, and at least 800 people from windows, in one hour, capability to fight fires at any floor of the building using an on board water source or ground based water pumps, and the capability to deploy 15 firemen at a time on the rooftops. These missions were to be co-ordinated by a sophisticated command and control platform with access to real-time data on the fire, building and city maps. The requirements imply the need for a multi-role system, with an advanced flight control system, capable of operating in urban canyons.

Configuration Selection

Aeneas is an optimally designed configuration capable of satisfying the unique requirements of this multi-mission operation. One of the initial challenges faced by the design team was to decide whether multiple rotorcraft configurations, tailor-made for each of the specific missions, were necessary. It was felt that a multi-role rotorcraft equipped with mission specific modules would result in lower production and acquisition costs. Furthermore, the RFP requirement of "system reconfigurability" was interpreted to mean that the same rotorcraft should be capable of performing all the defined missions. The optimum configuration was, therefore, arrived at after carefully choosing a fundamental set of critical design parameters based on the specific needs of a generic rescue mission. All the potential candidate configurations were carefully evaluated for each of the missions specified by the RFP. The results of the configuration evaluation study suggested that a co-axial rotor configuration was the most promising candidate for all the missions

defined by the RFP. A co-axial rotor configuration is the most geometrically compact design for a given payload capability and can, therefore, more easily operate in congested urban areas. A single rotor – tail rotor configuration requires a long tail boom to increase the moment arm of the tail rotor. The presence of a tail rotor is also a safety issue in a mission where one expects the movement of people around the helicopter. Tandem and tilt-rotors are not as compact as co-axials because of the horizontal separation between the rotors. The downwash from tilt-rotors is comparatively large, and could cause hazardous conditions both for the rotorcraft and people around it from flying debris. An intermeshing rotor or synchropter design was a close second to the co-axial configuration. However, the synchropter was felt to be a sub-optimal design for the following reasons. The rotor shafts have to be tilted, which means that the rotors must be set higher up on the mast to provide adequate clearance between the rotor tips and the ground to increase safety. The existing synchropter designs are two-bladed, and increasing the number of blades results in greater complexity of the design. Constraining the design to a two-bladed rotor placed restrictions on the minimum rotor radius that could be achieved for a given payload. Taking into consideration the primary mission requirements and associated flight environments, a co-axial configuration was decisively chosen.

Design Approach

Aeneas design was carried out in conjunction with the ENAE634 – Helicopter Design course at the University of Maryland in Spring 2003. No commercial codes were used in the design process. The study was performed entirely using tools developed during the course. The rotor dynamics analysis was performed using the University of Maryland Advanced Rotorcraft Code (UMARC), which was modified for trailing edge blade flaps. The graphics were developed using I-DEAS CAD software.

Aeneas – Design Features

Aeneas rescue system comprises of a heavy lift, co-axial helicopter, and an array of subsystems tailored for different missions. The helicopter has a gross takeoff weight of about 22,230 lbs. This heavy-lift capability was necessary to limit the number of independent systems required to perform the mission. The evacuation missions will be carried out using a versatile underslung pod. The compact firefighting subsystems can be installed on both the helicopter, as well as on the pod, enabling engagement of fires in narrow urban canyons. The schematic of Aeneas with its different subsystems is shown in Foldout 1.

Analysis of the Thermal Environment

The design team worked actively with the faculty of the Department of Fire Protection Engineering at the University of Maryland. With their advice, the team was able to develop a realistic picture of the aerodynamic and thermodynamic environment around a burning building. This analysis proved extremely valuable in determining the no-fly zones around the building, and the feasibility of rooftop and window extraction missions when the fire occurs at different heights above the ground. Based on this analysis, a simple fire modeling database was proposed, for the disaster command and control module, to aid in the decision making process of the flight management of vehicles.

Aeneas: Co-Axial Helicopter

Aeneas features an advanced swashplateless, three-bladed, bearingless, co-axial main rotor, a state-of-the-art MR landing gear, a cutting edge flight control system with simple operator interface, sophisticated avionics suite and a three engine configuration to ensure sufficient power for hovering at high effective density altitudes. The primary design features are:

Co-axial rotor configuration — The co-axial configuration is the most compact hovering vehicle system for a given payload capability enabling Aeneas to operate in narrow urban canyons. The absence of the tail rotor improves operational safety in ground operations. This is critical because a disaster rescue operation is usually carried out amidst widespread panic and mass movement of people around the helicopter. The rotor design is optimized for hover and low-speed forward flight. The rotor diameter is 52.35 ft. This is the most compact rotor possible for a vehicle of this weight class, without incurring severe downwash and induced power penalties.

Swashplateless control — Aeneas uses actuated trailing edge flaps on the blades for primary flight control. The swashplateless design eliminates the need for pitch linkages, resulting in an aerodynamically clean and mechanically simple rotor. Absence of failure prone, mechanical linkages enhances the reliability of the system and improves the Mean Time Between Failures (MTBF). In addition to primary control, the trailing edge flaps can be used for Individual Blade Control (IBC) providing vibration reduction. The present swashplateless concept uses recently developed piezo-hydraulic, compact, hybrid actuators to control the trailing edge flaps, in conjunction with a neural-network based adaptive controller perfected for individual blade control with a dissimilar rotor. The blades have an indexing angle of 20° and a low torsional frequency. Two trailing edge flaps per blade and two actuators per flap provide high redundancy in case of failure.

Magneto-Rheological landing gear — Aeneas is expected to land on unprepared landing sites during emergency operations. In addition, the takeoff weight is dependent on the type of mission performed. A semi-active landing gear uses a magneto-rheological fluid that has adaptive damping characteristics, and will absorb landing impact loads more efficiently decreasing susceptibility to structural fatigue failure, dynamic stresses and passenger discomfort.

Autonomous flight control system — Aeneas features a full authority, triple redundant, digital, Fly-By-Light (FBL) Flight Control System (FCS). The Autonomous FCS provides response shaping, stability augmentation and integrated flight and engine control that enhances operational safety in urban canyons. Mission specific auto-navigation relieves the pilot workload considerably, and enables a *trained operator* to fly the vehicle inside *urban canyons*.

Sophisticated avionics suite — Aeneas is required to hold hover position within one foot in all directions. The flight control system is assisted in this task by fast, responsive, high resolution inertial and position sensors. The instruments include a Zero-lock Laser Gyro and a Global Positioning System (GPS) which, when augmented with Differential GPS (DGPS) corrections, can provide very accurate position information to less than one foot.

Simple operator interface — Aeneas provides Multi-Function Displays (MFDs) capable of displaying different information depending on the pilot proficiency and mission performed. This enables a *trained operator* to fly the vehicle with considerable ease, when assisted by the automatic flight control system.

Three engine configuration — Rescue missions require the helicopter to hover for extended periods of time. One engine inoperative (OEI) condition is critical while operating in urban canyons and loading passengers from building windows. In addition, all these missions need to be performed in "a hot day in Denver" conditions. Aeneas was, therefore, designed with three engines. In the event of an engine failure, Aeneas is capable of sustained hover with two engines operating at intermediate power, ensuring successful completion of the mission.

Aeneas: Modular Subsystems

The capabilities of the helicopter subsystem are complemented by a highly modular, versatile array of mission specific subsystems. Considerable efforts were taken in the module design to ensure multi-mission capability with minimum reconfiguration. The subsystems are described in brief detail below.

Aerial Rescue Kit (ARK)

The primary module is the Aerial Rescue Kit (ARK), an underslung pod of dimensions 18.5 ft$\times$9.3 ft$\times$6.5 ft, designed to carry 40 passengers and one operator. The ARK is designed for a gross weight of 10,000 lbs. Structurally, the module is capable of resisting a limit load of 3.5g (35,000 lbs). The ARK is built from three modular sections for ease of manufacture and reconfigurability. The main design features of the ARK are:

Control with thrust fans — The ARK has three fans, two on the side and one on top, which provide precise longitudinal, lateral and yaw control. The thrust fans assist in positioning the box vertically below the helicopter in forward flight, enabling Aeneas to maneuver within urban canyons. The fans also serve to orient the box for precise landing on the rooftops and position the ARK alongside the building face during evacuation through windows. The thrust fans can be used to eliminate the oscillations arising from gusts and other unsteady aerodynamic effects within urban canyons.

Independent flight control system — The ARK is equipped with an advanced flight control system (FCS), similar to the FCS in the helicopter, to control the thrust fans. A continuous two-way data transfer between the ARK FCS and the helicopter FCS enables it to position the ARK vertically below the helicopter at all times.

Crash-worthy seats — Safety of the passengers was the primary concern throughout the design of Aeneas. The ARK provides seating arrangement to its passengers, ensuring enhanced operation safety. The seats can be folded easily to increase the standing floor space to accommodate 15 fully equipped firemen.

Heavy duty cables — The ARK is supported by the helicopter through high strength, lightweight, abrasion resistant Kevlar cables. The torque-balanced, double braid construction minimizes the oscillations of the ARK in the torsional mode.

Oleo-pneumatic undercarriage — The ARK is provided with landing gears to minimize passenger discomfort and structural fatigue during rough landings on unprepared landing sites.

Quick installation and reconfiguration — The installation and reconfiguration times are critical in emergency response situations. The ARK can be installed on the helicopter within 5 minutes, and can be reconfigured for different missions within 20 minutes.

Aerial Firefighting System

Aeneas is designed as an aerial firefighting system capable of engaging fires at any floor of a high-rise building using both on-board water tanks and ground based water systems. The on-board tank is capable of carrying 800 gallons of water and 40 gallons of additives. In addition, Aeneas can lift and direct a 5 inch water hose at any floor of the building. The main features of the firefighting module are:

Impulse nozzle water cannon — While fighting fires with an on-board water tank, Aeneas uses an impulse water cannon. These cannons require only about 10% of the water required by a conventional spraying system to control the fire. Aeneas' on-board water tank can fight fires for longer periods without the need for refilling the tank.

Conventional nozzle — In addition to the impulse nozzle, a conventional nozzle capable of delivering up to 2000 gallons per minute is installed on Aeneas. This nozzle is used with the ground based water pumps. A 5 inch hose connects the nozzle to the ground based pump, and this arrangement enables Aeneas to fight fires without the need for refilling.

Aeneas: An Ideal Disaster Response Package

Minimizing the number of systems required to carry out all the RFP specified missions simultaneously was the primary design objective. The mission strategy, the vehicle payload, and size were all chosen to maximize the utilization of available resources. Preliminary analyses of various mission scenarios was carried out to determine the minimum number of systems required to perform all the missions simultaneously. Based on the study, it was determined that a minimum of 10 helicopters with appropriate subsystems were necessary to successfully carry out all missions goals within the prescribed time limit on a representative 100 story building. Of the ten systems, three each are required to perform the rooftop and window evacuations, one for deploying firemen onto rooftops, two for aerial firefighting (assuming self contained water tank firefighting), and one for the aerial disaster command and control platform. The final number of systems was chosen based on an optimization study of different parameters such as the number of people to be evacuated, and restrictions on multiple systems operating simultaneously around the building.

A preliminary estimation shows the acquisition cost of the helicopter system to be around 10 million US dollars. The cost is comparable to existing helicopters of similar payload capability.

Conclusions

Aeneas offers the prospective customer a reliable and efficient rescue system that is responsive to the unique requirements of a disaster control operation. The incorporation of the latest technologies improves the performance with considerable reduction in maintenance and operating costs. Aeneas has been carefully designed to meet all the design requirements and expectations of the RFP to provide unsurpassed performance when the situation demands it.

Aeneas - Urban Disaster Response System

Command and Control Module

Aerial Rescue Kit

Self Contained Firefighting Module

1 Aeneas - The Urban Disaster Response System

This proposal presents the UM–911 Aeneas, a multi-role rotorcraft system designed for conducting rescue operations in congested urban areas. Aeneas was designed in response to the Request for Proposals (RFP) from the American Helicopter Society as part of their 2003 Student Design Competition. The RFP, sponsored by Sikorsky Aircraft and NASA, identified the need for a hovering disaster response system capable of evacuating civilians trapped in a high-rise building in the event of an emergency. In addition, the system was also required to aid in the containment and suppression of fires in tall buildings and to assist in supplying disaster relief materials and/or emergency evacuation of debris. The VTOL rescue system, combined with a ground-based system, was envisaged as the future of disaster response systems.

1.1 The Case for an Urban Disaster Rescue Vehicle

Current ground based systems, for containing fires and rescuing victims, are effective only up to a height of about ten stories from the ground. The need for a VTOL based disaster response system was highlighted by the September 11 terrorist attack on the World Trade Center in 2001. In the case of high-rise buildings, like the World Trade Center, the victims trapped in the floors above the fire have no means of safely exiting the building. Helicopters, with their hovering capability, offer an ideal escape route in such emergencies. However, helicopters are rarely used in rescue operations involving high-rise buildings, because of several reasons. High-rise rooftops are not designed with helipads, nor a clear approach and exit route. Aerial access to most rooftops is obstructed by the presence of antennas and other obstacles. Rescuing civilians from a high-rise often involves operation in congested urban localities. This requires high precision attitude and position hold capabilies in a highly, turbulent, unsteady aerodynamic environment. Rescuing victims from the rooftops is restricted to the top ten to fifteen floors. Victims might be incapable of climbing upstairs owing to physical infirmities and/or the debilitating effects of smoke and fire. No existing rotorcraft appear to be capable of extracting people through the windows of a high-rise building. Any attempt at conducting rescue operations involving high-rise buildings will require the helicopter to operate very close to these buildings. This can be a hazardous operation, even in the absence of a fire, because of the gusty, turbulent air around the buildings. In the absence of an advanced flight control system, the pilot does not have adequate time to react to disturbances, and this can have disastrous consequences. Thus, the requirements of such a rescue system are unprecedented and present daunting challenges.

Helicopter based rescue systems, when specifically designed for civilian rescue missions, can successfully deploy firemen into burning buildings, extract occupants trapped on floors above the fire (rendered inaccessible to ground rescue systems), and engage fires at the upper levels. In addition, aerial monitoring systems can obtain and analyze real-time data regarding the fire and victims, enabling firefighters to plan the mission more effectively. Availability of such helicopters, capable of controlled hover, along with appropriate rescue subsystems, could have potentially saved the lives of many who tragically leaped to their deaths on 9/11.

Therefore, Aeneas was designed with the objective of developing a reliable hover capable disaster response system with enhanced performance that will enable it to operate in even the most demanding environment.

In the following sections, a brief description of the operating environment in an “urban canyon” will be presented. This will be followed by the results of a detailed mission study that looks into greater detail at the important factors

that contribute towards an effective rescue operation. Finally, the criteria for vehicle and subsystem selection, based on the results of the study and mission requirements of the RFP, will be presented.

1.2 Conceptual Rescue Mission Scenario

The success of any design depends on the identification of the key operational requirements that will enable the potential system to be responsive to the unique needs of the mission with an efficient design. The choice of the helicopter configuration, the rescue mission modules, their sizing and performance, depend primarily on a thorough understanding of the requirements of typical rescue missions.

1.2.1 RFP Mission Requirements

The rescue mission scenario was studied in great detail to identify the primary issues that most impact the operations. A disaster response operation consists of the following parts:

Occupant Evacuation — The primary objective of this mission is to extract the victims trapped in the upper floors of a high-rise building and transport them to a safe location. The aerial modes of access to the building are the rooftops and the windows on the upper floors. This usually requires a helicopter to hover very close to the buildings while loading and unloading people. The success of this mission depends on long hover endurance and advanced flight control technology capable of precision attitude and position hold.

Fire-fighter Deployment — The objective of deploying firemen are two-fold. The firemen can enter the building with the necessary equipment and create exit routes for the victims trapped on the upper floors. They can physically transport people to safer locations, especially if they are incapacitated by smoke. In addition, firemen, when deployed near the floor on fire, can prevent the fire from spreading onto other floors and maintain the exit routes open until the building has been evacuated. The success of this mission depends on the capability to detect the extent of the fire and deploy firemen at the appropriate locations. Furthermore, provisions must be made to extract the firemen in an emergency and also to provide replacements. This requires quick access to the rooftop or the windows, and again high-precision hovering capability is required.

Aerial Fire-Fighting — The existing fire-fighting systems are capable of engaging fires only up to a height of about 10 stories. A helicopter designed to fight fires will be able to hover at any altitude beside the building and engage fires at any floor above the ground. This can be achieved by two schemes. One solution is to carry an on board water tank. This would depend critically on the speed at which the water tank can be refilled and on the availability of large water sources near the disaster area. This would require a high hovering efficiency and a fast tank refilling system. Another solution is to provide lift to a water hose attached to a ground-based water pump. The helicopter acts as a “hovering crane” by lifting and directing the nozzle in the direction of the fire. This assumes the existence of a powerful pump and pipe system that is capable of pumping water to a height of 100 stories.

Command and Control System — The success of the aforementioned missions depend critically on careful planning and execution of the flight plan. The objective of the command and control mission is to analyze the real-time

data obtained from the sensors and other sources, identify the extent of the disaster, plan rescue activities, schedule flight cycles, and direct and monitor the other rescue missions, including the ground-based systems, to ensure the operations are carried out efficiently.

1.2.2 Aerodynamic and Thermodynamic Environment

A study of the aerodynamic and thermodynamic environment around a burning high-rise building was conducted during the process of the initial concept exploration. The study provided insight into the unique mission requirements. The knowledge gained by this analysis was used to determine the design drivers for configuration evaluation and selection.

The environment associated with a fire, has an adverse effect on not only the survivability of humans but also the helicopter performance. A thorough understanding of the aerodynamic and thermodynamic environment around fires in high-rise buildings is essential for evaluating the operational envelope ("no-fly zones") around the building. Based on this knowledge, one can then build a "rescue-able mission scenario". As a result, one of the initial objectives was to obtain three-dimensional profiles of temperature and other properties around the building. In this aspect, the design team had the unique opportunity to avail the expertise of the Department of Fire Protection Engineering (FPE) at the University of Maryland. This department is one of a kind specializing in the analysis of fires in buildings. With their advice, the design team was able to develop a realistic disaster scenario on which the final design was based. One of the design team members, Joe Whitt, is a full-time student in this department.

Temperature Profile Around the Building

Most high-rise buildings are required to be equipped with a full sprinkler system and fire-alarms. Moreover, these buildings usually have multiple stairwells at different locations to provide downward exit routes. Any rescue scenario requiring aerial access should, therefore, assume complete blockage of these escape routes. This is possible if the fire engulfs one or more floors completely. The fire-alarm and sprinkler systems might have failed, preventing the early detection and control of the fire. This is an important conclusion that can provide an estimate of the magnitude of the fire. Discussions with the experts at the FPE suggested that a 50 MW energy output would be a typical estimate for a fire in a high-rise building. It was further suggested that the quantity of heat released would break the windows (Ref. 2). These broken windows not only act as vents for smoke and heat release, but also allow air to be entrained into the building. The fire, therefore, can be assumed to be fuel-limited. [1]

The smoke and heat released from the windows rise up as a plume. The properties of air around the plume vary as a function of the height from the origin of the plume (the venting windows) and the radial location from the plume centerline. Exact analysis of the fire and the heat convection requires a coupled thermodynamic, CFD analysis, which is beyond the scope of the present study. The present analysis, therefore, was carried out with empirical tools obtained from previous experience. The temperatures along the plume centerline as a function of height are obtained using the Zukoski fire plume equation (Ref. 3). Figure 1.1 shows the temperature variation along the plume centerline as a function of the height above the vent. One observes that the temperature decreases exponentially as the height increases. The temperatures can be as high as a 100° Celsius above the ambient temperature at heights less than 100

[1] Fuel-limited fire dies out when all the available fuel is consumed.

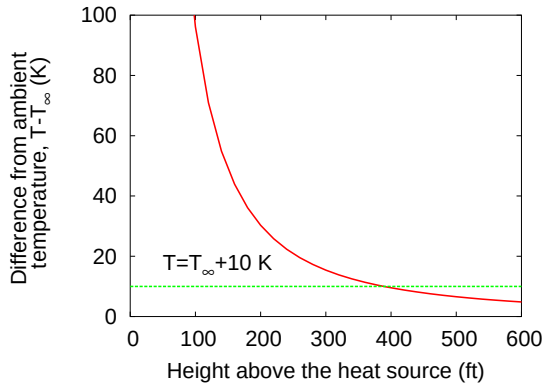

Figure 1.1: Temperature differences, above ambient temperature (T_∞) as a function of height above the fire vent.

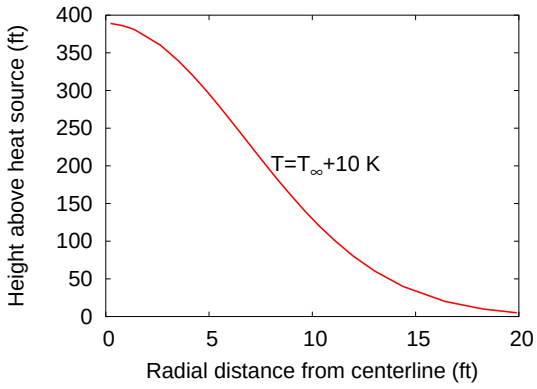

Figure 1.2: Combination of radial distance from plume centerline and height above the fire for a temperature difference of 10 K.

feet above the heat source. The radial distribution of temperatures around the plume centerline varies in a Gaussian manner (Ref. 3). Figure 1.2 shows the boundary, in terms of radial distance from plume centerline and height about the heat source, where the temperatures are 10 degrees Celsius above the ambient temperature. This helps one build a three-dimensional picture of the temperature variation around the burning high-rise. It must be emphasized that the above analysis is based on a number of simplifying assumptions, particularly the absence of winds. Nevertheless, this is a good first approximation in the preliminary design stage to assess the feasibility of a rescue mission. Experience suggests that the primary effect of wind velocity is to shift the plume at an angle to the vertical axis. Also the presence of winds will dissipate the heat faster. However, considering the temperature variation across the plume, operations involving flight through the plume is not recommended.

Temperature and Toxin Tenability

In addition to establishing the "no-fly zones" for the helicopter, the temperature and toxin tenability of humans also needs to be evaluated to determine the feasibility of a particular mission (rooftop or window extraction). Humans cannot survive the large temperature differences shown in Fig. 1.1. The temperature tenability of humans is defined as the heat flux that humans can tolerate at sustained exposure.

Figure 1.3(a) shows the incapacitation time as a function of the height above the floor, using Purser's temperature tenability relation (Ref. 4). The plume centerline temperatures are used in the calculations. This is a worst case scenario with the assumption that the immediate floors above the origin of fire are experiencing high temperatures. A time limit of one hour is assumed for performing the rescue operation. Based on an average floor height of 13 ft. people in the 20 floors above the fire will be incapacitated during this time period. In other words, if the fire occurs in the one of the 20 floors below the rooftop, evacuation through rooftop might not be feasible.

Toxin tenability is also an important issue. In enclosed spaces, people die inhaling poisonous gases like carbon monoxide (CO), carbon dioxide (CO_2) and hydrogen cyanide (HCN) (Ref. 4). Figure 1.3(b) shows the time to incapacitation from carbon dioxide poisoning. If the time of exposure is assumed to be an hour, then the concentration

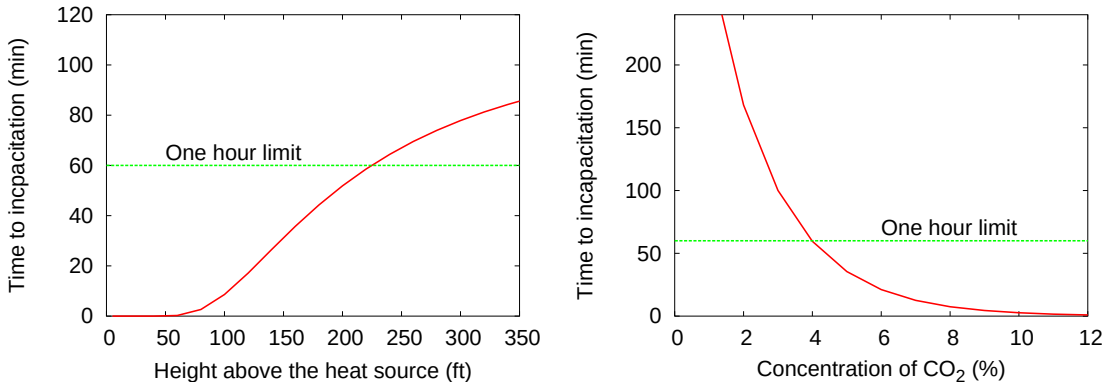

(a) Temperature tenability

(b) Toxin tenability

Figure 1.3: Time to incapacitation from high temperatures and toxin concentrations

of carbon dioxide should be less than 4%. Similar analysis could be carried out for toxin tenability of other harmful gases.

The analysis throws light on the overall thermodynamic environment around a burning building. It was found that operation inside the smoke plume was not advisable at heights less than 200 feet above the fire. The systems should be equipped with sensors measuring temperatures and toxin concentrations. This information will alert the operators of the rescue systems of adverse environmental conditions. The design team recommends that a comprehensive model of the temperature distribution around the building should be built into the data analysis computer of the command and control module. With corrections for prevailing winds, this model will enable the mission command to plan the missions effectively and also prevent rescue systems from accidentally flying into dangerous areas.

1.3 Critical Design Issues

Based on the generic requirements for each mission scenario and the realistic operation environment developed in Sec. 1.2.2, a fundamental set of critical design requirements or “design drivers” was established. The design drivers identified during initial concept exploration are listed below along with a brief description.

High payload capability — The helicopter is required to evacuate a minimum of 1,200 people per hour from the rooftop and at least 800 people per hour through the windows. To restrict the number of rescue systems required for each mission to a practical limit, each system must be capable of carrying a large number of people per trip. Also, the fire-fighting missions, with on board water tanks involving engagement of fires for long periods without refueling, result in a large payload requirement.

Compact size — The system performing the rescue operations is required to operate in narrow urban canyons in between buildings. This imposes severe restrictions on the maximum allowable dimensions of the rotor. This requirement is at variance with the need to evacuate people in large numbers per trip, because the size of the

vehicle scales up with the payload carried.

Hover endurance and efficiency — The rescue system should be able to operate for a minimum of two hours without the need for refueling, necessitating an efficient hovering system.

Low downwash — During rescue operations, the system will be expected to operate over different terrains and land on unprepared landing sites. The rotor downwash could disturb debris on the ground, which can, in turn, cause injuries to the personnel working on ground or around the system. It is, therefore, preferable to keep the rotor downwash as low as possible to prevent hazardous conditions to the people operating around the helicopter.

Adverse weather capability — The missions demand that the system be able to operate at night and in adverse weather conditions.

Operational safety — The rescue missions will be carried out in an adverse operational environment. The helicopters will operate in close proximity to other objects. Therefore, the rescue system should be as safe as possible both in operation and on the ground. Configurations without exposed tail rotors or tilted main rotors are, therefore, preferable.

CG range — A vehicle with an inherently large operational center of gravity travel, in both lateral and longitudinal directions, is preferable to enhance mission flexibility.

Reliability — Disaster response missions are not planned for in advance. The rescue vehicle must be able to respond to distress calls quickly. The system must be reliable and easy to maintain.

Design complexity — The use of unproven high-risk technology will impact adversely on the system reliability. This is not recommended for a disaster response operation.

Acoustic signature — A typical rescue mission will involve firemen relaying instructions to the victims trapped in high-rise building. A noisy rotor will hinder the efficiency with which these operations are performed.

OEI performance — Certain RFP specified missions require the helicopter to hover close to buildings for long periods of time. Transition into forward flight and subsequent autorotation may not be feasible when operating at such proximity to buildings and at low ground clearances. In addition, the helicopter should be capable of continued hover when passengers are boarding the rescue module during window extraction process. The ability to hover out of ground effect (OGE) with one engine inoperative (OEI) is, therefore, a critical requirement.

Multi-mission capability — The RFP defines six separate missions. However, the missions that will be carried out in a disaster operation is strictly situation dependent. As a result, the rescue helicopter should be reconfigurable in a short period of time.

Modular design — The response system should comprise of mission specific modules that can be installed on the vehicle with minimal reconfiguration time.

The design drivers, listed above, are the most critical issues that impact almost all fundamental design decisions. The final vehicle subsystem and the rescue modules were designed with these primary design drivers in mind. This

ensures a reliable, responsive Aeneas that will meet all the needs of the customer. Efforts were taken to incorporate the latest proven technology, which would enhance reliability and performance while reducing the maintenance requirements and costs.

2 Helicopter Down-Selection Methodology

This chapter describes the methodology adopted in the selection of the helicopter configuration that was determined most suitable for a rescue mission. The candidate configurations were evaluated based on the critical design requirements identified during the initial concept evaluation process – see Section. 1.3. However, there were certain issues that needed to be resolved before proceeding with the configuration evaluation matrix. One of the issues that needed to be addressed was: Will each one of the "RFP defined missions" be performed by the same helicopter subsystem, or, will each mission be performed by a different helicopter designed specifically for that task?

2.1 Choice of a Multi-Role Helicopter

The payload for which the helicopter will be designed for, follows from the answer to the this question because the RFP explicitly specifies the payload for certain missions. However, the RFP specifically states *"system reconfigurability"* as a design requirement. This was interpreted by the design team as: *"any helicopter in a disaster response system should be inherently capable of performing any of the defined missions with minimum modifications"*. Further, a mission specific helicopter might have very limited scope for operational enhancements in the future. It was, therefore, decided to design a single helicopter system which, when equipped with the mission specific module, could perform any of the missions by the RFP.

2.2 Determination of Mission Payload

After the decision for a multi-role helicopter was made, the payload was estimated. The RFP specified two payload requirements. One was a minimum lifting capability of 5,000 lb and the other, more stringent, requirement was to evacuate at least 1,200 people per hour from the rooftops. The two choices available at this point were to either design the helicopter for a payload of 5,000 lb and determine how many helicopters and/or trips will be required for rescuing 1,200 people in one hour, or optimize the number of helicopters and/or trips for rescuing 1,200 people per hour and design the helicopter for a payload that is greater than 5,000 lb.

A trade-off study was conducted to decide between these two choices. The details of the trade-off study are given in Sec. 3.3. The variables in the trade-off study were the number of trips, number of helicopters used for rescue purposes and the distance traveled in a round trip. These parameters, along with the RFP requirement of extracting 1,200 people per hour, determined the payload per trip, with the minimum acceptable payload being 5,000 lb. The time required for loading and unloading people was assumed to scale proportionately with the number of people evacuated per trip. The results of the analysis showed that the time spent by each helicopter on the rooftop of the burning high-rise was the bottleneck for the entire operation. Operational safety considerations dictated a limit of one helicopter hovering above the rooftop at any given time. The situation was further complicated by the additional

Table 2.1: Weighting factors used in the configuration evaluation process

Impact on mission	Ratings	Weighting
Essential for successful execution of the mission.	Excellent	4
Major impact on the mission performance.	Good	3
Minor impact on the mission performance.	Fair	2
Preferable but not essential.	Poor	1
No direct impact on the mission.	—	0

RFP requirement of fire-fighter deployment on the rooftops. This meant that the two missions had to be carried out simultaneously. A detailed optimization study was conducted and it was found that 40 people per trip was the optimum payload configuration that satisfied all the RFP requirements, while keeping the size of the helicopter as compact as possible. Forty passengers per trip translated into a payload weight of approximately 7,000 lb, which is well above the minimum RFP requirement for the other missions.

It should be pointed out that the 7,000 lb payload is just the weight of the passengers alone. To this, the weight of the mission specific modules should also be added as additional payload. A trade-off study conducted for the optimum design of rescue modules – see Sec. 3.3.1, suggested this additional weight to be around 2,000 lb. Therefore, a maximum payload of 9,000 lb was chosen as the design payload in the present study. A vehicle designed for a payload of 9,000 lb would be able to carry out all the specified rescue missions.

2.3 Configuration Evaluation and Selection

This section details the methodology adopted to select the optimal rotorcraft configuration for a disaster response mission. Eight different existing rotorcraft concepts were evaluated to avoid premature elimination of any one concept. Experimental and conceptual configurations were eliminated because of operational safety, affordability and technological maturity concerns.

Representative rotorcraft for all candidate configurations with the required payload limit of 9000 lb were used as a basis for comparison. The suitability of each configuration was analyzed for each of the five different missions to ensure that the final configuration was capable of carrying out all the RFP specified missions.

The merits and demerits of the selected candidate configurations were evaluated using certain evaluation criteria, derived from the design drivers identified in the initial concept exploration study (described previously in Sec. 1.3). A five point weighting scheme was used to assess the relative importance of each criterion on a mission-to-mission basis. A higher weighting indicated a stronger impact on the overall mission performance. The configurations were also rated on a five point grade system. A higher grade indicated better suitability for the specific mission – see Table. 2.1. The criteria and their weightings for the different missions are shown in Table. 2.2.

A configuration evaluation matrix was developed to enable a concise evaluation of the overall merits and demerits of the different candidate configurations. Table. 2.3 shows the detailed configuration ratings and the overall “mission suitability index” of each configuration. The ratings were multiplied by the appropriate weighting factors (for each individual mission) and the cumulative sum was divided by the total weights for each mission. A cumulative

Table 2.2: Table showing the weights given to different evaluation criteria for the five different missions specified by RFP.

Mission ⟶	Fire-fighter Deployment	Rooftop Extraction	Window Extraction	Fire-Fighting	Command & Control	Total
Criteria						**150**
Compactness	3	2	4	3	2	14
Precision hover	4	3	4	4	4	19
Downwash	4	3	4	2	0	13
Hover power	2	1	2	1	2	8
CG range	2	3	4	1	0	10
Rate of climb	4	4	3	3	1	15
Controllability	3	3	4	3	2	14
Adaptability	4	3	4	3	2	16
Affordability	1	1	1	1	1	5
Operational safety	4	4	4	3	3	18
Acoustic signature	4	4	4	3	3	18

average over all the different missions was also performed to obtain an overall "mission suitability index" for each configuration. The mission suitability indices for each individual mission is shown in Table. 2.4.

The study indicated that co-axial, synchropter and fan-in-fin configurations were all suitable for the present mission, with a co-axial rotor having a slight advantage over the other two configurations. Tilt-rotors and compound helicopters were the most unsuited for this operation. This was expected because these rotor configurations are optimized for high-speed forward flight applications. The mission at hand was more hover intensive. The conventional, tandem, and NOTAR configurations were better than the tilt-rotor and compound concepts but not as good as the co-axial, synchropter or fan-in-fin concepts. Of the three leading configurations, the co-axial rotor was chosen as the design choice based on its better all-round attributes. The synchropter was eliminated because of the following reasons. A compact vehicle was desired for the present mission. Reduction in rotor diameter could be achieved with increasing the number of blades. However, increasing the number of blades in an intermeshing rotor involves added complexity. Further, tilted shafts of synchropter meant that the rotors had to be placed higher to provide adequate clearance from ground. In the case of a fan-in-fin design, the presence of a fenestron requires the tail boom to extend beyond the rotor circumference. This increases the overall length of the vehicle which was undesirable. The synchropter was, therefore, eliminated in favor of a co-axial rotor configuration.

3 Mission Description and Subsystem Details

This chapter presents the details of individual missions for all six RFP missions. Firstly, detailed mission scenarios developed during initial concept exploration will be presented. Based on these mission scenarios, the optimum configuration for individual mission were determined. The configuration evaluation methodology adopted for the

Configuration	**Conventional**	**Synchropter**	**Co-axial**	**Tandem**	**Fan-in-fin**	**Tilt-rotor**	**NOTAR**	**Compound**
Compactness	1	2	4	1	2	1	3	1
Precision hover	4	4	3	3	4	1	3	1
Downwash	2	4	3	2	2	1	2	1
Hover power	4	4	4	3	4	1	4	2
CG range	3	2	3	4	3	3	2	3
Rate of climb	4	3	3	3	3	4	2	3
Side-wind operation[a]	4	4	3	3	3	2	2	2
Adaptability[b]	4	3	4	4	3	3	4	3
Affordability	4	4	4	3	3	1	3	1
Acoustic signature	1	2	2	2	3	1	3	1
Operational safety	1	3	4	3	4	2	4	2
Mission suitability index	2.76	3.11	**3.29**	2.78	3.12	1.86	2.93	1.81

[a] 1 ft. position hold in gust conditions

[b] Modifications required for reconfiguration to a different mission

Table 2.3: Configuration evaluation matrix showing the criterion ratings for different rotor/airframe configurations.

Table 2.4: Configuration evaluation matrix showing the mission suitability index for individual missions.

	Fire-fighter deployment	Rooftop extraction	Window extraction	Fire-fighting	Command & Control	Disaster response
Conventional	2.77	2.74	2.70	2.81	2.80	2.76
Synchropter	**3.14**	**3.06**	**3.05**	**3.15**	**3.20**	**3.11**
Co-axial	**3.29**	**3.23**	**3.30**	**3.30**	**3.35**	**3.29**
Tandem	2.77	2.84	2.78	2.74	2.75	2.78
Fan-in-Fin	**3.09**	**3.10**	**3.05**	**3.11**	**3.35**	**3.12**
Tilt-rotor	1.89	2.00	1.86	1.85	1.60	1.84
NOTAR	2.91	2.84	2.89	2.93	3.20	2.95
Compound	1.83	1.90	1.84	1.78	1.65	1.80

choice of individual modules will be presented next. Finally, detailed timelines describing the rescue operation from the 911 call to the end of the mission will be presented. The schematic of a typical urban disaster operation is shown in Foldout 3.14.

3.1 Disaster Command and Control

The disaster command and control module is an aerial survey team comprising of experts who assess and control the mission. Their mission can be divided into two primary tasks: conduct an aerial survey of the disaster area and determine if aerial rescue is necessary and supervise all the other missions so that they are performed in a coordinated manner. In order to perform these functions, the module must be equipped with a wide array of sensors that provide an accurate description of the severity of the fire, throughout the mission. In addition, the crew must be equipped with communication devices for relaying instructions to the other helicopters involved in the rescue mission.

The command and control module is contained inside a helicopter in which the main cabin has been adapted with a subsystem that accommodates the five crew members. A modular, low weight configuration is desired to allow for reconfiguration in a short period of time.

The choice of number of personnel and their respective tasks was based on the number of missions that would be performed simultaneously. In the worst case scenario, there would be two or more vehicles fighting the fire, another set of vehicles evacuating people from the rooftop while providing teams of firefighters to help evacuate or fight the fire, and a third set performing window rescue. The most important person in the command and control module is the chief commander, who would be an experienced firefighter, and whose responsibilities include overall assessment of the disaster, and decision making. Three of operators are in charge of specific missions, and the last operator, the second in command, oversees the interaction of vehicles and analyzes the fire data, weather data, external information, communication with ground units, etc. The three mission coordinators have the task of communicating and coordinating the vehicles in the mission they have been assigned. For example, the rooftop rescue coordinator will have to coordinate all the vehicles in that team, assign landing sites for evacuation and provide alternatives if the situation changes.

Each of the four operators will have a computer station and communication device to perform their task. All of the computer displays will be projected in a large screen, individually or simultaneously, for the chief (and the other Command and Control members if necessary) to evaluate. Besides having access to all this information, the chief will also have access to windows for visual cues, and be strategically positioned in the cabin to have access to all these features while being close to all the operators to optimize communication between the personnel.

3.2 Command and Control Module

The command and control module has been designed to fit within the existing fuselage of the helicopter and to accommodate the necessary number of personnel required to perform the mission successfully.

The personnel and their task were already addressed in the section 3.1. The choice of equipment is based on the RFP requirements and the recommendations of the faculty at the Department of Fire Protection Engineering. The RFP requires “capability for simultaneous multiplexed communication on 6 different communication frequencies, developing horizontal and vertical tactical situation displays with overlays of data such as sensor information, maps, and building schematics”, navigation system capable of enabling “rapid and accurate response to street addresses”, sensor systems with “the ability to locate occupants in zero visibility conditions” as well as “capable of developing thermal maps of building structures”. Moreover, the sensor data should be able “to be transmitted to other disaster relief systems on the ground and in the air”. In addition to these requirements, based on the recommendations from the Department of Fire Protection Engineering, the design incorporates capabilities to monitor the heat flux emitted by the fire and to model the fire plume and its characteristics to determine a “no-fly zone”. Moreover, a three-dimensional database of the city to provide accurate virtual views of the disaster area and its surroundings is also provided.

Four computer stations are installed in the module, and the information on each of the computer screens will be projected on a large screen, individually or simultaneously, for the commander to evaluate. A screen of at least 40” diagonal is recommended in order to see the four computer screens displayed simultaneously in a good size.

The command and control module is equipped with four General Dynamics C4 Versatile Computer Units (VCU) workstations (Ref. 5). The VCU’s versatile design includes a 12 in. XGA sunlight readable or an 18 in. SXGA touchscreen-equipped display. It features, among other things, single/dual 1.26 MHz Pentium III Processors and memory expansion up to 2GB of PC100 or 1.5GB of PC133.

The information processed and displayed depends on the task that each operator performs. The firefighting coordinator needs to communicate with all the firefighting units, supervise the operations in the canyons, monitor the temperatures around the building, and the locations at which fire needs to be placated, as well as sources of water for refilling the tanks. For this purpose, the firefighting workstation displays information regarding building thermal environment, plume temperature profiles, locations where usable water surfaces are found. The window rescue coordinator workstation displays the immediate environment of the disaster area and suitable landing sites, tracks the different evacuation routes and coordinates them with the rooftop rescue vehicles, analyzes the temperature and toxicity profiles of the building and determines which are rescuable windows and other similar jobs. The rooftop rescue coordinator, like the window rescue partner, organizes the timeframes of all the units to avoid overlapping of routes over the rooftop, communicates with all the different vehicles performing the mission, interacts with window rescue to avoid missions obstructing each other, evaluates potential landing sites for the evacuation, analyzes the thermal maps

to determine the number of people stuck in the upper floors, assesses the need for firefighters and the rate at which they need to be brought into and out of the building, appraises the fire evolution in order to determine the moment at which rooftop evacuation is no longer safe due to temperature or toxicity changes, etc. The second in command's task involves mainly assisting the chief gathering and processing the data for the other coordinators to perform their mission efficiently, like modeling the fire and the temperature profiles around the building, communicating with ground firefighters, administering the resources, overseeing the overall operation and the interaction of the different missions, observing the weather and predicting its possible effects on the fire and on the mission, etc.

The command and control module allows a commander to cope with all the requirements of such a mission. It provides high frequency channels (HF) for linking with ground or air command elements, ultra high frequency (UHF) for joint operations, very high frequency (VHF) for tactical communications. Connectivity through a information terminal suite will allow staff to receive and filter data from real-time and near real-time information. To allow for simultaneous communications with all the vehicles in the team, it includes 8 Multi-Band Transceiver Channels, 2.0 To 512.0 MHz, Expandable Beyond 2.5 GHz.

The seating arrangement in the command and control module was chosen to allow the maximum utilization of space available, offering the chief with access to the windows, access to the cockpit to communicate with the pilots and close interaction with all the operators on board — refer Foldout 1 .

3.3 Occupant Extraction — The Aerial Rescue Kit (ARK)

Aerial rescue missions involve rapid evacuation of large numbers of occupants from the building in a relatively short time. Given the complexity of the mission, such an operation can only be achieved through the efficient utilization of available resources and careful mission planning. The rescue modules used in the mission should provide safe egress to the victims trapped in burning high-rise buildings and safe transportation to suitable landing sites. These modules must be simple and easy to operate. Furthermore, the modules designed must be cost-effective and economically viable. In short, a robust, yet relatively simple solution was sought for performing the rescue mission.

3.3.1 Mission Evaluation for Rooftop Occupant Extraction

Most high-rise rooftops are cluttered with antennas and other obstructions that prevent a helicopter landing on a building. The lack of proper helipads and safe approach routes to high-rise rooftops necessitates the development of an evacuation strategy where no helicopter landing is necessary. This can be achieved by using an underslung pod to evacuate people. Helicopters have proven capable of transporting cargo and equipment in underslung mode. The helicopter can hover above the building while people are being loaded into the underslung module, thus eliminating the need for a rooftop landing. The underslung module can be designed for greater stability and control, thereby making it safe for human transport.

In the event of an urban disaster, it is desirable to evacuate a large number of people in a given time. This number is limited in practice by various factors. One of the primary limitations is that the size of the rescue module should be small enough to be able to land on most high-rise rooftops. The weight of the underslung pod translates into the payload of the helicopter. A larger payload will mean a bigger helicopter, rendering it incapable of operating in urban canyons. The engine power requirements for one engine inoperative (OEI) conditions will also increase with

Table 3.1: Preliminary study to determine the number of people transported per trip per hour.

No. of People per Trip	Weight (lbs)	Box Area (ft^2)	Number of Trips	Number of Helicopters for 1200 People
10	1750	32	120	2.40
20	3500	64	60	1.38
30	5250	96	40	1.03
40	**7000**	**128**	**30**	**0.85**
50	8750	160	24	0.75
60	10500	192	20	0.68
70	12250	224	18	0.65

increasing payload. As it is also desirable to have a control system on the pod for stability augmentation, the power requirements for such a system will increase with increasing payload.

At the same time, a limit on the minimum number of people that should be transported in each trip, arises from the RFP requirement to evacuate 1,200 people in an hour. Decreasing the payload per helicopter increases the number of helicopters required to complete the mission and is economically unattractive. More importantly, the helicopters performing the missions must be sequenced properly so that no two helicopters are operating over the rooftop at the same time. This presents a bottleneck for the entire operation and limits the number of helicopters that can be used to perform the mission.

In light of the aforementioned limitations and requirements, a method was developed to optimize the number of people carried per trip. The total mission time for different payload configurations was converted to an effective operation time for a single helicopter. In this approach, different parts of the mission, e.g., time for loading and unloading people, flying to and from safe drop-off locations, stabilizing and landing the pod on the rooftop etc., were converted to an equivalent distance that had to be traveled at a certain cruise speed. Initial estimates showed that the optimum configuration for evacuating 1,200 people in one hour is a 40 persons per trip scenario – see Table 3.1. This was chosen as the final design payload, as it was the optimum configuration considering the size and payload limit, while still being able to transport a reasonably large number of people per trip.

3.3.2 Mission Evaluation for Window Extraction

The window extraction missions must overcome the same difficulties as the rooftop rescue mission, as explained previously (see Sec. 3.3.1). In addition, rescue missions from a building face are further complicated by the need to “suspend” the rescue module alongside the building structure to facilitate loading of people. Such an operation is unprecedented, and the choice of the optimal and efficient procedure is unclear at the very outset. Initial concept exploration yielded several possible solutions for performing this mission, and a selection procedure to carefully evaluate the viability of each was developed. Criteria that are critical for carrying out a safe and efficient rescue operation, were determined and the candidate options were carefully analyzed. The final choice of the method of rescue was based on the compliance of the rescue options to meet these criteria.

Four viable solutions for window rescue were identified in the initial concept exploration study and explored in

greater detail. The four schemes studied were a flying platform, helicopter based rescue system, a building based rescue system and, finally an underslung pod similar to that for rooftop rescue mission. A brief description of the four schemes, along with their advantages and disadvantages is presented here. Schematics of the different concepts explored are shown in Fig. 3.1.

Flying Platform – The Flying platform (Fig. 3.1(a)), is an autonomous flying vehicle, with four ducted fans providing vertical thrust, and another forward thrusting fan, similar to that developed by DM AeroSafe (Ref. 6). This concept is designed to hover very close to the buildings. The shrouded fans offer safety during operations close to building walls. The primary disadvantage of this concept is that the ducted fans require large amounts of power as compared to a helicopter with the same lifting capabilities. Moreover, considering the projected cost for a similar system by Armstrong (Ref. 7), that can transport 6 persons at a time, makes the option economically unviable when designed to meet the RFP requirements.

Helicopter Based Extensible Platform – A second option (Fig. 3.1(b)) is to have a platform extending from the helicopter to the particular window from which people are being evacuated. The helicopter can then hover at a certain distance away from the window (with a minimum rotor-tip clearance of at least one rotor diameter) while people board the helicopter. This configuration will create large pitching moments on the helicopter which cannot be counteracted by the main rotor alone. The use of ducted fans to relieve these moments was investigated. However, the sluggish dynamic response of the tail-ducted fans could lead to disastrous consequences, endangering lives of the people. Furthermore, the use of ducted fans adds to the complexity and weight of the vehicle.

Building Based Platform – To eliminate these problems, the feasibility of building based platforms (Fig. 3.1(c)) was investigated. While such a concept is a mechanically simple, safe, and efficient design, it has economic and architectural drawbacks. Such platforms will be required at regular intervals, say every 10 floors, on each high-rise building, making this a very expensive proposition, both in terms of initial capital and recurring costs. These platforms will also take up valuable leasing floor space. In addition, considerable modifications will need to be performed on existing buildings to provide mounting points for such a platform, thus making it unattractive.

Underslung Rescue Kit – Finally, the use of an underslung pod (Fig 3.1(d)), similar to that used in rooftop rescue mission, was also investigated. This concept, when equipped with appropriate control systems, can be positioned along side the windows to load people. This involves no modifications to the building and is a relatively simple design.

A configuration evaluation study was carried out based on various parameters, using a procedure similar to that described in Sec. 2.3, to choose the optimum solution amongst the four concepts described above. The analysis (Table 3.2) showed that the underslung pod concept was the most attractive solution for performing this mission. It was, therefore, decided to use the same underslung pod designed for rooftop rescue for this mission too. This eliminates the need to design and fabricate different modules, thereby cutting down the production costs.

Table 3.2: Configuration evaluation matrix for window rescue mission.

Criteria	**Flying Platform**	**Building based**	**Helicopter based**	**Underslung pod**
People per trip	1	3	3	3
Operational safety	3	2	1	3
Compactness	1	2	2	3
Building Independence	3	1	2	3
Cost effectiveness	1	1	2	3
Deployment time	2	2	1	2
Initial setup time	3	2	2	2
Ingress/egress time	3	2	1	3
Total points	**17**	**15**	**14**	**22**

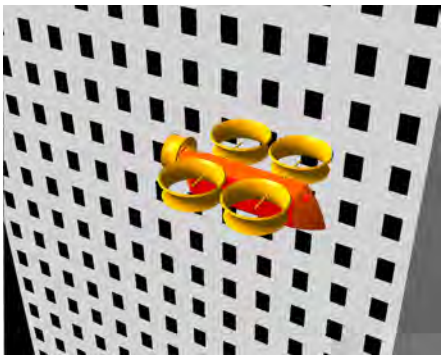

(a) Flying Platform

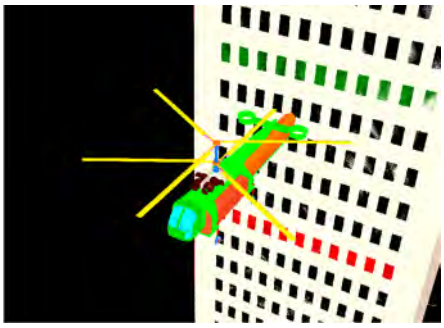

(b) Helicopter based platform

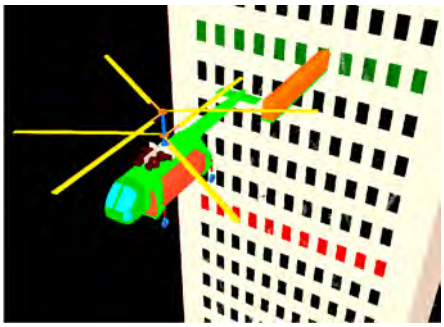

(c) Building based platform

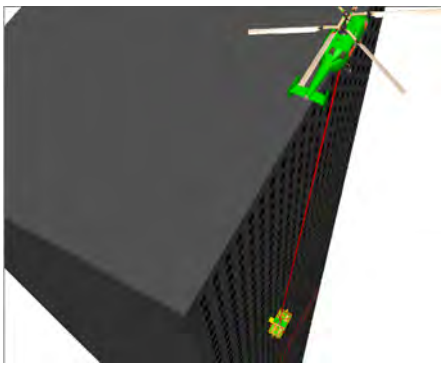

(d) Underslung pod

Figure 3.1: Schematic showing the various options explored for window extraction mission.

3.4 Design Considerations for the Aerial Rescue Kit

The Aerial Rescue Kit or the ARK is an underslung rescue module designed to transport people. The primary design considerations for the ARK are :

- Carry 40 people at one time and at least one trained operator.
- Transport 15 firefighters to building rooftops.
- Land on congested rooftops.
- Be capable of positioning itself close to building faces for window penetration and evacuation of occupants.
- Maneuver precisely for docking with windows.
- Have sensors that provide the exact position with respect to the building.
- Be capable of performing fire-fighting operations.
- Lightweight, cost effective and crashworthy.

One other important design consideration for the control system on the ARK was that the operator be able to control it using simple commands. During operations, the pod would tend to sway under the influence of gusts and helicopter maneuvers including transition to forward flight. If the occupants were standing, they would have to be densely packed. It was decided to seat the occupants while being rescued. This will enhance the operational safety of ARK because the passengers will be strapped in securely.

3.5 ARK Design Details

The Aerial Rescue Kit (ARK), shown in Fig. 3.2 is a highly reconfigurable, multi-mission rescue module. It can be configured to seat 40 passengers, or 15 fully equipped firefighters when standing, or to carry the aerial firefighting modules (see Sec. 3.7). The ARK features crashworthy, foldable troop seats, two wide doors for rapid ingress and egress, and three thrusting fans to control its orientation. The design details are presented below.

Each person is provided a floor area of 3 ft^2, and each fully equipped fire-fighter, typically weighing 300 lbs, is provided a floor area 10 ft^2. These requirements fix the internal dimensions of the underslung pod. The external dimensions of the underslung pod are 222 in$\times$ 112 in$\times$ 78 in. The pod has a height of 6.5 ft to accommodate the standing firefighters. The interior floor dimensions are 218 in $\times$ 108 in. The width of the pod door is 48 in so that it can interface easily with typical windows (usually wider than 36 in), to provide enhanced ingress and egress. The ARK is designed for a gross weight of 10,000 lbs. Structurally, the module is capable of resisting a limit load of 3.5g (35,000 lbs), and capable of withstanding a longitudinal or lateral compressive load of 1.0g (10,000 lbs). Other parameters considered in the design of the pod include weight, cost, maintainability, impact and wear resistance. In the present design, these parameters are optimized, with special emphasis being placed on cost and weight minimization.

The pod is assembled three sections (Fig. 3.2):

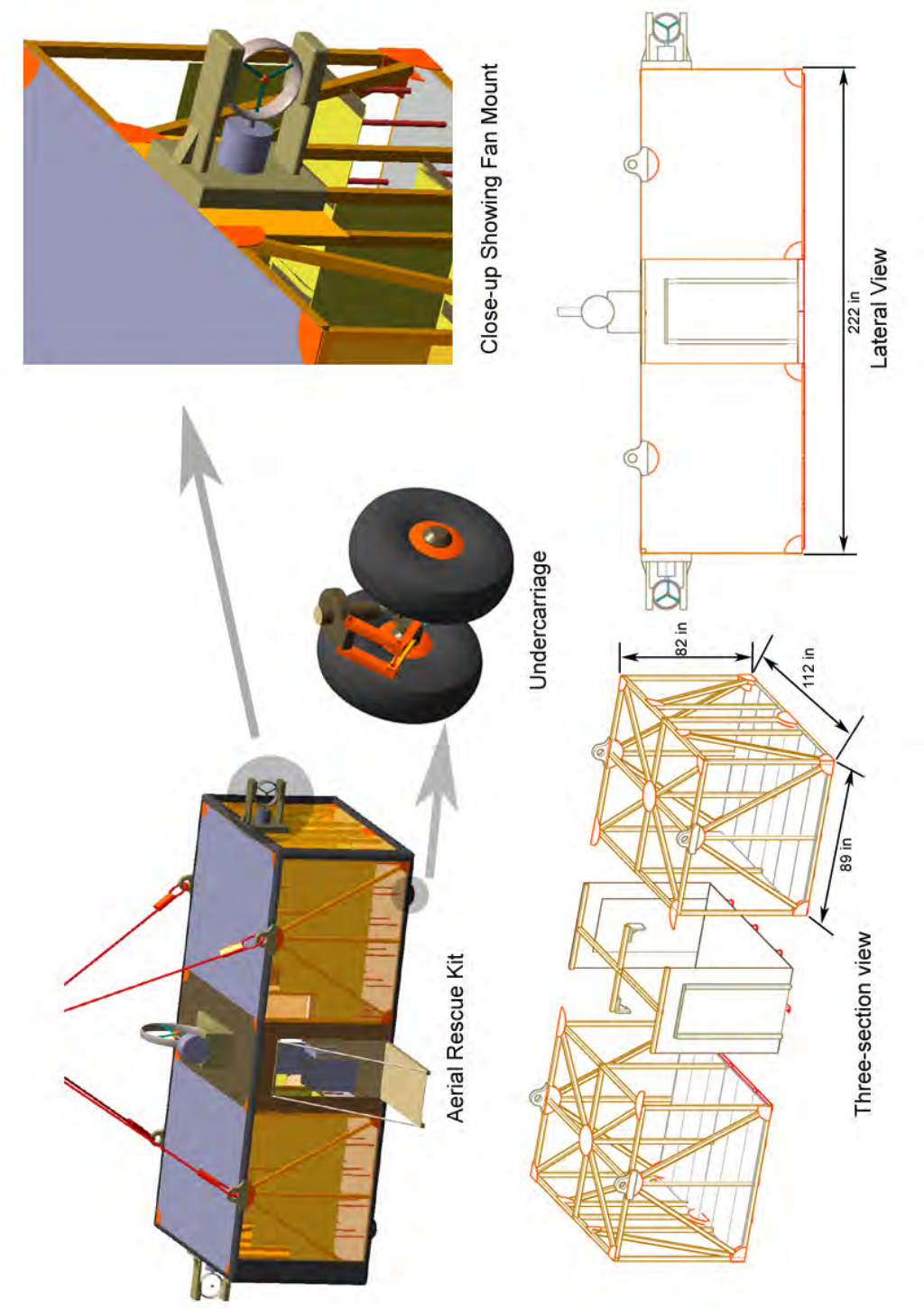

Figure 3.2: Details of the Aerial Rescue Kit (ARK).

- Two end sections with a floor assembly, side columns, center columns, beams, and diagonals and upper structures, and
- One center section consisting of floor assembly, doors and a top structure to support the weight of the fan.

The pod is constructed by bolting the beams of the center section to the columns on the two side sections, using the gussets. Such a modular design provides for easy reconfiguration capability of the interior of the pod. Moreover, the pod can be increased in length by connecting more such similar sections, such as for carrying large cargo.

3.5.1 Structural Details of the Pod

The structure of the pod has been designed according to FAR part 29.865, which requires that *"... both the rotorcraft external load attaching means and corresponding personnel carrying device system for rotorcraft-load combinations to be used for human external cargo applications can withstand a limit static load* (factor) *equal to 3.5 ..."* The structural design of the ARK consists of a lightweight aluminum lattice frame, built on top of a metal floor assembly, and an upper structure to support the weight of the thrust fan on the top of the ARK. Steps are provided on the side columns to aid personnel in attaching slings to the helicopter.

Design of the Floor Assembly

The floor assembly for all the three sections consists of a partly perforated metal deck supported by stringers to transfer the load acting on it to the vertical center columns that are connected to the cables, and eventually to the helicopter. The floor structure of each of the three sections of the ARK consists of a 3/16-inch thick deck plate. Adding perforations on the deck, below the position of the seats, resulted in a weight reduction of 110 lbs. The perforated deck structure allows for the easy installation of tie-down points for mounting troop seats or holding other cargo. The deck is supported by longitudinal stringers, end beams, side beams, transverse beams, and lower corner fittings on the two end-sections. Commercially available, 7476 aluminum alloy is used for its high resistance to corrosion, high strength to weight ratio, and low cost. For the two end-sections of the pod, the corner columns are welded to the perforated deck at appropriate locations.

The floor of the center section holds the door, which doubles up as a platform for ingress and egress. The door is held by tethers and is controlled by the operator in the ARK. The center of the floor has a pluggable hole, which is used during the ground based fire-fighting, for connecting the hose to the nozzle. The top structure of the center section supports the fan on the top.

Lattice Frame Structure

The lattice frame shown in three sections in Figure 3.2 provides a load path for the transfer of load on the floor deck to the cable connecting the ARK to the helicopter. It also supports two thrust fans on the sides, which are used for yaw control. The side columns supporting the upper structure are subject to both axial tension and compression. As such, they were designed for a critical compressive buckling load of 0.6g that could occur during hard landings. The columns are 0.125 in. thick, square cross-section measuring 2.25 in. a side. 6061-T6 aluminum alloy was chosen for its high yield strength and adequate as-welded yield and ultimate strengths in the heat-affected zones at the ends of the

columns. The columns are welded at the corner to the aluminum plate deck below and to the beams on the top. The joints at the bottom deck are reinforced with plate gussets to which the diagonal support struts are bolted.

The columns through the center of the two end-sections of the pod are provided to enhance the rigidity of the structure, and to provide support to the seats, and are provided with handles for the people and the fire-fighters to hold. The center columns are connected using quick connect joints, and are removable for reconfiguration of the module for fire-fighting purposes and other cargo carrying capability.

The purpose of the diagonal assemblies in the underslung pod is to provide lightweight, low-cost, impact and damage resistant structure for maintaining the shape of the module. It also provides a shorter load path for the load on the floor, thus reducing the support structure required in the floor assembly, and hence the cost of the structure. The diagonals are designed for a minimum ultimate load of 25,000 lbs, bolted to the plate gussets provided at the ends of the vertical columns. The diagonal and center columns on the side structure can be disconnected from the plate gussets to provide for rapid load/unload capability of cargo and other equipment.

The upper diagonals that form a part of the upper structure are used primarily to maintain the shape of the structure as a whole and to provide support for the columns through the center of the two end-sections of the pod.

Fan Mount

The ARK is equipped with three thrust fans - two small fans on the sides of the pod, and one larger fan at the top. Each of the small fans is bolted to the smaller face of the frame as shown in Figure 3.2. The fan-motor mount is bolted to the base plate provided on the pod side. The fan-motor mount has a cutout to match the contour of the duct, to hold the duct in place. The top fan is bolted to the top of center section of the underslung pod.

Skin

The ARK needs to be covered with a skin to prevent people inside, from accidentally falling off, and also to protect the occupants from any falling debris. Besides reducing the weight, a mesh structure has the advantage that it reduces the dragon the underslung pod, reducing the susceptibility to gusts, and, thereby increasing stability. Reducing the drag on the pod also is beneficial for the performance of the helicopter during forward flight. The skin has a rubber layer on the outside meant for cushioning impact loads when the pod docks with windows.

Undercarriage

The ARK is designed primarily for emergency rescue missions. In such situations, it is highly probable that the underslung pod would have to land in unprepared landing sites. To cushion the impact of hard landing in such places, it was decided to design a suitable undercarriage for the pod. A non-retractable quadri-cycle undercarriage configuration was selected. All the four struts are located such that they share the static loads equally. The wheels can swivel freely and are equipped with brakes.

Each of the landing gear axles consists of two tires. Low tire pressure were selected to land at unprepared sites. When fully loaded (design gross weight of 10,000 lbs), considering a factor of safety of 1.1 and weight variation of 1.15, each tire of the gear must carry a load of 1,500 lbs. A type-III 5.00-5 tire with rated load of 1,850 lbs and maximum load 3,500 lbs was chosen for each of the landing gears. Oleo-pneumatic shock absorbers were chosen or

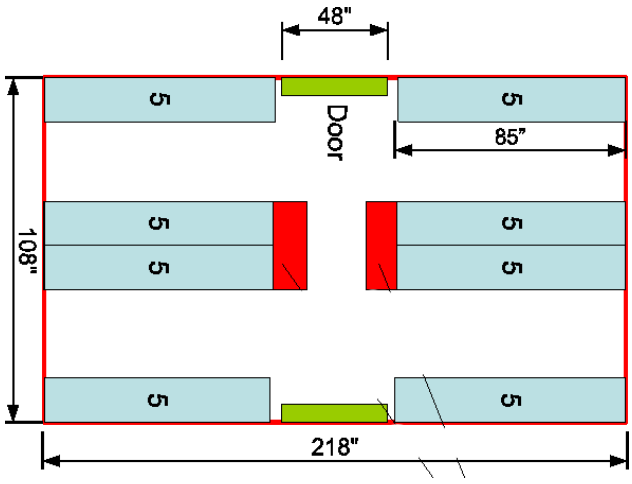

Figure 3.3: Seating arrangement with internal dimensions

the landing gears. The stroke of the landing gear was determined to be 2 in. This value is increased to provide for uncertainties in landing and provide a margin of safety. Using a technique similar to the helicopter landing gear sizing, results in oleo dimensions of diameter 1.25 in $\times$ 4.5 in.

3.5.2 Seating Arrangement

To provide rapid ingress and egress for the people being rescued, it is necessary to choose a suitable seat layout (Fig. 3.3) that provides sufficiently fast access from the seats to the doors, and yet optimize the overall dimensions of the pod. Troop seats were chosen because they are lightweight, low-cost, crashworthy and collapsible. The seats can be folded, to provide space for the firefighting team to be transported in a standing position in the pod. A seat is provided for one operator along with a working table, which can hold two control sticks. The center columns in the pod provide support for the seats. The seats and the center column can be removed for the reconfiguration of the pod for cargo and equipment carrying purposes.

3.5.3 Manufacturing Considerations

The individual columns and beams of the lattice frame are commercially available 6061-T6 aluminum alloy. All the members have the same cross-section and are from the same stock in order to reduce the cost of manufacturing. The modular, three-section design of the pod aids in easy transportability and storage. The reconfiguration time for the pod is reduced by using quick release attachments for the center columns. All other joints are semi-permanent and each individual column can be detached, if necessary, for storage or transportation.

3.5.4 Cable Considerations

For the cable bearing the ARK, a lightweight, high-strength, low-stretch material was sought. Kevlar has one of the highest critical temperature of about 400^{o}F, among various synthetic cables available. Being a good insulator the cable

Table 3.3: Specifications of the cable used.

Cable Material	Diameter (inches)	Rated load (lbs)	Ultimate Load (lbs)	Weight per 1000 ft. (lbs)
Kevlar	**7/8**	**13200**	**92600**	**190**
Galvanized - 7×19	7/8	9900	35000	590
Stainless Steel - 7×19	7/8	10000	36000	710

protects the pod from the static charge build-up on the helicopter. The double-braided, twelve strand, torsion-balanced Kevalr cable with UV protection coating, is abrasion resistant and has high strength to weight ratio when compared to stainless steel and galvanized cables – see Table 3.3.

During the rooftop rescue mission, the helicopter has to hover at a certain minimum distance above, so that people on the rooftop are not affected by the rotor downwash. Typically, this distance is of the order of two rotor diameters. Hence, the cable length for the rescue mission from rooftops was deemed to be 120 feet. During window rescue operations, the ARK should be capable of reaching windows at any floor of the building. Typically, for a high-rise of 100 stories, the biggest cable length that might be necessary is about 1,000 feet. Thus, it was decided to have cables of different lengths varying from, 200 feet to 1,000 feet, available.

When the underslung pod is fully loaded - with 40 people and an operator - the ratio of the underslung mass to the helicopter is 0.75. In order to maintain the dynamic coupling between the two bodies at a minimum, it was deemed necessary that the point of suspension for each body pass through their respective center of gravities. This effectively, ruled out the possibility of two and four-point suspensions. A long cable lengths, along with single point suspension is beneficial in reducing the frequency of oscillations as shown by Szustak (Ref. 8), and Gabel and Wilson (Ref. 9).

3.5.5 The Shrouded Thrusting Fans

Operation in urban canyon requires that the underslung pod have sufficient maneuverability to prevent collision with nearby building faces. This is also desirable during rescue missions on congested rooftop, where the pod has to perform maneuvers to land on a clear spot. During occupant extraction through windows, maneuvering the pod is required to dock the pod precisely with the window, for easy ingress of the occupants. Moreover, during forward flight or hover, aerodynamic disturbances can cause the pod to deviate from the original position relative to the helicopter. It is necessary to control these deviations for precise control of the pod. Thus, it was decided to have thrusting fans on the pod, for increasing the maneuverability of the ARK. This has the added benefit that the thrust can be used to keep the pod pushed against the window and prevent the pod from losing contact with the building during occupant rescue. The aforementioned requirements can be satisfied by three bidirectional thrusting fans. One fan placed atop the structural lattice (Fig. 3.4) provides longitudinal thrust control, while two fans (Fig. 3.4) provide both lateral as well as yaw control. The fans are shrouded to enhance the safety, and protect the system from stray objects or debris.

The most critical requirement for yaw control of the pod is damping oscillations that might setup during flight, as it can adversely affect the handling quality of the helicopter – see Sec. 3.5.7. A rudimentary analysis shows that for a two-body system connected by a 750 feet kevlar cable, the frequency of oscillation for the yaw mode of the underslung pod is of the order of 255 seconds. Typically, it has been observed (Ref. 8) that such oscillations in yaw, when setup,

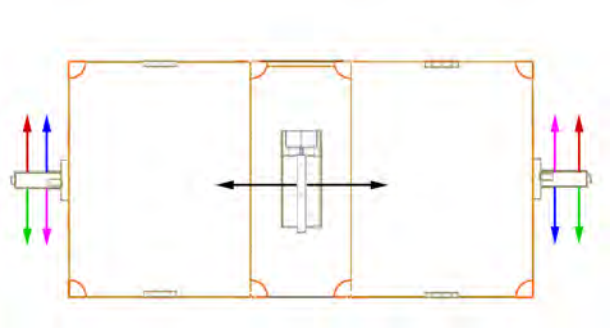

Figure 3.4: Schematic showing the three fans

do not damp out and the amplitude increases with time. It was found that this oscillation is critically damped with two bidirectional thrusting fans on either side of the box providing 55 lbs of thrust each – see Table 3.5.5 for further details. For pure yaw control, the fans thrust equally but in opposite directions (shown with blue arrows), while they provide pure lateral control when thrusting equally in the same direction (shown with green arrows).

	Units	Top Fan	Side Fans
Fan radius	ft	2	1.5
Chord	ft	0.21	0.16
Number of blades		3	3
Power	hp	30	9
Thrust produced	lbs	200	60

Forward flight with an underslung load could cause handling problems for the helicopter pilot for certain mass ratios, and cable lengths (Ref. 10). During forward flight, the underslung pod will tend to lag behind the helicopter because of aerodynamic forces acting on it. When the helicopter transitions from forward flight to hover while performing the rescue operation, the pod will tend to sway. This increases the time of the rescue operation as the pod cannot be landed on rooftop or docked to the building face, until the oscillations die down. Since, during the rescue missions, the distance traveled each trip is less than a mile, the speeds are low, and are of the order of 20-30 knots. At these forward speeds, the drag on the pod is 175 lbs. To reduce the angle of deviation of the cable from the vertical, and hence, the oscillation time, the fan needs to provide a thrust equal to the drag of the pod – see Table 3.5.5.

The ARK is equipped with a bi-directional three-bladed, thrusting longitudinally, shown with black arrows in Figure 3.4, placed atop the lattice frame. Each of the three fans consist of three blades, rotating at 4,000 RPM. Becasue the fans thrust in both direction, the blades have a symmetric NACA0012 airfoil cross-section. The thrust on the fans is controlled by changing the collective pitch of the blades.

3.5.6 Power Supply and Propulsion system for the ARK

One of the most critical components for the smooth working of the ARK, is a robust and reliable power supply system for the thrust fans and the avionics. A power cable coming down from the helicopter is not reliable as it is exposed to

the elements during flight, especially in cases of nearby fire and heat sources. Moreover, a low-loss power cable drawn from the helicopter power source would add to the payload weight, e.g. copper cables weigh 800 lbs per 1,000 feet. It was deemed preferable to have an on-board power supply for the ARK. Such efficient power supplies are in an experimental stage and are used in electric road vehicles. The AC-150 power system used in experimental electric cars, manufactured by AC Propulsion (Ref. 11), offers high performance and rapid convenient charging capabilities, thus making it ideal for the current purpose. The system includes a 3- phase AC induction motor, and an integrated power electronics unit that contains the AC motor controller, the controls and conditioning electronics for the onboard 20 kW charger, and a 100A, 13.5V DC power supply (Ref. 12). A battery pack of 28, 12V lead-acid cells provide a total power output of 16kW-hr for two hours without the need for intermediate recharges. The endurance of the system can easily be increased by adding more cells to the battery pack. The total weight of the system, for all the three fans is less than 100 lbs. The on-board charger accepts any normal line power, providing an endurance of 1 hour when charged for an hour through a 240V 50A power supply.

3.5.7 Flight Control System for ARK

For the smooth operation of the ARK in an urban canyon, a Flight Control System (FCS), similar to that on helicopters is required. Such an FCS should be capable of:

- Reducing the amplitude of oscillations arising out of aerodynamic and other disturbances.
- Maintaining the cable deflection from the vertical at a minimum, during forward flight.
- Controlling the orientation and position of the underslung pod during evacuation operations either on rooftops or through windows.

For this purpose, an FCS was designed for the ARK – see Fig. 3.5.7. The FCS on the pod maintains real-time data transfer with the helicopter FCS, through optic fiber cables running along the kevlar cable length. Based on the sensor data available on the ARK (see Sec. 3.5.8 for sensor details), the FCS adjusts the thrust of the fans to provide adequate damping to overcome the oscillations and stabilize the ARK. A similar strategy is adopted to minimize the cable angle relative to the vertical in forward flight. The positions and velocities of the helicopter are relayed to the ARK FCS. The relative position of the ARK with respect to the helicopter is then determined, and the FCS compensates for differences by controlling the thrust on the appropriate fans. In addition, controls are provided for the operator inside the ARK, with a much reduced authority, so that control can be achieved by simple translation commands.

3.5.8 Avionics and Operator Interface

The ARK is equipped with sensors for precise maneuvering within urban canyons. It is necessary for the pilot of the helicopter, as well as the operator in the ARK, to have the coordinates of the pod relative to the nearby building surfaces. To aid in safe landing, proximity sensors that measure the distance from the ground or rooftop on which the ARK is being landed, are installed on its underside. Moreover, a position and velocity sensor is needed to maneuver the pod safely in the urban canyon. For this purpose, a Microwave Doppler Radar (MDR) is installed on the sides of the module to measure the distance from the nearby building walls. This is particularly necessary when approaching

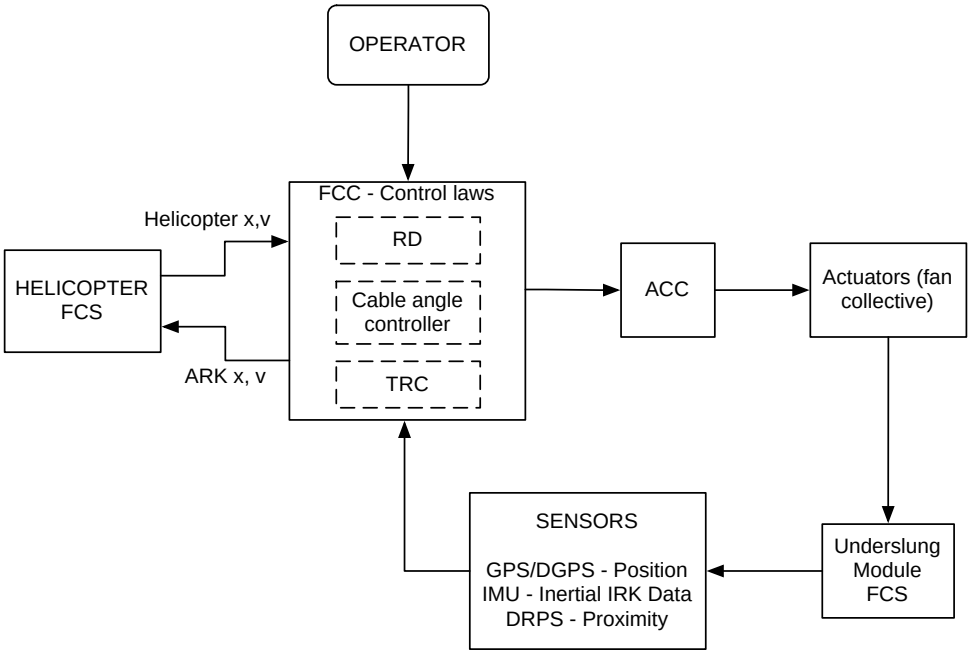

Figure 3.5: Flight Control System for the Aerial Rescue Kit

the building during window rescue. The ARK also has an infra-red camera (see Sec. 5.1) to provide the Command and Control module with a color thermal image of the building along with its occupants.

The Flight Control System (see Sec. 3.5.7) on the underslung pod requires the accurate position and velocity measurements to maintain the, RFP stipulated, 1 foot altitude and horizontal position hold. For this purpose a Crossbow AHRS400 (Ref. 13) inertial measurement unit, providing accurate pitch, roll and heading attitudes and rates, as well as three-axis linear accelerations is mounted on the rescue kit. This information can be coupled with corrected position and velocity measurements of a Trimble Force 5 GRAM-S GPS Receiver (Ref. 14), and fed to the FCS of the pod to control its position and to maintain the required position hold.

Since the ARK can position itself close to building faces, it is in a unique position to measure the environment around the disaster site. Hence, it is also equipped with infra-red sensor for creating a thermal map and other heat flux and chemical monitors (see Sec. 5.1 for more details).

The ARK is a semi-autonomous vehicle, and manual control is necessary only during landing on a rooftop or the ground, or when moving the ARK closer to a window for occupant extraction. The operator only has partial authority over the three thrust fans, and uses them for minor position and attitude adjustments when close to window, or when landing on congested rooftops. The operator controls the fans using a three-degree of freedom joystick, providing lateral, longitudinal and yaw control. This is augmented by another stick, for extended capabilities such as controlling the water cannon in case of aerial fire-fighting.

Table 3.4: Weight Breakdown for the ARK

Individual Components	Weight - lb	(kg)
Side Frame	180.7	(81.9)
Top Frame	86.0	(39.0)
Bottom Plates	333.1	(151.1)
Bottom Keel Beams	149.7	(68.0)
Top Thrust Fan Mount	75	(34.0)
Top Thrust Fan-Motor	170	(77.1)
Side Thrust Fan Mount	50	(22.7)
Side Thrust Fan-Motor	110	(49.9)
Power Supply	85	(38.5)
Doors	30.4	(13.8)
Landing Gear	236.3	(107.2)
Troop Seats	200.0	(90.7)
Skin	68.7	(31.2)
Cables	200	(90.7)
Fiber Optic Communication Cable	60	(27.2)
Avionics and Flight Control	50	(22.6)
Total	1727.3	(783.8)

3.6 Proposed Strategy for Occupant Extraction and Firefighter Deployment

A realistic scenario of the operational environment in the event of an urban disaster was presented in Sec. 1.2. The discussion gives a fair idea of the challenges involved in such operations and the precuations necessary for performing the mission successfully. Based on this information, a strategy can be developed to synchronise the different missions and perform them simultaneously.

3.6.1 Rooftop Rescue and Firefighter Deployment

In the proposed rooftop rescue procedure, the helicopter flies to the disaster site with the ARK, with the operators and fire-fighters in place. On approaching the building, the helicopter decelerates and hovers over the rooftop. Once the oscillations of the ARK are minimized, by the fans on the pod, the helicopter then descends vertically and lands the pod at an appropriate spot on the rooftop, as decided previously by command and control. The operator in the pod opens the two doors for people to enter. Once the people are seated, the helicopter ascends until the pod clears the rooftop antennas and other tall structures that might obstruct its flight path, and flies to the landing spot, also identified beforehand by command and control. The deployment of firefighting teams onto the rooftop also happens simultaneously. These missions use the same helicopter-module systems to minimize the resources needed for carrying out all missions. This is achieved by transporting firefighters onto the rooftop every alternate trip.

The number of helicopters required to carry out the RFP mission is a function of the distance of the safe landing

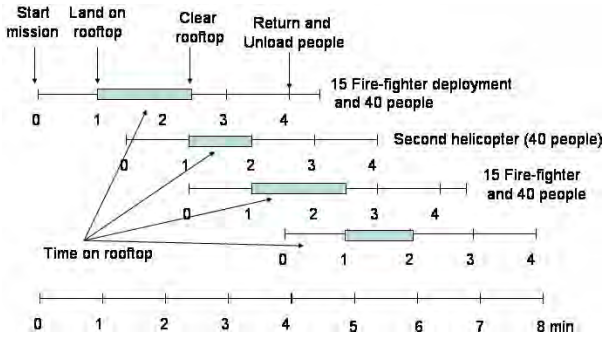

Figure 3.6: Time line for rooftop rescue and firefighter deployment.

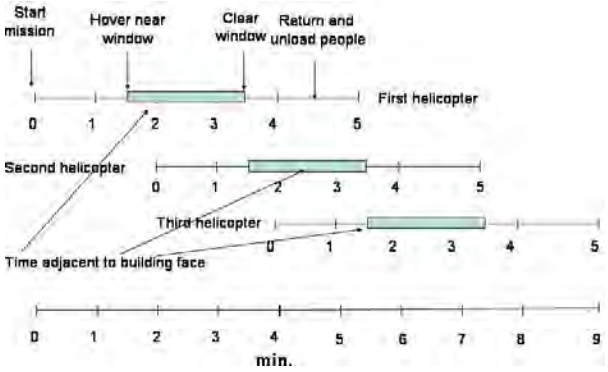

Figure 3.7: Time line for window rescue operation.

zones from the building and the height of the burning building. In the present scenario, the four landing zones identified were rooftops of buildings within a half mile radius of the high rise. In such a situation, it was found that a minimum of four helicopters were required to carry out both the missions simultaneously. The flight patterns of these helicopters have to be staggered in time to ensure that there is always one, and only one, helicopter hovering over the building at any given time. A schematic timeline explaining the procedure is shown in Fig. 3.6. Based on the timeline details, and the optimum payload per trip (discussed in Sec. 3.3.1), it is found that 160 people can be evacuated every cycle (each cycle consisting of four helicopters). The RFP requirement of 1200 persons per hour can be achieved in eight such cycles, spanning 44 minutes. The remaining time is sufficient to extract the firefighters deployed in the eight cycles. It must be understood that even though there is provision for deploying 15 firefighters in two minute cycles, deploying about 200 firemen onto a rooftop is not realistic. Firemen, typically, work in 15 minute shifts and in small groups. However, provision has been made for the two minute cycles to enable emergency evacuation of firefighters and force replenishment.

3.6.2 Window Penetration and Occupant Extraction

The window rescue module is required to rescue 800 people per hour from the windows of the building on fire. The window rescue mission is extremely critical and requires precise hovering of the helicopter at desired locations. The underslung rescue method avoids the operation of the helicopter near the building face, making it a viable and practical option. The helicopter approaches the building faces and hovers ensuring minimal safe distance of the ARK from the window designated for window evacuation. Now, the collective pitch of the side fans is modified to translate the ARK towards the window, while the thrust of the top fan is actively modified to align the ARK door to the window. The door of the ARK is then dropped inside the window. The thrust of the side fans ensures contact of the ARK to the building face, enabling faster ingress of the people. The helicopter is translated towards the building to a position vertically above the ARK to reduce thrust requirement of the side fans once people begin loading into the ARK. The pilot in the helicopter switches to the autopilot mode before people start loading to avoid pilot induced errors. Once 40 people sit down in the ARK, the door of the ARK is closed and the helicopter leaves the window and flies towards the safe landing site.

A time line for the window rescue mission is shown in Fig. 3.7. This time line is very similar to the one for rooftop rescue. It involves operation of 3 helicopters to comply with the RFP. Each rescue trip carrying 40 people takes 5 minutes. The sequencing of helicopter ensures evacuation of 120 people every 6.5 minutes after the first trip. This mission plan would require 45 minutes to rescue 800 people, leaving a spare time of 15 minutes. This spare time is sufficient to account for off design operation from the mission plan. Off design operation conditions include additional time required to adjust the position of the ARK relative to the window because of gusts and slow loading of passengers from windows. This mission assumes operation of only one helicopter for window rescue near the building at a time. This is a worst case scenario when window rescue is only possible on one face of the building. The mission would be much more effective and faster in less dire conditions.

3.7 Aerial Firefighting on Urban High Rise Buildings

Firefighting is an important aspect of an urban disaster response system. While ground based operations can effectively contain and even extinguish fires up to a height of about ten stories, they are quite ineffective on fires on higher floors. Helicopter based firefighting systems overcome this disadvantage and enable enagement of fires at any floor.

3.7.1 Self-Contained Tank Water Cannon Fire-Fighting

Choice of firefighting system

Fires are usually engaged by directing a stream of water from a spray nozzle at the core of the fire. The water provides a cooling effect that reduces the temperature of the fire below its flashpoint.[1] This reduction in temperature creates conditions more suitable for firefighters to target the fire from closer range, i.e, within the building. Conventional fire-combating techiques involve directing a continuous stream of water at the fire to extinguish it. However, recent tests suggest that the impulse spraying technique is more effective than continuous spraying (Ref. 15). The impulse nozzles shoot small amounts of water at very high velocities, during a short period of time. Under these conditions, the water breaks down into very fine droplets, increasing the net cooling surface area. The high velocities ensure that the fine droplets have enough kinetic energy to penetrate the fire ball. Typically, an impulse system requires only about 10% of the water required by conventional systems to achieve the same cooling effect (Ref. 15). The weight savings achieved using an impulse cannon system will allow the helicopter to operate 10 times longer for a given quantity of water, as compared to a conventional system. The impulse fire extinguishing system for this mission has been based on the system developed by Ifex Technologies,[2] that has been successfully demonstrated on the Kaman K-Max.

Equipment

Figure 3.8(a) shows the self-contained tank firefighting mission kit mounted on the helicopter. There are two identical impulse water cannons, each capable of firing loads of 25 litres of water per impulse shot, installed in a rigid aluminum framework that incorporates all the valves, and control equipment. The impulse cannon consists of a power chamber and a water barrel separated by a high-performance quick opening valve. The power chamber is pressurized using

[1] The lowest temperature at which the vapour of a combustible liquid ignites momentarily in air.
[2] IFEX GmbH : 18 Hansestrasse, Sittensen D-27419, Germany

25 bar compressed air from a pneumatic system consisting of a diesel motor driven air compressor with a large high pressure buffer tank, air pressure regulators, and piping. The water chamber is recharged from an 800 gallon carbon fibre water tank and a 40 gallon additive tank, mounted rigidly on the floor of the fuselage. The water tank is equipped with baffles to prevent sloshing of the fluid, a venting system that allows fast refuelling, an inspection cover and a water level sensor. The water and agent are mixed and pumped to the impulse cannons through 3 inch diameter pipes by dual electrically powered water pumps. It takes each impulse cannon less than 5 seconds to reload the water after firing, which means that the maximum combined firing rate of the system is about 160 gallons per minute. The impulse unit is capable of firing 121 impulse shots on a full 800 gallon tank of water, which allows the system can operate for a minimum of 5 minutes without refilling the water tank.

In addition to the impulse system, there is a water cannon fitted with a high capacity continuously operating nozzle capable of firing water at flow rates from 300 to 2,000 GPM, which is not utilized in this mission. The three water cannons are mounted on a pneumatic tilt mechanism that allows them to be tilted 90 degrees from the horizontal. This tilt mechanism is fitted with an automatic recoil reduction system that minimizes the impulse reaction forces. Aiming of the cannon at the fire is accomplished by an infrared sensor, which detects the portion of the targeted region where the temperature is maximum and a video camera, which provides a visual tool for aiming and monitoring. A micro-processor based control unit adjusts the tilt of the cannon automatically, using the inputs from the aiming mechanism to accurately target the fire, with programmed compensation for the downwash of the rotor and the range. The control input in the cockpit consist of a joystick, which controls the aiming and firing of the cannons. The control system also allows the operator to program the system to aim and target the fire at a particular frequency.

A ‘hover snorkel’ mechanism consisting of a 20 foot long flexible water hose of 3 inch diameter with a submersible electric water pump mounted at the end allows the tanks to be refilled in 54 seconds from standing water sources or from water supplies in adjacent buildings. The control unit controls all aspects of the firefighting system including refilling the water tank, recharging and operation of the impulse cannons and water/additive mixing ratio.

When the system needs to target a fire located in an urban canyon, this firefighting system is mounted inside the underslung box (ARK) used for the rooftop and window rescue case, as illustrated in Fig. 3.8 (b). The water carrying capacity of the system is slightly reduced for this case as the helicopter will have to provide lift for the ARK as well. There are two water tanks with a total capacity of 700 gallons. The belly mounted frame containing the remaining components, is attached to the floor of the ARK. Because the frame is a bit longer than the box, the cannons will protrude through the doors on one end. The hover snorkel is attached to the frame through a cut-out on the floor of the box.

Installation

The water tank slides in through the cabin door by means of guide rails mounted on the cabin floor, and is bolted to the bulkheads on either end of the doors. The rest of the components are mounted to the belly of the fuselage using two rear mounting points and one preloaded mounting point at the middle of the nose landing gear. The preloading prevents vibration of the setup and also provides easy jettisoning of the unit. The total time required for installation on the helicopter is 12 minutes. When the system is mounted on the ARK, the system is installed on the floor of the box. The total time required for installation on the ARK is 17 minutes.

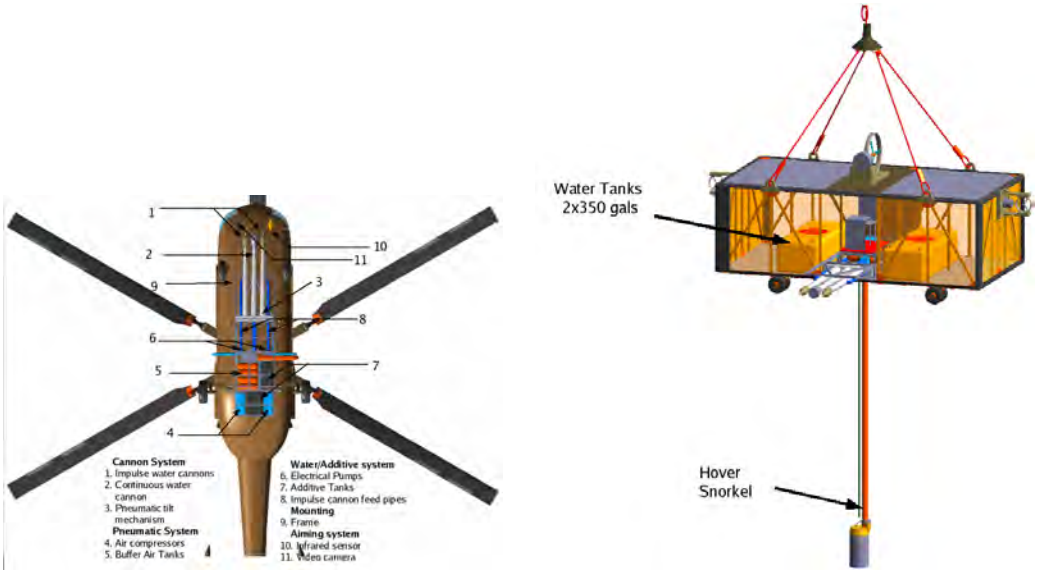

(a) Helicopter Mounted

(b) ARK mounted

Figure 3.8: Self Contained Tank Firefighting Mission Kit

3.7.2 Ground Pump Water Cannon Firefighting

This subsystem enables the system to lift 5 inch diameter water hose upto a minimum of 100 stories, which corresponds to a height of 1,200 feet. Because the RFP calls for a flow rate of 1,500 gallons per minute in this mission, a continuously spraying nozzle is used in addition to the impulse nozzles, which have a combined maximum flow rate of 160 gallons per minute. This nozzle is an automatic, remotely electically controlled Monsoon® fire fighting nozzle (Ref. 16) that can spray the water in a jet, with a maximum range of about 200 feet. This nozzle has a flow range from 300 to 2,000 GPM and is mounted on the same tilting mechanism as the impulse nozzles of the self-contained system, which allows it to tilt upto 90 degrees from the horizontal.

This mission shares a lot of the components used by the self-contained firefighting mission such as the frame, two impulse water cannons, the continuous water cannon, the pneumatic tilt mechanism, hover snorkel and the control unit. This system also has the following additional components, as shown in Fig. 3.9(a). There is 200 feet of 5 inch diameter fire hose attached using a quick disconnect coupling, which allows jettisoning of the hose if necessary. The three-way inlet that splits the flow between the impulse nozzles and the continuous nozzle. The two outlets that feed the impulse nozzles have automatic valves that open when the nozzles need to be refilled with water. These valves also regulate the pressure and the flow rate within acceptable limits.

When this system is to be operated in a urban canyon, the unit is mounted inside the ARK, as shown in Fig. 3.9(b). However, there is no modification to the kit whether it is mounted in the ARK or directly on the helicopter. The frame is directly fixed to the floor of the box and the hose is connected through a cutout in the floor.

The equipment required at the ground level are:

Table 3.5: Self-Contained System Specifications

Water/Agent Capacity per Impulse Shot	25 litres - each cannon
Velocity at Cannon Outlet Muzzle	400 feet per second
Valve Opening and Closing time	50 milliseconds
Peak Recoil Reduction System	Automatic - Pneumatic
Impulse Shot Throw Distance	Horizontal - 200 ft, 45° through Vertical - 250 ft
Mean Droplet size	100 micron
Time of Recharge and Refilling	5 seconds
Compressed Air Supply	Two 300 bar 5.5 hp diesel 4 stroke compressors
Air Buffer Tanks	4 x 20 litre 300 bar
Fuselage Mounted Water Tank	Carbon Fibre, 350 lbs, 800 gallons, 6'×4.5'×4'
Underslung Box Mounted Water Tanks	Carbon Fibre, 325 lbs, 2×350 gallon, 8'×2.25'×3'
Additive tanks	40 gallons
Hover snorkel pump	Submersible electric pump 15 hp @ 400 Hz 230 V
Hover snorkel hose	3 inch diameter hose, 20 feet long
Water Supply to Cannon	2×2 hp Dual Electric Impeller Pumps
Total Empty Weight of Helicopter-Mounted System	1060 lbs
Total Weight of Helicopter-Mounted System	7810 lbs
Total Empty Weight of Underslung System	2990 lbs
Total Weight of Underslung System	8812 lbs

- Ground water pump capable of pumping water and/or additives at a flow rate of 1,500 gallons per minute at a pressure of 900 psi
- Ground water hose of the required length, capable of sustaining a pressure of 900 psi at the base

To attach the subsystem to the ground pump, the helicopter hovers vertically above the ground pump unit at a height of 200 feet with 200 feet of suspended air hose. The ground personnel connect the ground hose to the air hose by means of a quick connect coupling. The helicopter then climbs to the required height, and assumes the attitude for nozzle operation. The ground pump then starts pumping the water at the required pressure to operate the system.

The pump pressure required is a sum of elevation head, friction losses, dynamic head and nozzle pressure. The maximum pressure required is 900 psi to pump to 100 stories at 1500 GPM. To achieve such a high pressure, ground based pumps need to be upgraded to handle this capacity . The heavy duty fire hoses that are available today are rated for a burst pressure of about 1,200 psi and a proof pressure of 600 psi[3]. Although the margin of safety will be low, the required pressure is still within the allowable burst pressure. In order to increase the margin of safety, it would be recommended to use a pump mounted on an adjacent rooftop, if available, for cases when the required pressure exceeds 600 psi (i.e, when the height of fire is above 900 feet).

Operation of the continuous water cannon causes a nozzle reaction force of 760 lbs when the flow rate is 1,500

[3]NFPA Standards

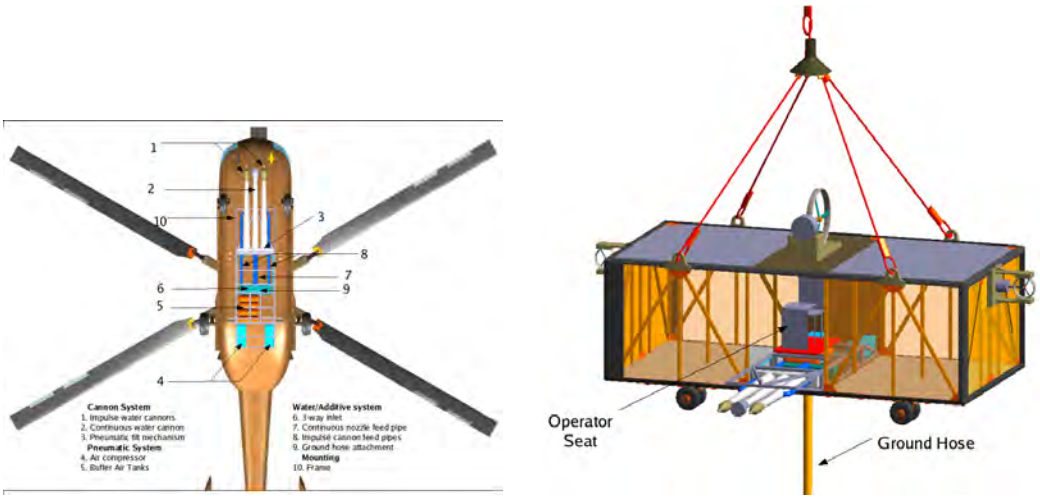

(a) Helicopter mounted

(b) ARK mounted

Figure 3.9: Ground pump water cannon firefighting mission kit

gallons per minute. The installation of this system, both on the helicopter and on the ARK is similar to the installation described in Sec. 3.7.1. The total time needed for installation on the helicopter is 12 minutes, and it is 15 minutes for installation on the ARK.

3.8 Proposed Strategy for Aerial Firefighting

3.8.1 Self-Contained Tank Water Cannon Firefighting

This mission requires a fire fighting system with directable nozzles that are capable of precisely aiming a stream of water from a self-contained water tank, at a fire at any floor. Because the source of water is limited, the water tank needs to be refilled at regular intervals, either from standing water sources or water supplies of adjacent buildings. The helicopter, equipped with the hover snorkel, is capable of refilling the water tank in 54 seconds. For this, the system needs to fly from the disaster site to the nearest standing water source, such as a lake, pond or the sea, or to the rooftop of an adjacent building, refill the tank and return to the firefighting operation.

The mission plan for execution of the mission depends on the height of the floor at which the fire is located and the space available between the building on fire and adjacent buildings. Fig. 3.10 explains the several situations that were studied and appropriate stragies to encounter them.

Figure 3.10(a) shows how the system would tackle a fire when there is enough space for the helicopter to hover level with the fire. When the fire is located in an urban canyon or in a highly smoke-filled environment, the firefighting system is placed inside the underslung box (ARK) used for the rooftop and window rescue missions. The helicopter descends to a height such that the ARK is level with the fire, as shown in Fig 3.10(b), and operates the fan thrusters on side of the box to hold the box stationary while the cannons are being operated. Inability of the fans to provide

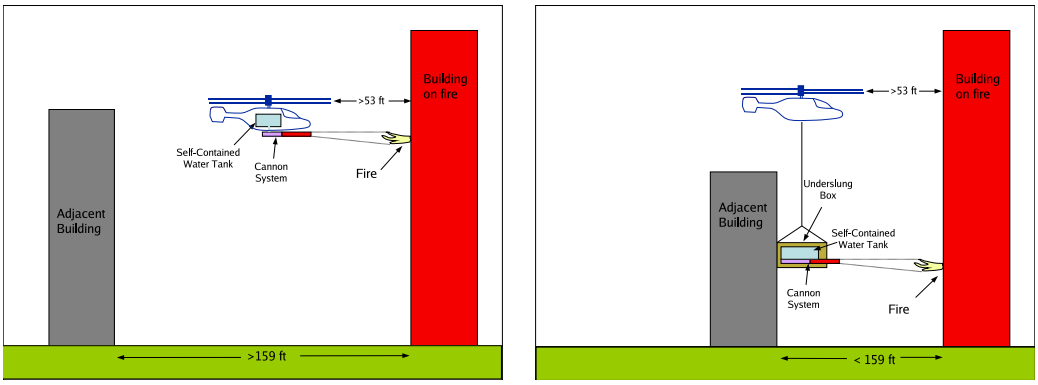

Figure 3.10: Self Contained Tank Firefighting Scenarios

sufficient thrust to counteract nozzle reaction forces limits the nozzle flow rates to lower values.

The timeline for operating this mission is explained in Fig 3.11. The helicopter flies in from the base with the mission kit, including the self-contained tank and the hover snorkel, and descends to the height of the fire, which in this case is assumed to be on the 30th floor. The helicopter hovers and operates the cannons until the tank is exhausted and then climbs to the cruise height of 1,200 feet. The helicopter then cruises to a water source, which is assumed to be 2 miles away, and descends to a height of 20 feet, where it refills the water tank in about 1 minute. The system then climbs to the cruise height and returns to disaster site. As the time taken for the refuelling stage is approximately the same as the time taken for the firefighting stage, two helicopters are needed to perform this mission continuously.

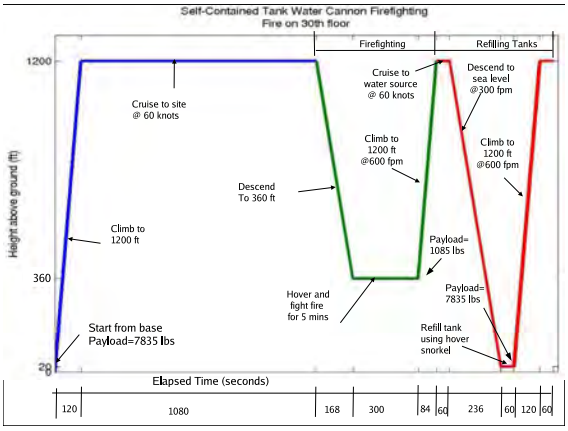

Figure 3.11: Timeline for operation of self-Contained tank firefighting mission

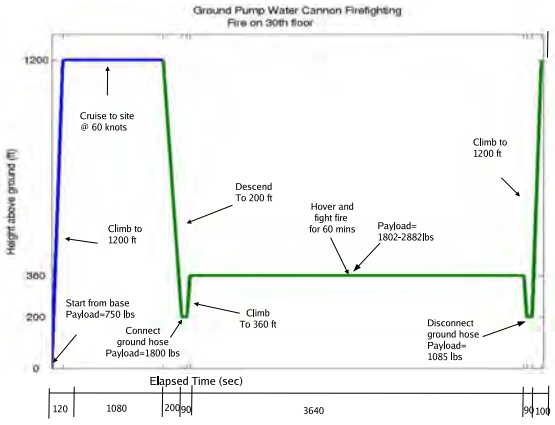

Figure 3.12: Timeline for operation of ground pump firefighting mission

3.8.2 Ground Pump Water Cannon Firefighting

This mission is similar to the self-contained tank firefighting mission, except that the source of water is from a pump, located on the ground or an adjacent building, which could pump water to the firefighting system at 1,500 gallons

per minute, to a maximum of 100 stories. The helicopter acts as a crane for lifting a 5 inch hose, which connects the ground based pump to the water cannons on the helicopter.

As in the self-contained firefighting mission, the strategy required to execute this mission depends on the height of the floor at which the fire is located and the space available between the building on fire and adjacent buildings. Several situations were studied and appropriate stragies to encounter them are shown in Fig. 3.13.

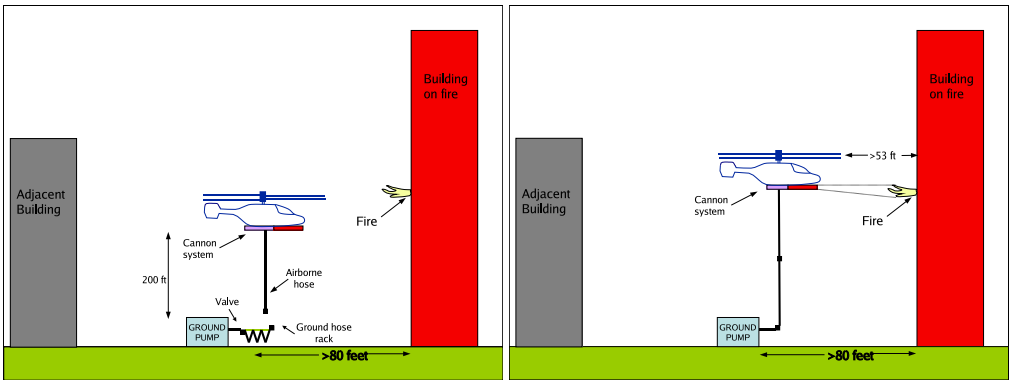

(a) Hose Attachment

(b) Firefighting

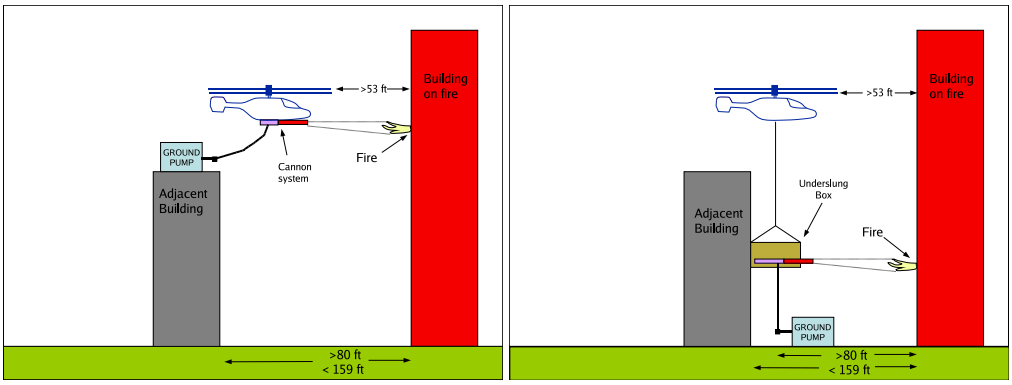

(c) Pump on Adjacent Building

(d) Underslung box

Figure 3.13: Ground pump water cannon firefighting scenarios

The first case, as shown in Fig. 3.13(a), is the simple scenario, when the fire is on a building face which is more than 3 rotor diameters away from the adjacent building or any vertical structures. The helicopter will have a separation of 1 rotor diameter from the building walls and can operate safely. Here, the helicopter descends with an installed firefighting system, the ground based hose is connected, the helicopter rises to the floor on fire and directs the nozzle into the fire. The next two cases illustrate a situation where the fire occurs on a building face that is less than 3 rotor diameters away from adjacent faces. As shown in Fig. 3.13(c), if the fire occurs on a floor that is higher than the adjacent building, it would be safe for the helicopter to engage the fire. However, it is not recommended to operate

within the urban canyon to have the hose connected. To solve this problem, it would be preferable to have the system connected to a pump system located on an adjacent rooftop. This would also reduce the pumping pressure required to be handled by the pump and the hose. Figure 3.13(d) shows a scenario when the fire is itself located in the urban canyon. To avoid operating the helicopter within the urban canyon, the firefighting system is placed inside the ARK. This allows the helicopter to lower the box to the required height and have the ground hose connected as described earlier in Sec. 3.8.1. The helicopter then climbs to a height such that the box is level with the fire and operates the nozzles in a similar fashion to the self-contained firefighting mission.

Figure 3.12 explains the timeline for this mission, for a case where the fire is on the 30th floor. The helicopter flies in from the base, which is 20 nm away and descends to a height of 200 ft with 200 feet of suspended airborne hose to have the ground hose connected. It then climbs to the 30th floor and operates the nozzle for 1 hour after the hose is turned on. After 1 hour, the hose is turned off and then, the helicopter waits for the water to drain from the hose and descends to 200 feet, to have the ground hose disconnected. The helicopter then climbs to the cruise height of 1,200 feet and flies back to the base. Only one helicopter is needed for this mission as it is capable of operating continuously for more than 1 hour.

3.9 A Day in Life of System Description

The fire station, equipped with the systems to carry out rescue operations, must be prepared to respond to emergency situations at all times. Some regular operations would be required to be performed to ensure immediate resopnse. The subsystems required for such rescue operations are designed to be simple, enabling fast assembly. The need for the command and control helicopter is most imminent in an emergency situation, so it should always be fueled and prepared to fly to the disaster site after sufficient warm up. Other operations required to be performed on a regular basis for immediate response are regular charging of battery pack in the Aerial Rescue Kit, ensuring proper functioning of water cannon and most importantly, the maintenance of the helicopters.

In the event of an emergency, the command and control helicopter is flown to the disaster site after 10 minutes warm up of engines. Helicopters for rooftop and window rescue also begin to warm up, once the information regarding the severity of the disaster is relayed by the ground based firefighting systems. command and control develops a mission plan, which involve, finding safe landing sites for window and rooftop module, and ensuring availablity of water for the firefighting module. The Aerial Rescue Kit and firefighting kits are assembled appropriately for the missions requirements, simultaneously. The rescue helicopers, equipped with rescue and fire fighting kits, fly to the disaster site. command and control monitors the operation of other rescue helicopters, once they reach the disaster site, for safe, effective and organised rescue mission. The time line for the entire mission is shown in Foldout 3.14. The figure shows that the rescue helicopters begin to perform their respective mission 10 minutes after command and control reaches the disaster site. The rescue modules performing window rescue fly to the disaster with 120 feet cables, in order to reduce the drag on the vehicle in forward flight, and improve maneuverability in urban canyons. The length of the cable is modified as per the requirement of the mission. The rooftop rescue systems also deploy firemen on to the rooftop of the burning building. The tasks performed by vairous helicopters are clearly shown in Foldout 3.14.

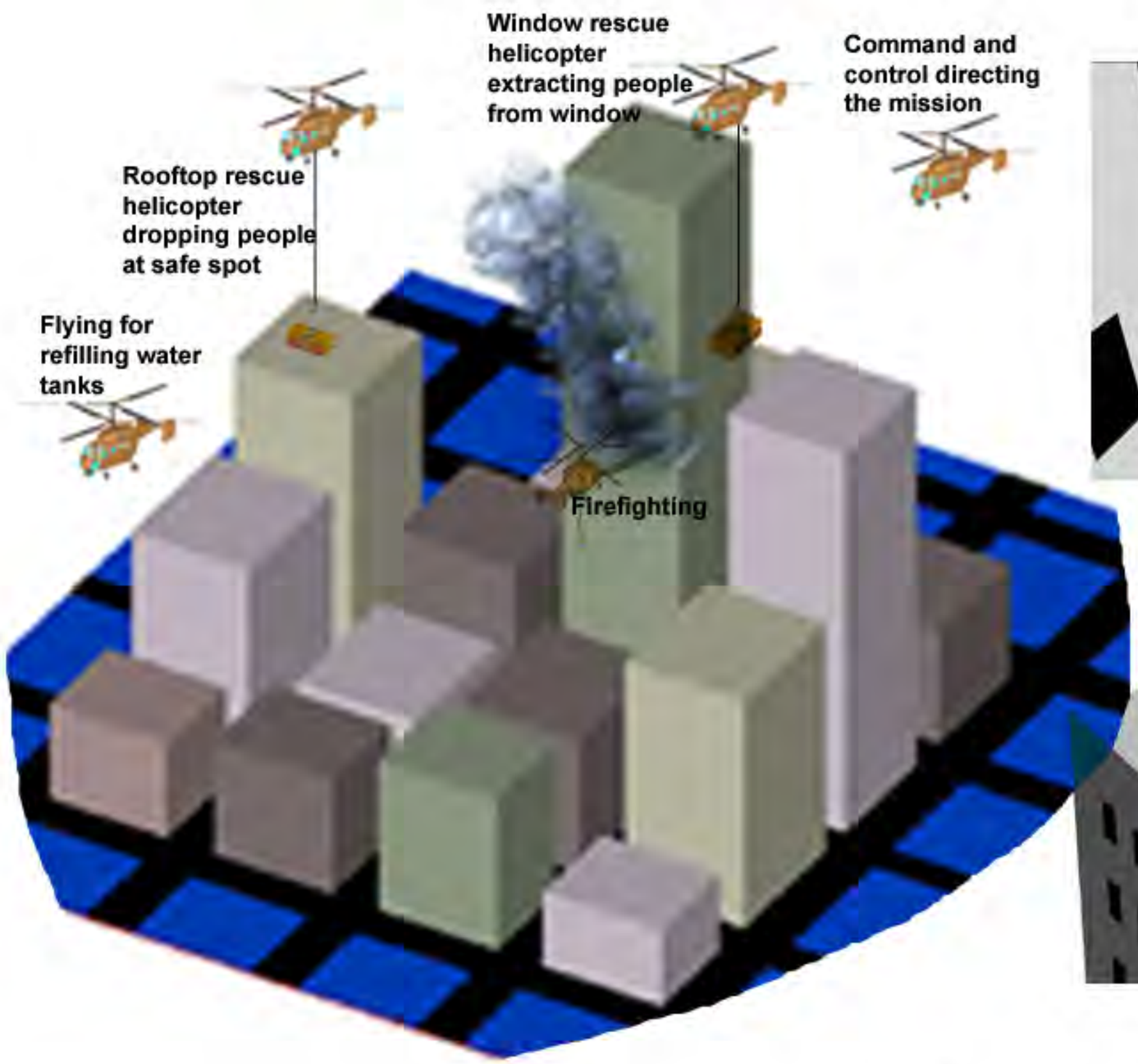

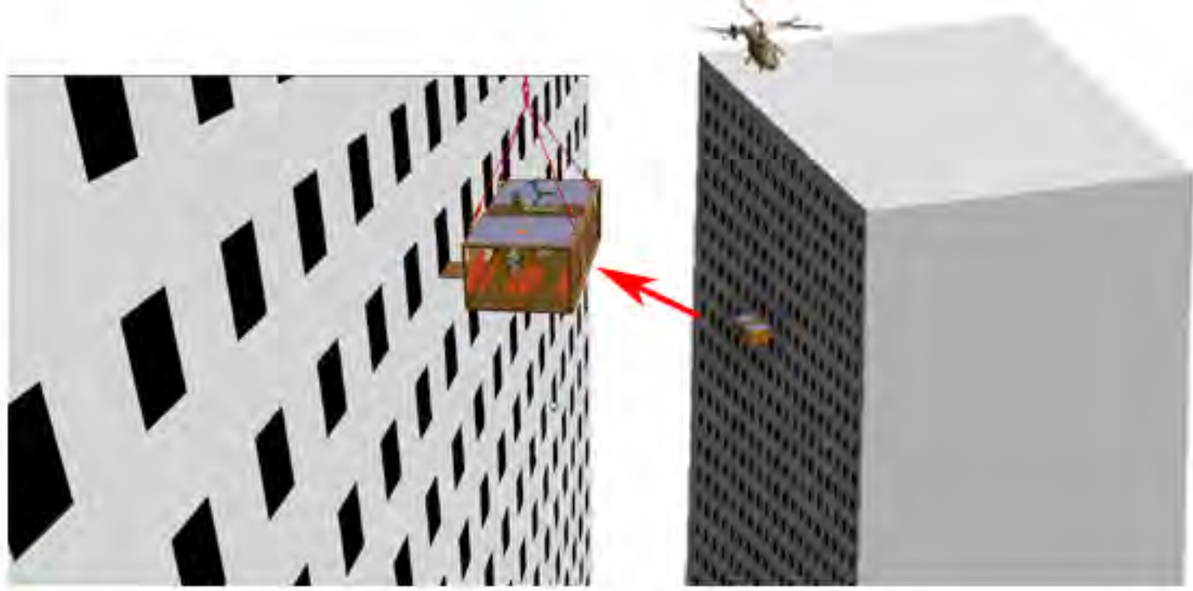

Window rescue

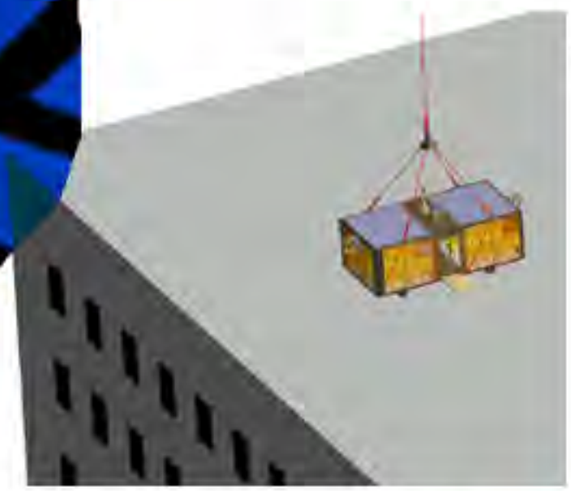

Rooftop rescue

Self contained Firefighting

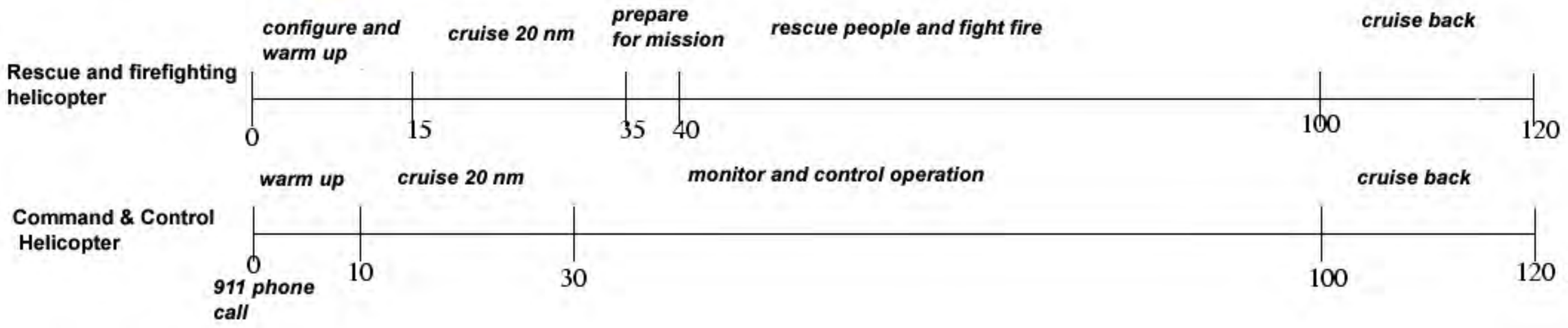

4 Details of Primary Vehicle Design

4.1 Design of the Rotor System

The Aeneas features a state-of-the-art swashplateless, co-axial rotor system. The co-axial design eliminates the need for a tail rotor, thereby reducing the overall size and complexity. The use of trailing edge flaps for primary control eliminates the need for swashplates and complex mechanical linkages at the hub, which results in an aerodynamically clean and mechanically simple hub design. In addition, fewer moving parts reduces maintenance costs. This section elucidates the design of the baseline rotor, the structural design of the blade, the trailing edge flaps, and the state-of-the-art piezoelectric-hydraulic hybrid compact actuators.

4.1.1 Baseline Rotor

The baseline rotor is a rotor with conventional swashplate and no trailing edge flaps, which is used for the preliminary design. The rotor diameter, airfoil section, tip speed, solidity and twist of the baseline, co-axial main rotor were designed to achieve good hover and low-speed forward flight performance. During the preliminary design process, the aerodynamic analysis of the co-axial rotor was conducted using an equivalent single rotor model with 3 blades, but having the same solidity as the co-axial rotor (Ref. 17). For the dynamic analysis, a detailed modeling of co-axial rotors was carried out. The final main rotor design was a compromise between various conflicting requirements such as compactness, low downwash and low induced power requirements, a light rotor hub system, good autorotational characteristics, and low noise. The important parameters of the main rotor are discussed in the following subsections.

Rotor Diameter

The need to hover and maneuver between close buildings in urban canyons requires a compact vehicle. Therefore, minimizing the rotor diameter was a key objective. Small diameter rotors also result in lighter hubs and lower drag. However, decreasing the diameter of the rotor results in an increase in the rotor downwash and induced power requirements as well as a degradation of autorotational characteristics. This requirement is less critical, as the three engine configuration (Sec. 4.4) can provide enough hovering power in One Engine Inoperative (OEI) condition. Based on the maximum take-off weight requirements and the disk loading obtained from the blade loading and solidity considerations, the rotor diameter was determined to be 52.35 ft.

Blade Loading and Solidity

The blade loading is a critical parameter that affects the blade stall limits. In low-speed forward flight regimes, rotors can be designed to have a high blade loading while staying within the stall limit. A moderate blade loading, $C_T/\sigma = 0.1$ was chosen for the main rotor in the present design. This corresponds to a disk loading of 10.68 lb/ft^2, an average of 5.34 lb/ft^2 per rotor. A moderate blade loading of 0.1 ensures that the rotor solidity and diameter can be minimized for a given Gross Take Off Weight (GTOW).

A three-bladed rotor design appears more suited for a co-axial configuration. With the number of blades fixed, solidity can be lowered by increasing the blade aspect ratio. Because the blade loading (C_T/σ) is fixed, a decrease

Table 4.1: Main rotor dimensions.

Parameter	Units	Value
No. of Blades	—	2×3
Diameter (each rotor)	ft	52.35
Chord (each rotor)	ft	1.45
Disk loading (each rotor)	lb/ft^2	5.34
Solidity (each rotor)	—	0.053
Twist (linear)	deg	-12°
Airfoil section	—	SC1094-R8
Root cut out	%	20
Tip speed	ft/s	722

in solidity would result in an increase in rotor diameter. A blade aspect ratio of 18 was chosen in the present design, which translates into an acceptable rotor radius, while still ensuring that $C_T/\sigma = 0.1$. The final solidity of the each individual rotor was 0.053, and the equivalent single rotor solidity was 0.106.

Tip Speed

Compressibility and rotor noise issues are less critical during hover and low-speed forward flight operations, permitting a high tip speed. This also reduces the rotor torque requirement, allowing for a lighter transmission system. However, the choice of very high tip speeds, can result in noise even at low-speed forward flight, which should be avoided as Aeneas operates primarily in densely populated civilian areas. Therefore, nominal tip speed of 722 ft/s was chosen.

Airfoil Section

For this helicopter, forward speed requirements were modest ($\mu < 0.2$) and compressibility effects on the advancing blade tip and retreating blade stall were not critical. Therefore, it was not necessary to use different airfoil sections at the root, middle and tip of the blade. A single airfoil section (SC1094-R8) was used throughout the entire blade span.

Twist

Blade twist can be employed to improve hover performance, delay retreating blade stall and reduce vibrations in forward flight. However, large twist can degrade autorotational performance. The optimum twist was determined using Blade Element Momentum Theory (BEMT) by minimizing the induced power factor during hovering flight. While a range of linear twists resulted in low induced power factor for hover, a linear twist of -12° was selected to optimize the hover performance without causing a significant degradation in autorotational characteristics.
The parameters of the main rotor are summarized in Table 4.1.

4.1.2 Swashplateless Primary Control Mechanism

The benefits of the swashplateless rotor concept for the current co-axial design were examined and are discussed below. Elimination of the swashplates and the complex linkages makes the co-axial rotor light, mechanically simple and aerodynamically clean, thereby enabling easy maintenance, improved performance, increased payload ratio and decreased maintenance costs.

Weight penalty – A conventional co-axial rotor system requires two swashplates, hydraulic system and multiple linkages, which result in a heavy hub. The on-blade actuators, controllers, slip ring units, pitch springs and pitch spring supports used in the swashplateless system are considerably lighter, resulting in significant weight saving for the helicopter.

Mechanical complexity – Conventional co-axial rotor system requires a minimum of three linkages to maintain the lower and higher swashplates in the same orientation. Additional linkages are necessary to apply differential collective for yaw control in co-axial configurations. Individual control of the blades using trailing edge flaps achieves these results with less mechanical complexity, which lowers maintenance costs.

Drag penalty – The swashplates and the mechanical linkages increase hub drag. Swashplateless hubs are aerodynamically cleaner than conventional hubs.

Vibration control – The trailing edge flaps used in swashplateless technology can also be used for vibration control.

Recently, several studies have been conducted, to explore the feasibility of using an embedded trailing edge flap for primary control (Ref. 18). Recent improvements in the smart materials technology (Ref. 19) and successful testing of smart actuators in model rotors (Ref. 20, 21) have established the feasibility of using actuated trailing edge flaps for primary control and vibration reduction. These factors have contributed to the feasibility of the swashplateless rotor technology.

Study of Alternate Swashplateless Rotor Control Concepts

The suitability of various potential rotor control concepts were studied to evaluate the best design solution. A preliminary analysis of these other concepts demonstrated that they are not well suited for primary control and were, therefore, eliminated. The alternative concepts explored were blade camber control, blade twist control, individual blade pitch control and shaft tilt concepts. Sufficient change in camber or twist, required for primary control, cannot be obtained with the stroke available from existing smart materials. Individual blade pitch control needs actuators and pitch link for each blade resulting in greater complexity, hub mass and higher drag. Since the complete blade is actuated, it requires a large actuation power in comparison to actuation of the plain trailing edge flap. The actuation forces and stroke for tilting rotor shafts are enormous, and require complex and heavy actuation mechanisms.

The deflections and hinge moments required for the use of plain trailing edge flaps for primary controls can be met with existing smart structures technology. The selection and design of the trailing edge flap is discussed in detail in the following subsections.

Trailing Edge Flaps vs. Servo flaps

Servo flaps are auxiliary airfoil sections located aft of the blade trailing edge and can be used for primary control. This technology is being currently employed by Kaman for controlling the K-Max. Kaman also has an ongoing research program to use trailing edge flaps for primary control (Ref. 22), that are integrated into the main lifting section of the blade. This configuration produces less drag as compared to servo flaps. Further, the plain trailing edge flaps require shorter linkages and are, therefore, better suited for actuation using smart materials embedded in the blade. Short actuators reduce the aft movement of the blade center of gravity. In light of the aforementioned advantages, plain trailing edge flaps were chosen over servo flaps in the present design.

Lift Flaps vs. Moment Flaps

Flaps located on a torsionally stiff blade (say torsional frequency > 3/rev), which form a large percentage of the blade chord ($> 35\%$), function primarily as lift flaps. A downward deflection of the flap (taken as positive) increases the effective camber of the section and produces an increase in sectional lift and nose down pitching moment. Because the blade is torsionally stiff and the moment produced on the main blade is low, the nose down twist produced on the blade is relatively small. The change in lift of the rotor is primarily because of the lift produced by the flap.

Moment flaps form a small percentage of the blade chord ($< 25\%$) and are used on torsionally soft blades (torsional frequency < 2/rev). The change in pitching moment causes the torsionally soft blade to twist elastically, thereby controlling the lift of the entire blade. Because they are relatively small and very effective in twisting the whole blade, moment flaps require small hinge moments and deflections. This reduces the force and stroke required from the smart actuators. Hence, moment flaps were chosen for the current rotor design.

4.1.3 Sizing and Location of Moment Flaps

The key parameters influencing the performance of trailing edge flaps are the blade torsional frequency, indexing angle, flap span, flap chord, the spanwise location of flap, and the location of flap hinge (Ref. 23, 22). The selection of these parameters is discussed in detail below. Optimization of the size and location of the flap was performed using the University of Maryland Advanced Rotorcraft Code (UMARC) (Ref. 24), incorporating trailing edge flaps (Ref. 18).

Torsional frequency – Low torsional stiffness decreases the trailing edge flap deflection and hinge moment, which in turn reduces the actuation requirement. However, blades with low torsional frequency (< 1.7/rev) are prone to aeroelastic instabilities. Torsional frequencies close to 2/rev lead to resonance and were avoided, whereas torsional frequencies well in excess of 2/rev require relatively large flap actuation requirements. A torsional frequency of 1.79/rev was chosen for the current design.

Indexing angle – A pre-collective is provided at the blade root using an indexing splice. This collective indexing of the blade reduces the flap deflection requirements during normal flight operation. The optimum collective angle was determined by examining the flap deflection requirements for a series of indexing angles. A large index angle not only reduces the collective requirement enormously, but also provides beneficial lift. Also, the cyclic requirement is reduced with increasing index angle. Increasing the indexing angle results in higher lift. Therefore, when the indexing angle is increased beyond the optimum value, higher collective flap deflection

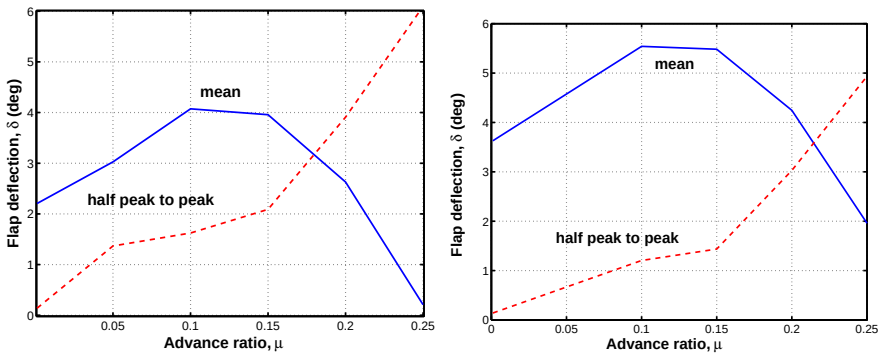

(a) Indexing angle=20° (b) Indexing angle=22°

Figure 4.1: The collective and cyclic trailing edge flap deflections required as a function of advance ratio for indexing angles of 20°, and 22°

is necessary to produce a nose-down twist of the blades. Hence, the choice of the indexing angle is a tradeoff between reducing the mean and collective flap deflections. To demonstrate the effect of indexing angle, the collective and cyclic deflection requirements for different indexing angles are shown in Fig. 4.1. A 20° indexing angle requires a 4° cyclic deflection at the maximum advance ratio of the Aeneas helicopter ($\mu = 0.2$), while requiring a mean deflection of 2.75°. Increasing the indexing angle to 22° reduces the corresponding cyclic deflection to 3° but increases the maximum collective requirement to 4.25°. The optimum collective indexing angle of 20° is chosen as it minimizes the total flap (mean+cyclic) deflection requirements (Fig. 4.1).

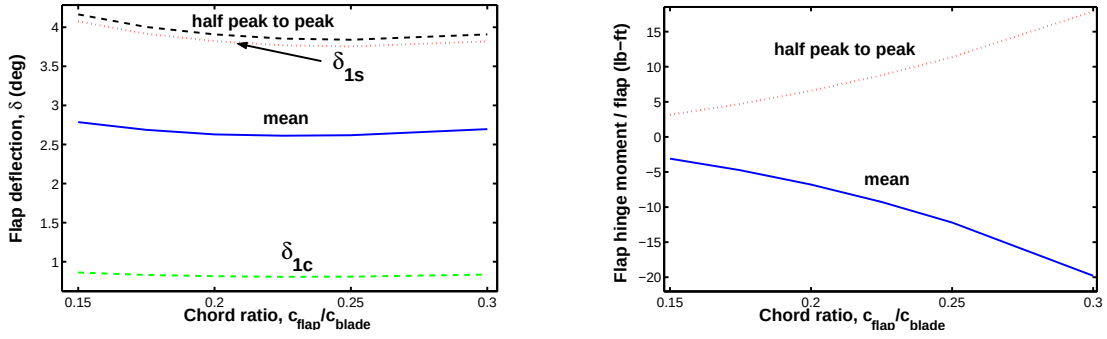

(a) Flap deflections (b) Hinge Moments

Figure 4.2: Effect of flap chord size on the flap deflections and hinge moments indexing angle=20° and μ=0.2.

Flap spanwise size – A flap with a larger spanwise length needs a smaller deflection. The power requirement of a flap also decreases as the flap length is increased from 10% radius to 20% radius. Further, an increase in flap length does not decrease the power requirements (Ref. 23). A flap span of 20% radius was chosen to reduce

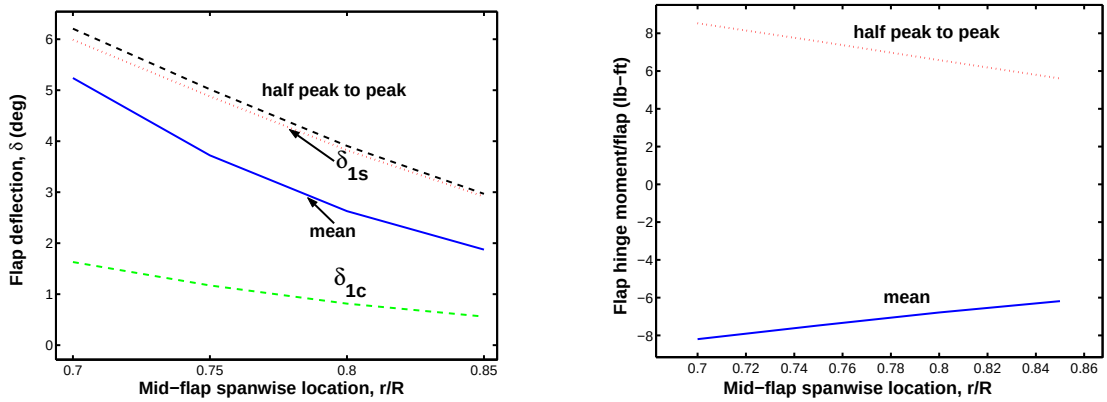

(a) Flap deflections

(b) Hinge moments

Figure 4.3: Influence of the spanwise flap location on the flap deflections and the hinge moments, indexing angle=20° and μ =0.2.

deflection and power requirements as well as to decrease the weight of the actuator-trailing edge flap assembly. Two flaps of length 10% radius each, are used for redundancy. The two flaps are separated by a distance of 0.5% radius to ensure that there is no mechanical interference between them.

Flap chord size – Figure 4.2(a-b) shows the flap deflections and the hinge moments generated as a function of flap chord size. Flap deflection decreases as the flap chord to blade chord ratio is increased from 0.15 to 0.2, but remains fairly constant thereafter. The hinge moment increases monotonically with flap to blade chord ratio. A flap to blade chord ratio of 0.18 is designed as an optimum solution for reducing deflection requirement while keeping hinge moments low.

Spanwise flap location – Moving the flap outboard decreases its deflection and hinge moment – see Fig. 4.3. The two flaps were placed between 69.75% radius and 90.25% radius as a compromise between reducing actuation requirements and blade structural integrity issues arising from placing the flap and actuator close to the blade tip (large centrifugal force).

Location of flap hinge – The location of the flap hinge close to its own quarter-chord reduces the hinge moment requirements (Fig. 4.4) but makes the flap susceptible to an aeroelastic instability. The flap hinge was located at 20% of flap chord from its leading edge to minimize hinge moment requirements while avoiding aeroelastic instabilities.

The flap deflection (Fig. 4.1(b)) and hinge moment (Fig. 4.5) requirements for different forward speeds for the optimum flap form the basis for the design of the actuator.

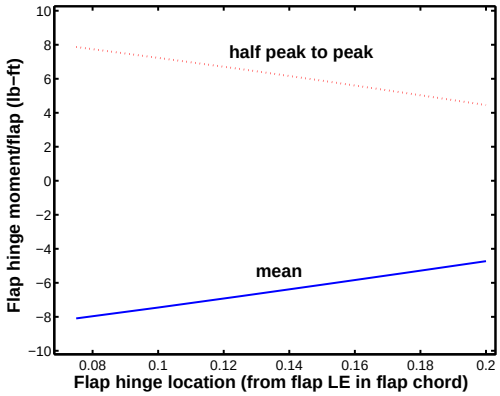

Figure 4.4: Hinge moments produced as a function of the flap hinge location, indexing angle=20° and μ =0.2.

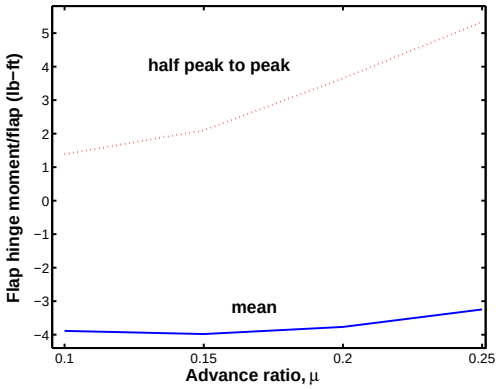

Figure 4.5: Hinge moments produced for the optimum flap.

4.1.4 Actuator Design

The trailing edge flap actuators were designed to meet the extreme requirements of both collective and cyclic deflections and hinge-moments over the entire range of forward flight conditions, which were evaluated in the previous section. This requires a maximum collective and cyclic flap deflection of 4° each. Based on this, the stroke and force required by the actuator were estimated. Using two actuators per flap, a stroke of $\pm$0.021 inches about the mean displacement, and a force of 150 lb needs to be applied by each actuator.

Table 4.2: Table showing the properties of various materials considered for the actuators.

Material	Maximum Strain	Blocked Force	Bandwidth	Considerations
Shape Memory Alloys	High (6-8%)	Large	Slow (<1 Hz)	Low frequency applications such as rotor tracking (not feasible for primary control)
Magnetic Shape Memory Alloys	High (6%)	Low-moderate forces	Fast (0-1 kHz)	Bulky, high weight penalty
Magnetostrictives	Low (0.2%)	Moderate (500-600 lb)	Fast (0-10 kHz)	Bulky, high weight penalty
Piezostacks	low (0.1%)	Large (1000 lb)	Fast (0-100 kHz)	Stroke amplification is necessary for rotor application

Different smart materials available were evaluated (Table. 4.2) for actuating the trailing edge flap. It was concluded that a piezo-stack in conjunction with a stroke amplification mechanism is best suited for the design of the actuators because of its high energy density and bandwidth. Especially, if the piezo stacks are be driven at a high frequency of

about 1000 Hz, it is possible to harvest an enormous actuation energy. Using frequency rectification the small output displacement produced by each stroke of the piezostack can be converted into a large output displacement of lower frequency.

Compact Piezo Hydraulic Pump Design

The piezo stack can produce large forces but has a low stroke that is amplified using frequency rectification with a compact piezo-hydraulic pump (Ref. 25, 1) developed recently at the University of Maryland. The dimensions and estimated weights of the components are summarized in Table 4.4. The working principle of this actuator is described below (Fig. 4.3 adapted from (Ref. 1)) :

First Half of the Output Stroke – During the positive stroke of the piezostack, the hydraulic fluid is pushed into the lower half of the output cylinder, pushing the output piston upwards (Fig. 4.3). The fluid displaced from the upper chamber of the output shaft is stored in the accumulator. During the negative stroke of the piezostack, the hydraulic fluid from the accumulator is drawn into the pump chamber. Hence, the output piston moves in one direction while the pump piston moves up and down.

Second Half of the Output Stroke – The operation of the valves is reversed. The positive displacement of the piezostack causes the hydraulic fluid to be pushed into the accumulator. During the negative stroke of the piezostack, the hydraulic fluid is drawn from the lower chamber of the output cylinder, while fluid from the accumulator gets drawn into the upper chamber, causing the downward movement of the output piston.

The design of the primary components of the actuator are discussed below:

Pump – The pump consists of a piezo stack and a piston enclosed in a steel casing. The casing was designed to be 10 times stiffer than the piezostack assembly to minimize pumping losses due to expansion of the pump body. The 1/rev flap deflection required determines the actuator output which in turn fixes the stroke of the piezostack. The maximum load on the actuator was determined to be 150 lbs, from the hinge moments. It was found that 8 piezostacks (each of dimensions 0.4 in $\times$ 0.4 in $\times$ 0.7 in) and a piston diameter of 0.63 inch (Fig. 4.6) was required to produce the required stroke. The power needed by the piezostack assembly in the current design was estimated to be 40 W. This results in an actuation power requirement of 160 W/blade.

Output Cylinder – This consists of the output piston (9/16 inch) enclosed by an aluminum casing of length 2 inches and connected to a push rod of quarter of an inch diameter.

Accumulator – The main function of the accumulator is to make the pump insensitive to air entrained in the fluid and store energy, which is necessary if there is a sudden load.

Mounting and Operation of Actuator

The actuator pump assembly is placed behind the blade spar (Fig. 4.19). The heaviest component of the assembly, the pump, is placed parallel to the spar and rigidly attached to it. The output cylinder of the actuator assembly is placed along the blade chord and the push rod is connected to the flap hinge. The output cylinder, being relatively light, is

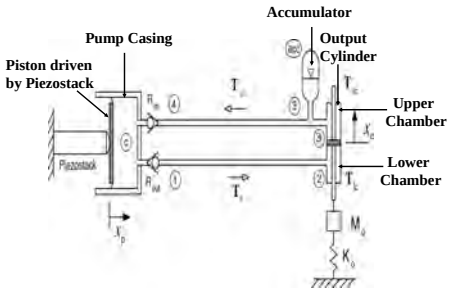

Table 4.3: Piezo-Hydraulic Compact Actuator Schematic (Ref. 1).

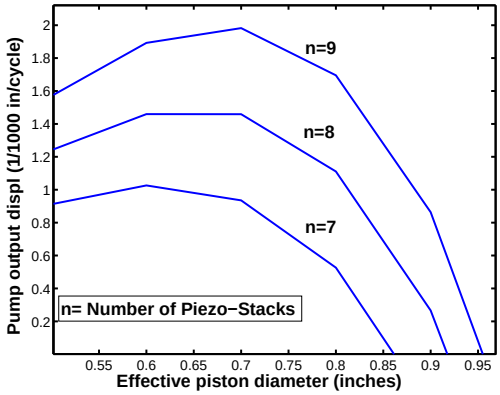

Figure 4.6: Output displacement of pump per cycle as a function of piston diameter.

Table 4.4: Estimated weights and dimensions of piezo-hydraulic hybrid actuator.

Component	Inner Diameter (in)	Length (in)	Outer Diameter (in)	Mass (lb)
Piezo-Stack	—	5.67	0.40	0.26
Pump Casing (includes piston and valves)	0.63	6.60	1.08	1.20
Output Casing (includes accumulator)	0.56	2.00	0.80	0.17
Fluid and Tubing	—	—	—	0.08

supported by a reinforced rib. An elliptical hatch is provided so that the actuator assembly can be easily accessed for repair or replacement. Countersunk screws with caps are used to reduce drag.

The push rod is connected to a hinge tube (flap hinge) using a pitch horn. The hinge tube is attached to the main blade through two flange mounted roller bearings on each side (Specifications: shaft diameter 5/16 inch, height 0.64 inch, dynamic load per bearing 266 lb (Ref. 26)). The mean and cyclic displacement of the push rod produced by the pump translates into mean and cyclic flap deflection. The actuator can achieve and hold a particular displacement and does not require a bias force, eliminating the need for a torsional spring.

Safety Issues

Even with only one of the flaps functioning, on each blade, the helicopter can hover and attain very slow speeds. The flap deflection required under these conditions is less than half of deflection required at an advance ratio of 0.2, for which the actuators are designed. The actuator can provide a mean displacement in excess of the normal requirement, which can be used to provide a high collective for flare when landing during autorotation.

The current compact actuator is low weight and reliable. Further reduction in weight and improvement in reliability can be achieved by using magneto-rheological fluids. The viscosity and stiffness of these fluids change on applying a magnetic field, thus eliminating mechanical valves needed to control the flow and thereby improving the high-frequency energy harvesting. Prototypes have already been built and tests have shown potential benefits.

Table 4.5: Properties of materials used in the blade structure.

Material	Density (lb/in^3)	Young's modulus (Msi)	Shear modulus (Msi)	Nominal ply thickness (in)
Glass/Epoxy	0.072	6.3	0.66	0.008
Graphite/Epoxy	0.055	8.03	6.31	0.01
Nomex Honeycomb	0.00116	0.0105	0.0042	—
Tungsten	0.700	40	19.2	—

4.1.5 Slip Ring

The power for actuators is supplied by the electrical systems in the helicopter. Therefore, a slip ring (Ref. 27) is necessary to transfer electric power from the non-rotating to the rotating frame. The arrangement consists of a stationary housing and brushes which are in contact with the rotating slip rings.

For co-axial rotors, separate power is required for both the contra-rotating rotors. This is achieved by using two slip rings. One slip ring is located on the outer shaft and transfers electrical power from the helicopter to the lower rotor. Housing and brushes located on the lower rotating hub transfer power to a second slip ring located on the upper shaft, rotating in the opposite direction. This is used to transfer power from the hub of the lower rotor to the upper rotor.

A small dust particle or mechanical imperfection may cause a momentary loss of contact between the brushes and the ring, which is detrimental to the reliability of the swashplateless rotor concept. Multiple brushes and rings are used to ensure that the transfer of power is not affected by loss of contact between any single brush and ring.

4.1.6 Blade Structural Design

The Aeneas blade must withstand flapping, lead-lag and torsion moments, and support the compact actuator and trailing edge flap assembly. Because of the low torsional frequency of the blade, the chordwise location of the blade center of gravity is critical to avoid pitch-flap divergence and flutter. Simultaneously, the blade mass must be sufficient to produce good autorotational properties. The final design of the blade is determined, taking into consideration these requirements (Ref. 28).

Structural Details

The blade primary structure consists of a D-spar consisting of twenty four uniaxial layers of glass/epoxy composite enclosed in a torsion wrap consisting of eight $+45^\circ/-45^\circ$ layers of graphite/epoxy. The outer skin comprises of two layers of glass/epoxy ($+45^\circ/-45^\circ$). Nomex honeycomb is used for the remaining internal blade structure as it bonds well with the skin and has low moisture absorption. Tungsten ballast weights are placed in the inner nose cavity at discrete sections along the blade to ensure that the blade center of gravity is slightly ahead of the quarter-chord. Blade sections between 69.75% and 90.25% span have additional tungsten ballast weights to compensate for additional mass due to actuator and trailing edge flap assembly located aft of quarter-chord. This outboard mass also contributes to improvement of the autorotation index of the blades. The properties of the various materials used are given in the

Table 4.6: Design parameters of the swashplateless rotor.

Parameter	Value
Lock Number	8.33
Blade Feathering Moment of Inertia	757.3 slug-ft^2
First Torsional Frequency	1.79/rev
Collective Index angle	20° (at blade root)
Trailing Edge Flaps span	69.75%R to 79.75% R and 80.25%R to 90.25%R
Flap chord	18% of main blade chord

Table 4.5.

A cut away of the blade section (refer to Fig. 4.19) shows the titanium erosion protection cap mounted over the leading edge of the blade and the electrically insulated de-icing blanket (heating element) is placed between the D-spar and the erosion protection cap.

Lightning Protection and Electromagnetic Shielding

The composite blades need to have proper electrical continuity and protection against lightning strikes. It should withstand a 200kA lightning strike and still permit safe landing (Ref. 29). Further, actuators are susceptible to damage by large currents and the composite blade internal structure can disintegrate because of the heat generated. Blade sections, which susceptible to heating and large currents, are covered externally with doublers made of conductive materials that conduct the current to a titanium abrasion strip. The current flows spanwise to the root end attachment of the blade. The actuator housing is wrapped in a nickel/iron alloy foil to shield it from stray low frequency electromagnetic signals.

Blade Folding

The helicopters need to be stored in compact spaces, such as in fire-stations, and should be transportable using ground based systems, which necessitates blade folding. The connection between the indexing splice and blade root is exploited for the blade folding. An indexing splice is used to provide a collective at the blade root. It connects the flex-beam end to the blade root providing a twist of 17° and is attached with a set of wire-locked bolts to each end. One of the bolts at the hub end can be removed and the blade can be folded about the axis of the other bolt. The gear box is indexed so that one of the blades of the bottom rotor is aligned with the tail boom. Two blades on the top rotor are folded to align with the tail boom. The remaining two blades on the bottom rotor are folded to align with the nose.

4.1.7 Final Blade Parameters

The blade polar and feathering moment of inertia and Lock number are influenced by the mass distribution which is determined from the blade structure, leading edge weights and actuator design. These parameters along with flap sizing are summarized in Table 4.6.

4.1.8 Hub Design

The main rotor hub provides an attachment to the blade, permits blade motion, and transfers blade loads from the rotating frame to a fixed frame. Conventional hubs require hinges for flap and lag and a feathering bearing. A bearingless rotor design is used to eliminate the hinges and bearings and reduce mechanical complexity and number of moving parts. This improves reliability, decreases maintenance costs, and reduces parasitic drag by providing an aerodynamically clean surface. Compared to conventional articulated designs, the higher equivalent hinge offset of a bearingless rotor provides faster response of the blade to control inputs and more control power (Ref. 30), both of which are extremely important when operating in urban canyons.

Design of Bearingless Hub

The bearingless hub, refer Fig. 4.19, consists of a flexbeam for pitch, flap and lag motion, a torque tube, a soft pitch link (pitch spring) to provide desired feather stiffness of the blade, and an elastomeric damper to provide lead-lag damping. Details of the individual components of the hub are explained below.

Flexbeam – One end of the flexbeam is cantilevered at the hub support structure while the other end is bolted to an indexing splice (which is in turn bolted to the blade). The flexbeam is fabricated from unidirectional S-glass/epoxy tapes. The spanwise sectional properties are tailored by adding S-glass fabric. It has low flap, lag, and torsional stiffness at the center while the stiffness at both ends are high. The taper is optimized in plan form and thickness. This helps to increase its structural integrity (improve ply delamination due to gradual ply drop). The length of the flex-beam is 20% of the blade radius.

Torque Tube and Pitch Spring – One end of the torsionally stiff torque tube is bolted to the flexbeam and indexing splice. The other end is attached to a soft pitch spring. The torque tube comprises of carbon fiber filaments with the chordwise stiffness enhanced by unidirectional tape. The flexbeam is torsionally soft. It is necessary to incorporate a pitch spring, which is essentially a pitch link replaced by a spring of low stiffness in order to transfer torsion load to the airframe as well as to maintain sectional geometry. The pitch spring stiffness was designed to obtain a torsional frequency of 1.79/rev.

Elastomeric Damper – As mentioned previously, the flexbeam is relatively soft to reduce lead-lag moments on the hub. The rotor is susceptible to ground resonance and air resonance, necessitating the augmentation of lead-lag damping. The elastomeric damper consists of alternate layers of elastomer and metal shims. Silicone-rubber elastomeric dampers can withstand high temperatures and are, therefore, selected (Ref. 31). Also, the relative movement between the flex-beam and torque tube produces a shear in the elastomeric damper, increasing the lead-lag damping.

4.1.9 Autorotational Characteristics

The autorotative index, used by Sikorsky (Ref. 32), is the ratio of the main rotor kinetic energy to the product of the design gross weight and disk loading. While an autorotative index (AI) of 10 or higher is considered safe for a multi-engined helicopter, it is also necessary to compare the AI of the designed helicopter with that of helicopters of similar Gross Take Off Weight (GTOW). The Aeneas has good autorotative characteristics as shown in the Table 4.7.

Table 4.7: Comparison of autorotational characteristics.

Helicopter	GTOW (lbs)	I_ω (slug-ft^2)	Rotor rpm	Disk Loading (lb/ft^2)	AI (ft^3/lbs)
Aeneas	22,230	6,174	27.57	5.16	20.5
Black Hawk	22,000	6,941	27	9.75	11.8

4.1.10 Rotor Dynamics

The soft-inplane bearingless rotor with trailing edge flaps must be carefully examined to ensure proper placement of its flap, lag and torsion frequencies and provide adequate safety margin from aeromechanical instabilities. This section describes the methodology adopted to study the susceptibility of the main rotor to instabilities and the steps taken to avoid them. The structural characteristics of the blade are plotted in Fig. 4.7.

Dynamic Analysis

The rotor fan plot was obtained using the University of Maryland Advanced Rotorcraft Code (UMARC) with the flap, lag and torsional stiffnesses calculated from the blade structure. The attachment of the actuator to the spar does not affect the stiffness, but it causes a large change in the mass distribution, as shown in Fig. 4.7. Several design iterations were performed to optimize the flexbeam and blade stiffness and appropriately place the blade frequencies. It was found that the changes in first lag and flap frequencies were influenced greatly by the flexbeam properties, while the change in higher flap and lag frequencies were primarily influenced by the blade stiffness distribution. The fan plot is shown in Fig. 4.8 and the rotor natural frequencies are summarized in Table 4.9. The lag and torsion frequencies are well separated from the rotor frequencies. This separation is essential, especially for the lag frequency, as the lag mode damping is low.

Stability Analysis

An aeroelastic analysis was performed to ensure that the rotor does not encounter aeromechanical instability in its flight regime. A pitch-flap flutter analysis (Fig. 4.10) shows that the critical CG location for the designed torsional frequency (1.79/rev) is 2% aft of quarter chord. Tungsten ballast mass was added at the leading edge to place the blade cg slightly ahead of the quarter chord (at 22% chord). This ensures that pitch-flap flutter and divergence are avoided. A comprehensive analysis of the critical damping of the rotor modes (Fig. 4.11) showed that all the rotor modes are stable over the entire flight envelope.

Ground and Air Resonance

Because the bearingless rotor in the current design is soft in-plane, it may be susceptible to ground resonance. Therefore, it should be ensured that the rotor and support modes are well damped at all rotor speeds.

A ground resonance analysis of the co-axial rotor was carried out, modeling the interaction of the lag modes of both the rotors with the body pitch and roll modes. In this analysis, the body pitch and roll frequencies of a typical helicopter were used. The analysis shows that the rotor in-plane modes of both the rotors are stable and their damping

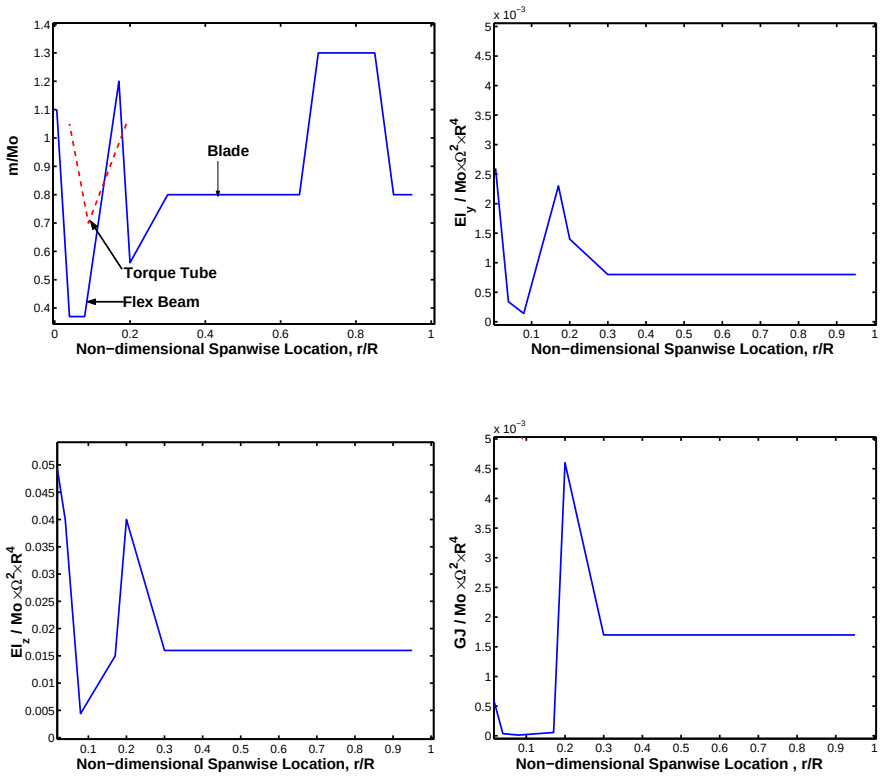

Figure 4.7: Blade stiffness and normalized mass distributions.

can be maintained above 0.8% throughout the flight envelope(Fig. 4.12).

Soft-inplane hingeless and bearingless rotors are susceptible to air resonance. It is caused by coupling of low frequency rotor flap and lag modes with fuselage rigid body pitch and roll modes. A comprehensive stability analysis was carried out, modeling the fuselage undergoing rigid body motions. The analysis shows that the rotor lag mode is stable over the entire flight regime (Fig. 4.13).

Blade Phasing and Vibrations

The 3-bladed rotors of Aeneas, feed large 3/rev forces and moments to the airframe. By phasing the contra-rotating rotors appropriately some of the 3/rev forces and moments produced by one of the rotors can be cancelled by those produced by the other rotor, assuming both rotors experience equal airloads at corresponding azimuth angles. A blade phasing, such that the reference blade of the bottom rotor points towards the tail when the reference blade of the top rotor points towards the nose, cancels the 3/rev vertical forces, longitudinal forces and pitching moments, while the lateral forces, rolling and yawing moments tend to nearly double (Ref. 33). This phasing corresponds to blades crossing each other at azimuth angles $30^\circ \pm n60^\circ$. An intermediate phasing may lead to optimum vibratory loads and moments in each mode. However, longitudinal, vertical, and pitch 3/rev vibration levels are more critical than the lateral vibrations and the rotors are phased to minimize the former in the current design. An added advantage of this

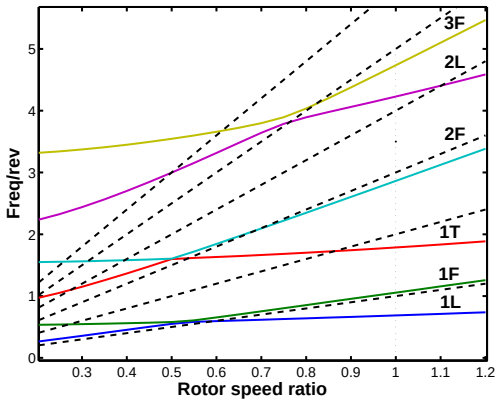

Figure 4.8: Rotor fan plot.

Figure 4.9: Flap, lag and torsion natural frequencies of the main rotor.

Mode	First	Second	Third
Flap	1.06	2.86	4.73
Lag	0.68	4.23	—
Torsion	1.79	—	—

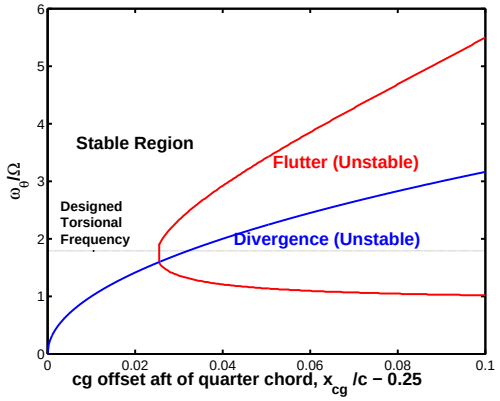

Figure 4.10: Pitch-flap flutter and divergence stability analysis.

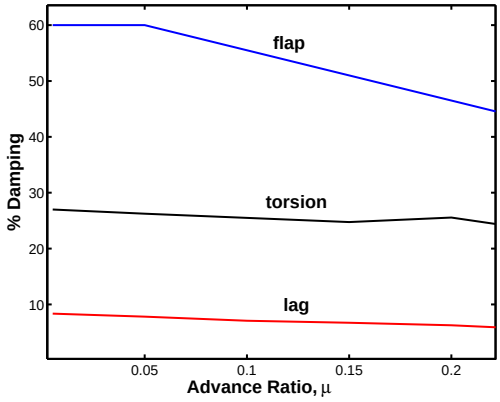

Figure 4.11: Flap/lag/pitch stability.

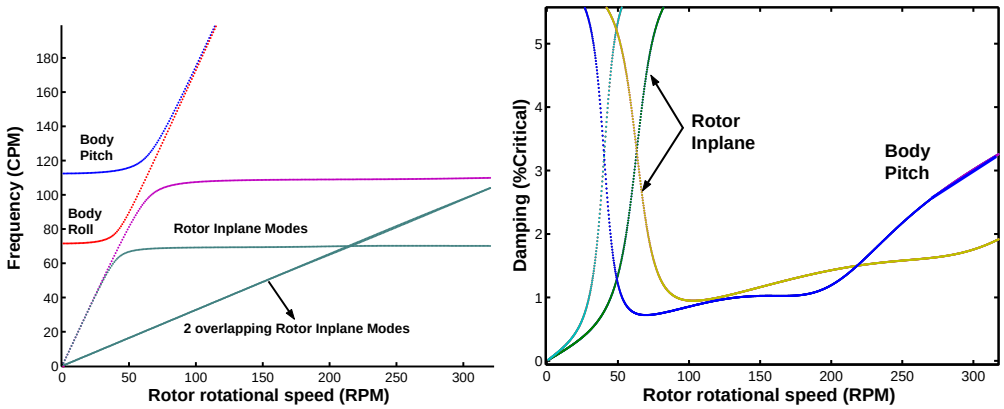

Figure 4.12: Frequency and damping in different modes for ground resonance analysis.

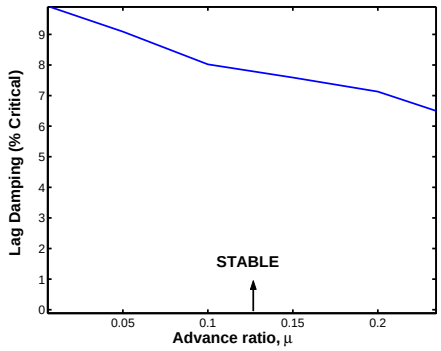

Figure 4.13: Air Resonance Analysis.

phasing is that the blade folding can be achieved in a simple manner. Four blades, each folded through 60° can result in aligning all the blades along the longitudinal axis of the helicopter.

Blade Tracking and Higher Harmonic Control

Since, the piezoelectric compact actuator has an input frequency which is about 200 times the output (1/rev) frequency, the actuator can also be employed to produce small, higher harmonic flap deflections (typically 3/rev and 4/rev) necessary for vibration control, by appropriately timing the valves. Further, the actuator is capable of sustaining a mean displacement, which makes blade tracking possible. Hence, the existing actuator hardware, coupled with a robust, neural-network based adaptive control methodology, will enable both blade tracking and higher harmonic control. A radial basis neural network structure is used to evaluate control inputs to the trailing edge flaps. The controller samples hub loads and control inputs on a per rev basis, performing system identification and vibration reduction in real time. It has been shown that such a controller can minimize vibration (Ref. 20). The use of a neural network based controller to individually actuate each blade enables tracking of each blade, based on sensing the hub-loads (Ref. 34).

4.2 Airframe Design

The Aeneas is designed as a multi-role helicopter. The airframe must be highly adaptable to meet the different mission requirements. During the initial stages of design, the concept of a crane-fuselage, similar to Erickson's Skycrane, was explored. However, this design was rejected, in favor of a semi-monocoque design, because of higher weight penalty. A crane design requires additional stiffening of the main airframe and is, therefore, inefficient in comparison to a semi-monocoque design. To satisfy all the RFP requirements, the fuselage must have the following features: suspension points capable of sustaining an underslung load of about 9,000 lbs, cabin space to house the Command and Control module, large doors for quick reconfiguration, a large fuel tank to satisfy hover endurance requirements. The overall fuselage dimensions are restricted by the RFP requirement that the system should be capable of being transported on wide flat bed trucks.

Figure 4.14: Figure showing the structure of the airframe.

4.2.1 Airframe Layout

The airframe layout is shown in Figure 4.18. The airframe consists of three primary modules: a cockpit section, a center fuselage section and a tail section. The airframe cross-section varies along the fuselage length to improve the aerodynamic and structural characteristics. The cockpit houses the avionics and control systems, in addition to the two pilots. The center fuselage consists of the main cabin area and a baggage compartment, with the fuel tanks beneath the cabin. The transmission deck above the cabin supports the engine, the main rotor gear box, and the rotor assembly. The maximum width of the fuselage was determined by the space required to house the three engines around the main rotor transmission. The dimensions of the internal cabin is determined by the space required to seat a five member command and control team. Finally, the tail section consists of the horizontal and vertical stabilizers along with a semi-monocoque structure to provide moment arm to the stabilizers.

4.2.2 Structural Details

Bulkhead Design

The skeleton airframe structure consists of four lightweight, primary load bearing bulkheads connected by four keel beams – refer Fig. 4.14. The first primary bulkhead is used to connect the cockpit to the center fuselage and supports the two nose landing gears. The second primary bulkhead forms the front support for the engine and transmission deck, in addition to supporting the two front legs of the rotor mast support standpipe. The third primary bulkhead forms an intermediate support for the engine and transmission deck and the two aft legs of the rotor mast support standpipe. The fourth, and the final, primary bulkhead connects the central fuselage with the tail. Support points for underslung loads are provided at the base of the second and third primary bulkheads. These bulkheads also support the strengthening frames around the large cabin doors. The doors are wide enough to provide easy access to the interior in the event of reconfiguration. The airframe also consists of two secondary bulkheads which provide additional supports. The first secondary bulkhead connects the nose and cockpit and supports the avionics bay. The other secondary bulkhead provides support for the aft engine mounts and the baggage compartment.

Four keel beams placed between the first secondary bulkhead and the third primary bulkhead supports the cockpit

and cabin floor. The two center keel beams extend from the third primary bulkhead to the rear secondary bulkhead. The keel beam sections have sine wave webs, which exhibit good energy absorption characteristics.

Engine and Transmission Deck

This deck provides structural support for the three engines and the main rotor transmission, along with the auxiliary power units, and electrical and hydraulic systems. The deck is a Kevlar-graphite-epoxy sandwich panel, that is bonded to the second and third primary bulkheads and the rear secondary bulkhead.

Tail Section

The tail section consists of the horizontal and the vertical stabilizer. The co-axial design eliminates the need for a tail rotor. This results in a short, light weight tail boom. The tail boom is a semi-monocoque structure, and has only two main bulkheads. The vertical and horizontal stabilizer are made of a hybrid sandwich structure using Kevlar-epoxy face sheets and a honeycomb core to ensure light weight. The spars of both stabilizers are made using composite graphite-epoxy.

4.2.3 Structural Materials Used for Construction

The primary objectives that determine the selection of materials for the structure are static strength efficiency, fatigue life, thermal limitations, corrosion resistance and cost. To minimize the overall structural weight, a hybrid composite-metal frame consisting of a composite skin and an aluminum-lithium alloy was selected. The alloy has superior strength-to-weight and stiffness-to-weight characteristics and is an ideal choice for the present vehicle.

4.2.4 Manufacturing and Construction Issues

The Aeneas features a modular airframe consisting of three modules namely, the cockpit, the central fuselage and the tail section. These modules can be manufactured separately, equipped with the required electrical wiring and hydraulic lines, and other subsystems prior to final assembly. This facilitates the ease of manufacturing and also results in low maintenance costs.

4.3 Landing Gear

The final landing gear design was based on the different mission requirements, crash-worthiness standards, ground handling characteristics. The landing gear arrangement is shown in Fig. 4.18.

4.3.1 General Arrangement of Landing Gear

Two different landing gear designs were considered – retractable and non-retractable wheel systems. The retractable landing gear are heavier, while the non-retractable landing gear incurs more parasite drag penalty in forward flight. Hovering and low-speed forward flight are the primary operating regimes of the current mission. The reduction in

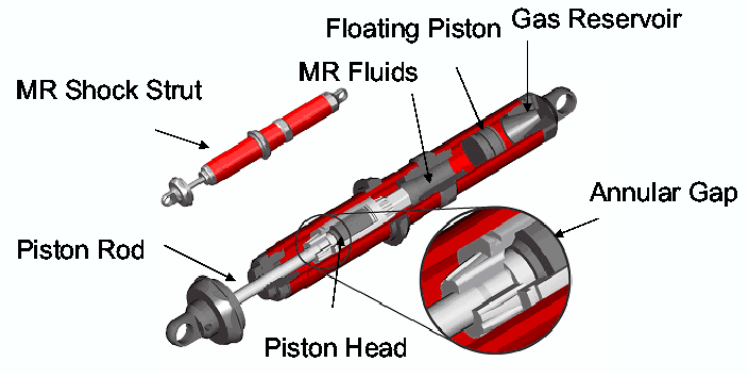

Figure 4.15: Figure showing the schematic of an MR damper landing gear system.

parasite drag in these regimes of flight did not justify the weight penalty incurred by using a retractable landing gear. Therefore, a non-retractable *quadri-cycle* landing gear arrangement was chosen for the present design.

The nose and the main landing gears are placed about the CG in a manner that the main wheels support 70% of the gross weight, while the remaining 30% of the weight is carried by the nose landing gears. The *quadri-cycle* configuration satisfies the overturn and tip back angle requirements to avoid helicopter turnovers and tip backs during landing or ground maneuvers.

4.3.2 Magneto-rheological (MR) Landing Gear

The helicopter is expected to land in all kinds of terrains and unprepared landing sites. The landing gear will experience harsh impulsive loads during operation. This landing impact is an important factor in structural fatigue damage, dynamic stress, and passenger discomfort. Therefore, a smart landing gear system, with adaptive damping characteristics, proportional to the impact velocity, is desired. In addition, the present helicopter is expected to perform different missions with different payloads. The gross takeoff weight for the command and control mission is almost half of the gross takeoff weight for the rooftop rescue mission. With such varied mission requirements, the design of an optimum landing gear is not possible without some sort of active damping system.

Magneto-rheological fluids are known to have outstanding advantages of continuously controllable rheological properties and fast response time under the influence of a magnetic field. Considerable research has been conducted investigating the utility of MR fluids for semi-active damping control in fields such as civilian building structure dampers, automobile suspension systems, and helicopter lead-lag dampers etc. Therefore, an MR shock strut was chosen in favor of a conventional oleo-pneumatic shock absorber in the present landing gear system. A sliding mode controller provides continuous damping control in response to the impact velocity.

A schematic of the flow-mode MR shock struts is shown in Fig. 4.15. The shock struts are composed of gas and hydraulic reservoirs, similar to oleo-pneumatic landing gear. The piston head divides the hydraulic reservoir, which is fully filled with controllable MR fluids, into upper and lower chambers. The fluid moves in between chambers through an annular valve. A gas chamber is located above the upper chamber to compensate the changing fluid volume because of the movement of the piston rod. In the absence of magnetic field, the MR shock strut produces the same damping force as a passive oleo-pneumatic strut. However, when a magnetic field is applied to the controllable

fluid, additional damping force is generated, by the field-induced yield stress, in the annular valve. This damping force can be continuously controlled by adjusting the intensity of the applied field with a velocity feedback control.

4.3.3 Tire Sizing

Low pressure tires were selected to allow the helicopter to land at unprepared sites. At the maximum gross take-off condition, each main tire is required to carry approximately 9,923 lbs. Therefore, the main tire was chosen to be a type III 8.5-10 tire with a rated load of 9,900 lbs, 16 plies, and an inflation pressure of 129 psi. A type III 6.50-10 type tire was chose for the nose landing gear. This has a rated load of 4,750 lbs, 10 plies, and an inflation pressure of 100 psi.

4.3.4 MR Strut Sizing

In the absence of an external field, the MR dampers and conventional oleo-pneumatic dampers behave identically. Therefore, the sizing methods employed for oleo-pneumatic struts can be used to estimate the MR strut dimensions.The stroke of the oleo was determined by the FAR 29.727, which states that each gear must be able to withstand a 12 in drop test, corresponding to a sink rate of 8 ft/s. Using recommended values for the tire strokes (1/3 tire radius) and shock absorber efficiencies of 0.8 for the oleo and 0.47 for the tires, results in a stroke requirement of 8 inch. This value is was increased to 9 in to account for any uncertainties in loading and to provide a margin of safety (Ref. 35). The diameter of the oleo was determined using a typical oleo internal pressure of 1,800 psi, an external diameter of 1.3 times the internal diameter. The length of the strut is typically 2.5 times the required stroke. The resulting strut dimensions were: nose gear outer diameter x length: 2.36 in $\times$ 23.6 in; main gear strut diameter x length: 3.54 in $\times$ 23.6 in.

4.4 Engine Selection and Transmission Design

The performance capability of a helicopter is determined by its engine and transmission limitations. The RFP requirements state that the helicopter should be capable of operating on a hot summer day in Denver. This is equivalent to operating at ISA+30 conditions at an altitude of about 6,000 ft. Under these operating conditions, the power requirements are significant. Further, a co-axial design complicates the design of the main rotor transmission system. The following sections describe the methodology adopted in the engine selection process and the rotor transmission design.

4.4.1 Engine Selection

It is obvious that the final engine configuration is determined by the total power required by the helicopter and its subsystems. However, the unique needs of this mission dictated certain other requirements. The additional constraints imposed by the mission at hand are:

- As mentioned earlier, the helicopter is required to perform all the specified missions at an altitude of about 6,000 ft and at ISA+30 temperature conditions. The increases the net power required to perform all the operations mentioned in the RFP.

Table 4.8: Engine specifications after accounting for IHPTET improvements

Rating	**Duration** (sec)	**Power Ratio**	**Power** (shp)	**SFC** (lb/hp.hr)
Emergency (OEI)	30	1.25	2975	0.38
Takeoff (max.)	120	1.00	2380	0.39
IRP[a]	1800	0.92	2199	0.39
MCP[b]	Continuous	0.8	1882	0.42
Partial Power	–	0.5	1190	0.51
Idle	–	0.2	476	1.27

[a] Intermediate Rated Power
[b] Maximum Continuous Power

- Existing helicopters hover at intermediate power for very short periods of time. Typically, the period of hover is not more than 30 minutes. The present missions require the helicopter to hover for much longer periods of time.
- Certain missions, e.g., window rescue and ground based water cannon firefighting, require the helicopter to operate dangerously close to buildings. In the event of an engine failure, transition into forward flight and subsequent autorotation is impossible. This imposes the very stringent requirement that the helicopter be able to hover and complete the mission in case of failure of one engine.

Based on the above constraints, it was decided to choose a three-engine configuration in which the engines provide the power required for hover when operating at the maximum continuous power rating. However, in the event of one engine failure, the other two engines switch to the intermediate rating and still provide the power required for hover.

Engine Performance

Performance estimates indicated the maximum operating power required by the helicopter and its subsystems to be 4,200 hp at sea level under ISA conditions. A survey of the existing engines, with a take-off rating of 2,100 hp, was conducted. It was found that the General Electric turboshaft engine (T700-T6E) had the best combination of power-to-weight ratio and specific fuel consumption (SFC) characteristics. Improvements in these parameters are expected with the efforts made by the Integrated High Performance Turbine Technology (IHPTET) program, a joint venture by the government and the industry with the objective of developing a new generation of engines with improved performance (Ref. 36). Table. 4.8 shows the static, uninstalled engine specifications at sea level, ISA conditions. The IHPTET improvements were factored in when calculating the engine parameters. Figure 4.16 shows the power output of a single engine as a function of the altitude at two operating conditions, ISA and Denver conditions ($\sim$ ISA+30).

Installation Losses

The power specified by the manufacturer is the uninstalled power. In reality, the power output from the engine is less than the uninstalled power. These engine installation losses can be divided into following: inlet and exhaust losses,

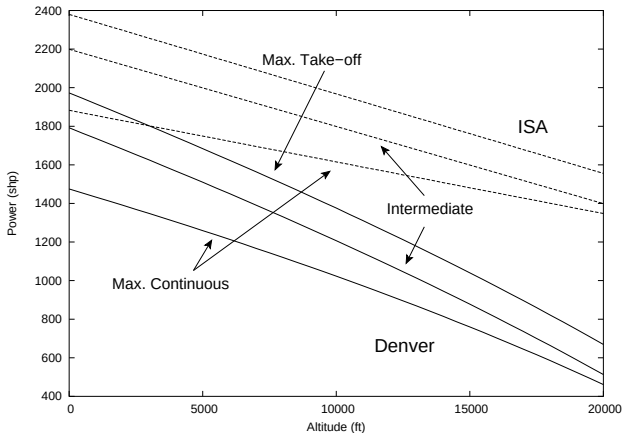

Figure 4.16: Engine power as a function of altitude at different operating conditions

losses from bleed air extraction and losses in the auxiliary gear box. Installation losses were assumed to be 3% in the engine take-off power (Ref. 37).

Structural Integration

The engines are installed on the transmission deck behind the main gear box, allowing for good accessibility for maintenance and inspection. The engines are mounted onto the transmission deck using two bipods and two linkages. The engine cover doubles up as a work platform when the systems are serviced. Torque transfer to the main transmission is achieved through flexible couplings.

Oil System

Independent oil systems are provided for each engine, thereby, improving the operational safety and reliability of the engines. The oil systems consist of a pump, tank, filter, cooler and two particle detectors. The particle detectors are monitored by the FADEC system – see Sec. 4.4.1. Preliminary estimations suggest that each engine requires 1.5 gallons of oil.

Particle Separator

Rescue missions require the helicopter to operate very close to airborne smoke. A particle separator is provided, as an integral part of the engine, to minimize the risk of engine damage from dirt or debris ingestion. The particle separator incorporates three filtration areas to increase its efficiency. Easy access is provided to each particle separator for periodic cleaning and maintenance. The separator blockage is monitored by the FADEC system.

Full Authority Digital Engine Control System

The flight control system features a Full Authority Digital Engine Control (FADEC) system to ensure optimum engine performance. The FADEC controls the engine settings, both during nominal as well as OEI operating conditions,

enabling the engines to perform at peak performance. In addition, FADEC also monitors the oil system and the particle separator system and reports any malfunctions to the integrated mechanical diagnostic health and usage management system (IMD HUMS) for compensation. This guarantees enhanced flight safety, reduced pilot workload, longer engine life between overhauls, in addition to significant reductions in life cycle costs.

Environment Sensors

During operations in smoke filled environments, the engine will ingest contaminated air (deficient in oxygen), thereby, degrading its performance. A special unit is, therefore, necessary to detect the presence of harmful gases. Various off-the-shelf sensors are available for this function. A Shack Rat II sensor, manufactured by BW Technologies was chosen for this purpose owing to its high sensitivity, low volume and weight (12 lb), wide operating range, and an easy-to-use operator interface. In the event of oxygen depletion, the sensor relays the data to the FADEC, which adjusts the engine parameters. In addition, this unit can also detect the presence and concentration of toxic gases and alert the pilot to fly out of that area.

4.4.2 Transmission Design

A schematic of the transmission is shown in Fig. 4.19. The first stage of the transmission is a spiral bevel gear with a reduction ratio of approximately 1:1.5. This stage turns the shaft direction of outboard engines by 90° – see Fig. 4.19. Clutches are provided just before the collector gear to disengage the engine in the event of engine failure. The power from the three engines is transmitted to the face gear, with a reduction ratio of 1:3.75. Triplex ball bearings and one roller bearing support the bevel gear shaft in an over-hung configuration. The next stage in the transmission system is a planetary mesh, consisting of one sun and four planetary gears, which provides a third reduction stage. The first stage bevel gear and the sun gear of the planetary mesh, are supported by the same shaft. The planetary gears are supported by double rows of spherical roller bearings attached to the planetary carrier. The sun gear drives the four planets, which in turn mesh with a fixed ring gear attached to the transmission housing. The planetary carrier is connected to four spiral bevel gears. The spiral bevel gears turn the two rotor shafts in opposite directions. The overall reduction achieved by the main transmission system is 24.2, which allows the rotational speed to be reduced from 6,050 rpm to 250 rpm required by the rotor. The rpm reductions at intermediate stages are tabulated in Table. 4.9. The first stage face gear also drives an accessory gear, which runs the oil pump. The oil pump supplies lubrication to the transmission through jets and channels located in the transmission housing.

Parameter Optimization & Weight Analysis

The gear mechanism was designed using the methods presented by Dudley (Ref. 38). The main rotor transmission is rated to transmit a maximum power of 4,200 hp. In order to satisfy the OEI requirements, the transmission components linking each engine and the main gear box are individually rated to transmit a maximum power of 2,100 hp.

The Lucas Aerospace flexible coupling is used to transmit torque from the engine to the gear box inputs. The chosen coupling is a single piece, light weight, reliable, and easy-to-maintain design. The torque input at the interface occurs through a spring-type overrunning clutch. The input point is the location of the lowest driveline torque and, therefore, allows considerable weight minimizations for the clutch.

Table 4.9: Speed reductions achieved at various stages of the main rotor transmission system

Reduction Stage	**Input Speed** (rpm)	**Output Speed** (rpm)	**Ratio**
Auxiliary gear box	21000	6050	3.47
Bevel gear	6050	4033	1.50
Face gear	4033	1143	3.75
Planetary gear	1143	250	4.57
Spiral bevel gear	250	250	0.00

Table 4.10: Weight breakdown for the main rotor transmission system

Component	**Weight**	**Component**	**Weight**
Bevel gear	164.3	Transmission casing	27.6
Face gear	268.5	Lubrication	41.7
Planetary gear	289.1	Accessories	45.0
Spiral bevel gear	336.8	Structural support	24.7
Shaft	42.3		
Total Weight		**1240 lbs**	

Gear size, bending and compressive stresses were calculated. Weight estimation is performed using the stress values calculated with the detailed model of the drive system. A non-dimensional Hertz stress index factor Sa, function of Hertz stress (Sc), Pressure angle (θ), and helix angle (Φ) is used to compare the effect of Hertz stress on weight. The Hertz stress index factor Sa is given by

$$Sa = \left[\frac{Sc}{158793}\right]\left[\frac{\sin 2\theta}{\cos^2\Phi}\right] + \left[\frac{\frac{Sc}{1000}}{140\Phi^2 - 9.5\Phi + 315}\right]^{\frac{1}{0.494}} \tag{4.1}$$

The equation for estimating each gear box section weight is given by

$$W = 150\left[\frac{Q.P.U.A.B}{Sa.N}\right]^{0.8} \tag{4.2}$$

where Q is a non-dimensional weight factor defined for every gear configuration (spur, bevel, planetary), P is the design horsepower of the gear assembly, N gear rotational speed, Sa is a hertz stress index, and A, B and U are factors used to include structural characteristics and special features of the transmission in the weight estimation. Weights of the shafts, bearings and lubrication system were also calculated using a series of empirical relationships.

The ratio of gear box weight to power is found to be 0.295lb/hp. This is lower than the nominal value of 0.3. The weight savings can be attributed to the use of ceramics, high contact gears, composite housing, and improved surface treatments.

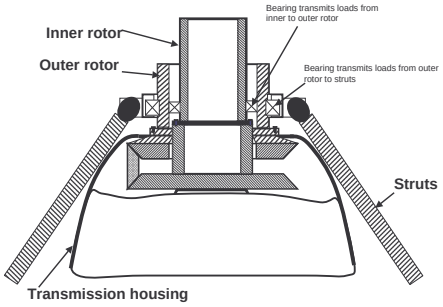

Figure 4.17: Mast support system

Gear Box Design

The gear box performs two functions, it encloses the transmission and provides support to the rotor shafts. Cored passages are incorporated into the housing to transfer lubricant to the gear meshes and bearings and an oil sight gauge is included to check the oil level. The transmission housing is composed of an upper and a lower casing bolted together and mounted to the transmission deck via vibration isolators.

Typically, rotor mast loads are transferred to the helicopter fuselage by the transmission housing. However, the co-axial configuration subjects the rotor mast support system to load environments that can be more severe than those experienced by a conventional helicopter. In order to minimize the rotor loads experienced by the transmission housing, four struts connected to the rotor housing have been incorporated. The rotor shafts carry the mast moment, thrust, side loads and torque and transfer 80% of loads directly to the fuselage through the struts. This configuration reduces the weight and increases the fatigue life of the transmission. Forces from the inner rotor are transferred to the outer rotor and then to the rods by ball bearings. The outer rotor transmits forces through a bearing to the struts. The bearing housing contains two tapered roller bearings and the rotor shaft. The active struts are attached to the bearing housing and then mounted to the transmission deck. In case of leakages, the gear box has a 30 minutes dry run capability.

Oil System

The components of the transmission oil system include the oil filter, magnetic particulate trap (MPT), cooler, pump, and fan. Two separate oil filters are installed, one at the sump and the other at the MPT output. The MPT will detect metallic particles and burn up small particles with a high voltage spark. Both filters will contain element detect switches (to ensure the filters are installed and operating properly) and bypass valves allowing for continued transmission operation if the filters are clogged. The MPT and filters each have integral alarms and any abnormal operation will be reported to the integrated mechanical diagnostic health and usage management system (IMD HUMS)

Integrated Mechanical Diagnostic Health & Usage Monitoring System (IMD HUMS)

IMD HUMS refers to equipment, techniques, and/or procedures applied to helicopter rotors, transmissions and engines by which incipient failure or degradation and/or selected aspects of service history can be determined. Provisions are made for the installation of a state of the art IMD-HUMS which not only increases safety, but also allows operators using information from the system to develop more effective maintenance and logistics practices. These changes result in increased aircraft availability, reduce maintenance, increased flight hours, and more effective management of spare parts and maintenance personnel. The IMD HUMS performs a number of tasks, the most important being:

- Automatically records, analyzes, communicates, and stores information about the operation, condition, and usage.
- Continuously records all state parameters from power up through power down, and provides a complete usage record.
- During each flight, a comprehensive vibration diagnostic system automatically acquires and processes data on rotor induced vibration, engine, rotor, and shaft balance, and gear and bearing condition, at frequent intervals.
- The on board system displays selected information to the aircrew, while the PC-based ground station serves as the primary means for communication with maintenance, logistics, and planning functions.

4.5 Vibration Isolation

The primary source of vibration, the rotors, transmit a vertical forcing of 6/rev and in plane vibration of 3/rev to the hub. The absence of a tail rotor, the co-axial configuration, and low speed flights imply relatively simple methods are sufficient for vibration control. Rotor loads are transmitted to the transmission deck through four struts and the transmission housing. The struts transmit eighty percent of the rotor loads. The struts are connected to the transmission deck via a Liquid Inertia Vibration Eliminator (LIVE) force isolator system. The LIVE isolator is composed of outer and inner cylinders joined by a co-axial rubber bushing. The inner cylinder is attached to the struts, while the outer cylinder is connected to the fuselage. Cavities connected by a tuning port within the cylinders serve as reservoirs for a dense hydraulic fluid which acts as the tuning mass of the isolator. By varying the diameter of the tuning port, the device may be calibrated to isolate the desired frequency. The system is of reduced mechanical complexity, bearingless, low weight and has a linear response at high gs. The state-of-the art of this type of isolators weigh approximately 18 lbs each, and can isolate a minimum of 65% vibratory forces.

UM-911 AENEAS Co-axial Helicopter

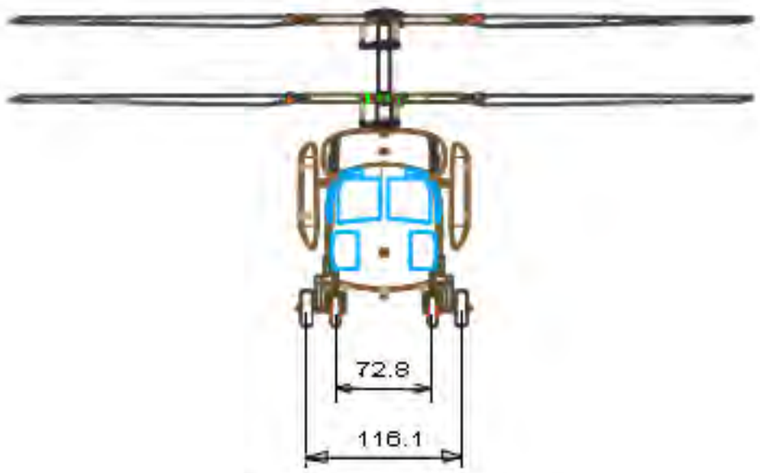

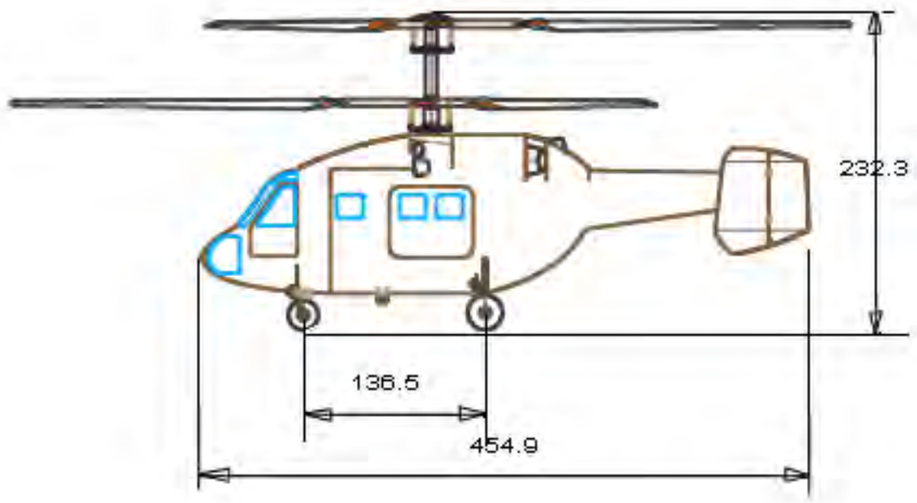

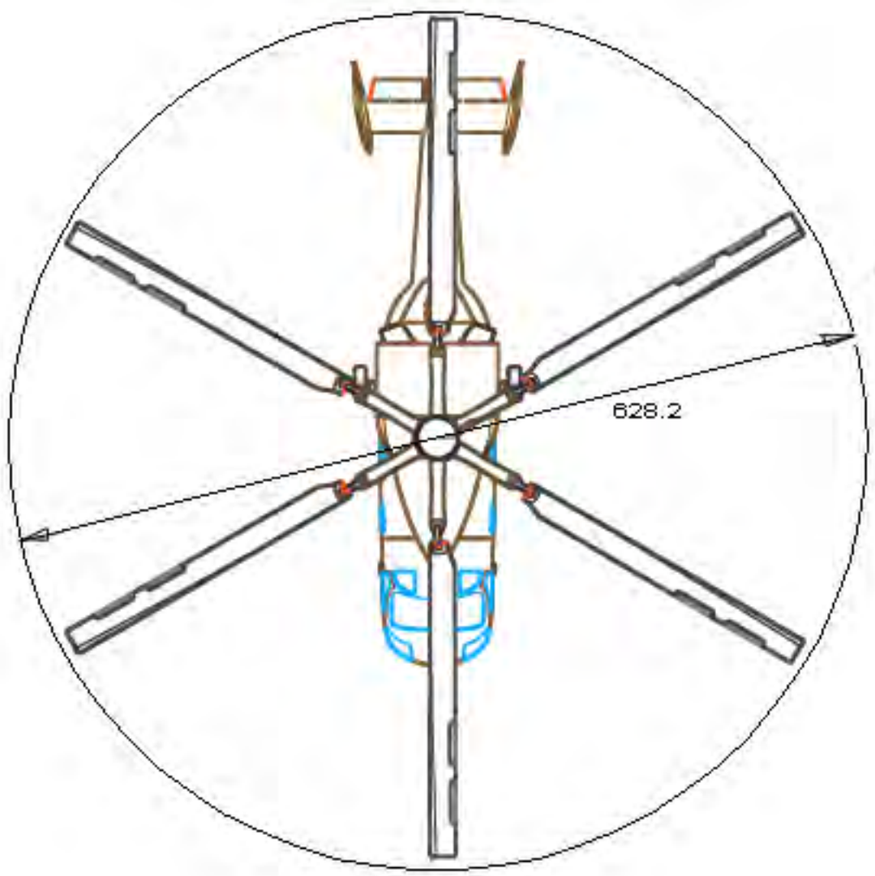

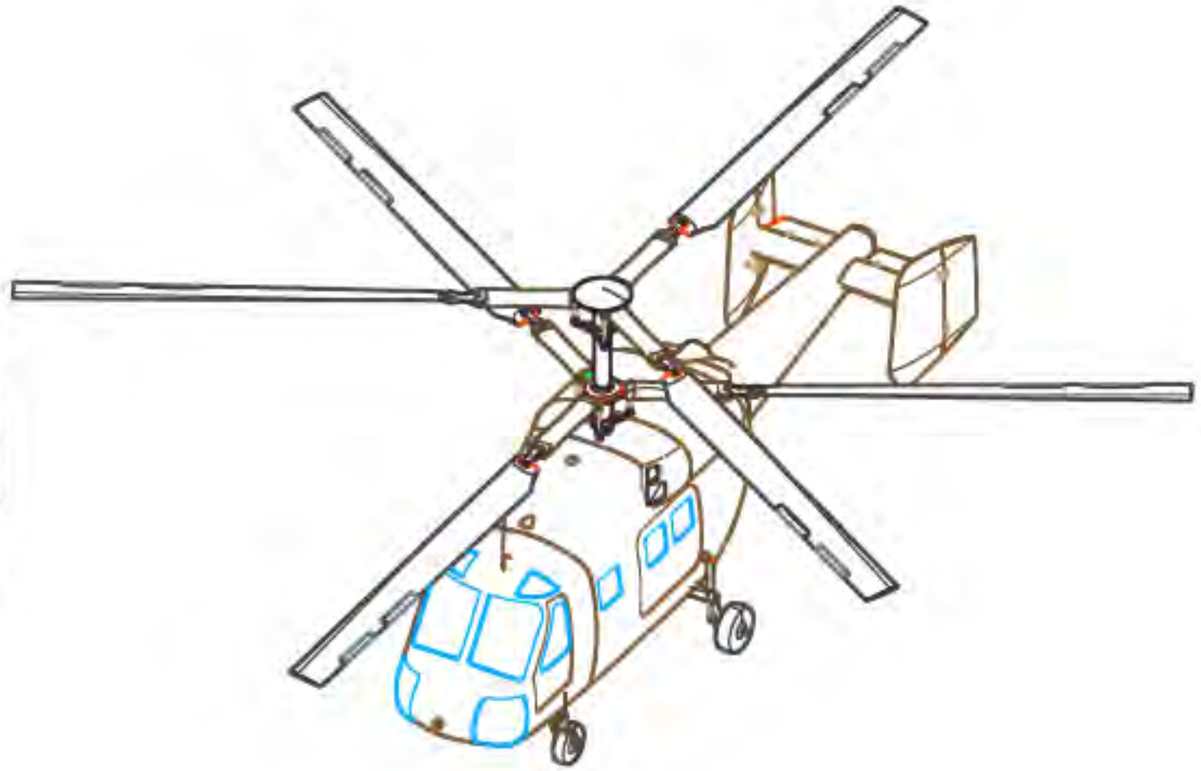

All dimensions in inches.

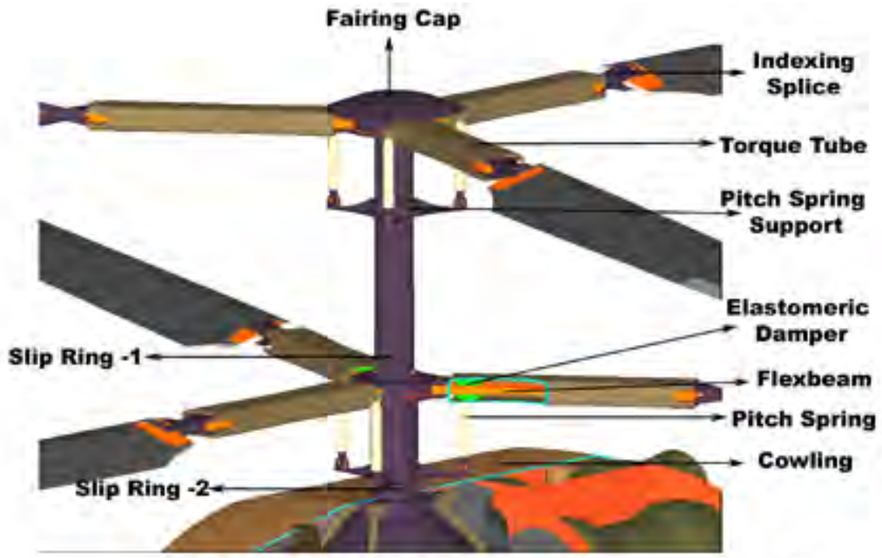

Hub Details

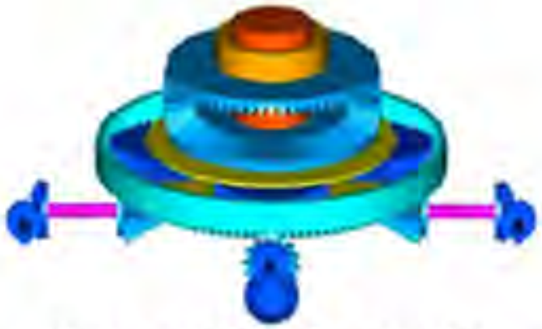

Gearbox Configuration

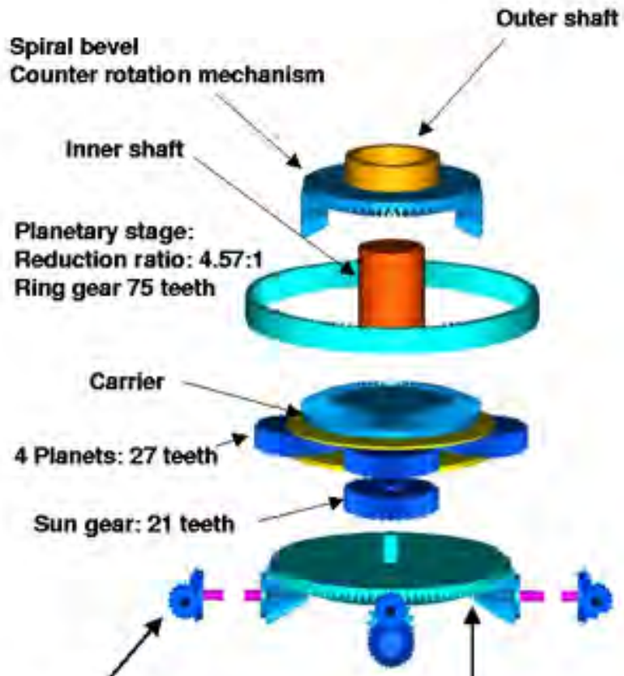

Gearbox Configuration

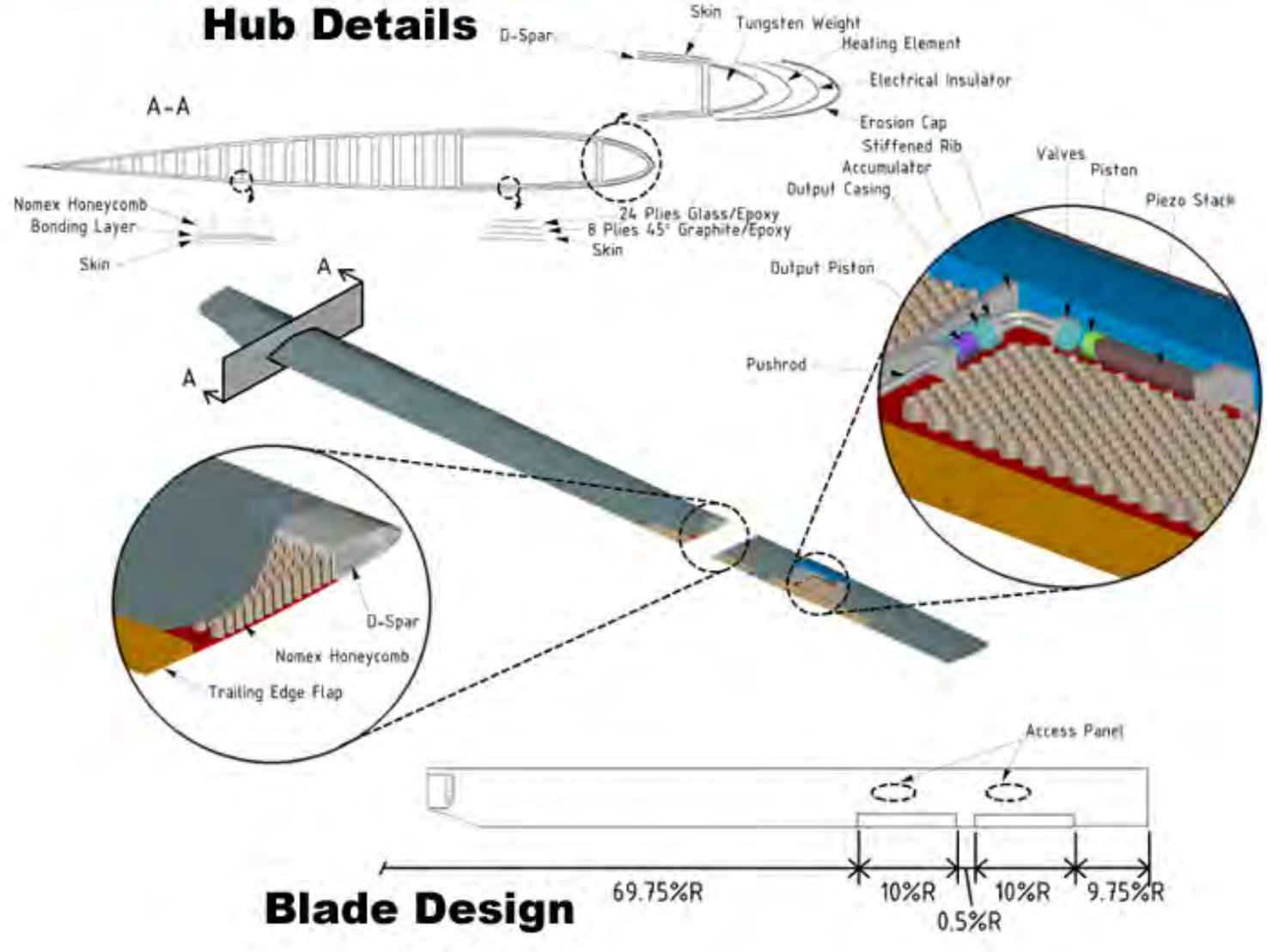

Blade Design

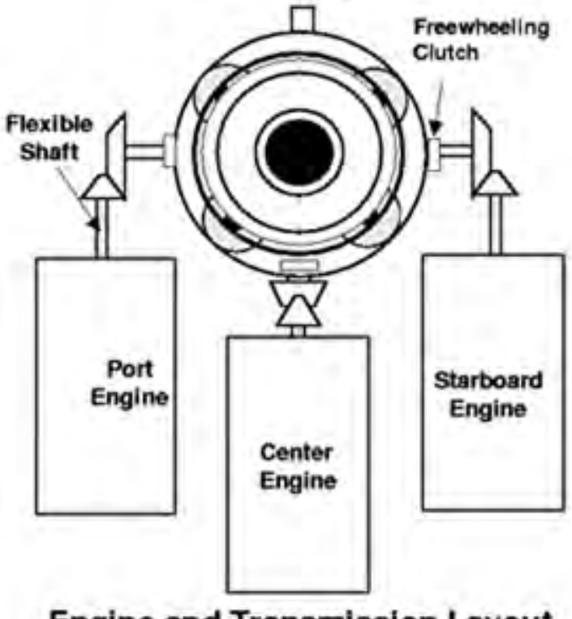

Engine and Transmission Layout

5 Details of the Autonomous Flight Control System

5.1 Avionics

The two primary considerations influencing the avionics design of Aeneas are, the requirements to operate in narrow urban canyons and the ease of operation of the system. The system needs a highly sophisticated flight control system that can provide autonomous control of the helicopter in urban canyons. An enhanced autopilot is absolutely essential if the system is to be flown by a trained operator who is not a professional pilot.

5.1.1 Sensor suite

Operations in urban canyons require that the flight control system have access to precise and accurate position, velocity, attitude and angular rate information. By coupling the Zero-lock Laser Gyro with the latest technology electronics and Global Positioning System (GPS), the LN-100G represents one of the highest quality INS/GPS in the market. It combines the high reliability and performance of nondithered laser gyros with the latest GPS receiver technology (Ref. 40). The INS/GPS unit outputs true heading, pitch, roll, position, velocities and accelerations and provides them directly to each of the Multi-function displays. The INS/GPS sensor unit is placed next to the engines, near the center of gravity, to provide the most accurate measurements.

The accuracy of the GPS receiver can be improved by providing differential corrections from a nearby Differential GPS (DGPS) reference station. For the accuracy of the measurements needed for this particular mission, the reference station should be within 20 miles. Therefore, it is strongly recommended that each city using the Rescue Vehicle establish a reference station within the city.

While the GPS receiver with DGPS corrections can provide position measurements with a precision of one centimeter, an additional system of measuring position relative to the walls was desirable. For that reason, it was decided to incorporate a series of Microwave Doppler Radars (MDR) in the helicopter to measure the proximity to the surfaces to safeguard from any possible crash with the building. These sensors are placed on both sides of the fuselage, at the nose and on the tail to measure the proximity of the helicopter in all four directions. Microwave Doppler Radars are currently available for use in luxury cars for Adaptive Cruise Control, a new method that measures the position and relative speed of other vehicles around the car and adapts the speed to maintain a safe distance from other vehicles. These Radars operate at a frequency of 77 GHz, use Frequency Modulated Continuous Waves (FMCW) and have a range of about 150 meters (Ref. 41). However, their accuracy, about 1 meter, is not sufficient for the precision needed in the present design . MDRs with different frequencies, sub-resolution techniques and other characteristics offer improved ranges and accuracies. Nalezinski (Ref. 42) and Klotz (Ref. 43) describe sensors for high-precision measurements. These FMCW radar sensors, operating at 24 GHz, offer an accuracy of ± 3 cm at distances up to 20 meters. They are not commercially available at present, but are expected to mature in the next five-year period.

Other sensors, included in the system, are necessary to measure changes in the surroundings of the helicopter. An infrared camera, provides color thermal maps of the buildings. It is capable of identifying a person from a distance of 500 ft with the standard 50 mm lens (Ref. 44). Besides obtaining thermal maps, inclusion of a heat flux monitor to determine the magnitude of the fire and measure the heat emission is recommended by the Fire Protection Engineering

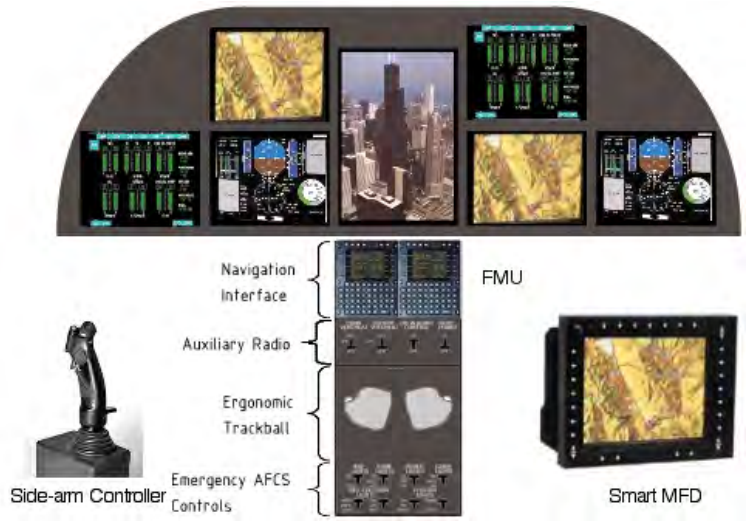

Figure 5.1: Cockpit layout for the Aeneas.

Department. Chemical sensors are also incorporated (see description in Section 4.4.1), to measure the toxicity of the environment.

5.1.2 Multi-function Displays

The principal components of the glass cockpit are the color Smart Multi-function Displays (MFD). There are seven Northrop Grumman All-Glass Cockpit Smart MFDs (Ref. 40) inside the cockpit, three on each side for each pilot/operator, plus a larger central display for maps, navigation, views of the building, and other mission related information.

Each MFD, shown in Fig. 5.1, contains its own industry standard single board computer, a high-performance and graphics processor, a universal video module and a custom input-output module; this independence provides another level of redundancy, as in case of failure of one of the MFDs, the same information can be displayed in another monitor. The MFD has a bezel size of 11.6 in$\times$9.3 in (294 mm$\times$236 mm), with an actual viewing area of 9.7 in$\times$7.3 in (246 mm$\times$185 mm), and is installed in a landscape orientation. The cockpit layout is shown in Fig. 5.1. The screen allows for a large viewing envelope (45 degrees left and right, 30 degrees up and 10 degrees down) and a unique dual backlighting system makes the MFD the brightest available for sunlight readability, while being sensitive enough for night vision systems.

The main advantage of the MFD is that the information displayed is interchangeable between the displays, can be reconfigured to adapt to new technology and each of them can show different screens with different fuctions, as required by the pilot and the mission. This way, a lot more information can be provided in the cockpit panel than with regular fixed instruments alone. Some of the functions provided include electronic flight instrumentation, engine instrumentation, sensor video (Forward Looking Infrared (FLIR), acoustic, radar) and maps – see Sec. 5.3 for more details.

5.1.3 Communications

The communications system includes cockpit-to-cockpit and cockpit-to-cabin channels, the latter required for the Command and Control mission. Each helicopter is also provided with a communications channel to the Command and Control Module. The equipment incorporated to provide these functions include a dual VHF-FM Ground and Airborne radios, a VHF-AM radio, a UHF-AM radio and a high-frequency radio for non-line-of-sight communications.

Every rescue system provides sensor and location information to the Command and Control. For this purpose, an Improved Data Modem is incorporated to transmit and receive digital information. All radio and communications can be controlled via the Flight Management Unit, through the Communications Display or with a back-up radio control located in the central console.

5.1.4 Flight Management System

The benefits of Helicopter Flight Management Systems (FMS) are:

- It allows for real time accurate map positioning, and also provides an "easy correlation between map and terrain."
- It provides an easy-to-use navigation management with both basic and complex FMS functions, which is a very important characteristic for the untrained pilot operator.
- It improves mission efficiency by providing a valuable aid to the decision-making process.
- It provides control of the Autopilot modes.

The Thales Avionics HelicopterFlight Management System (Ref. 45) is used in the present design. Two Control Display Navigation Units (CDNU), see Fig. 5.1, are provided in the central console, one for each pilot. The CDNU interfaces with communication equipment, location and tactical sensors to provide an integrated flight management system. It supports navigation from different sources, including DGPS and Inertial systems. For the former, the CDNU displays full GPS data and status information. In addition, it is capable of maintaining up to 200 way-points and 25 different routes, each referencing up to 100 way-points, for navigation. A Data Transfer Device (DTD), which is a portable memory card, can be used to transfer navigation data to the CDNU. Data typically transfered would include: a way-point database, a Navaids database, route database, as well as larger city database and software in the larger memory cards.

The CDNU provides control of the three V/UHF radios, and communication at different frequencies can be preset in different channels.

The CDNU panel is comprised of a high brightness, electro-luminescent display and multi-function keyboard with alphanumeric, function and line keys. The flat panel display is configured for 11 lines of 22 characters of text. The CDNU front panel measures 8.23 in$\times$5.71 in (209 mm$\times$145 mm), weights less than 8.8 lbs (4 kg) and requires +28V DC power.

5.1.5 Controllers

The untrained operator was the determining factor in the selection of the type of controllers for the Aeneas. The controllers of the helicopter were selected in such a way as to allow a pilot to handle the helicopter in a conventional

(or almost conventional) way, while keeping the concept easy enough for an untrained operator to use it.

The controllers chosen to meet these requirements are a three-axis side-arm controller (see Fig.5.1) for longitudinal and lateral cyclic control as well as yaw control, and a collective lever. The side-arm controller would be on the right hand side for both the pilot and the copilot, and an arm rest would be provided with the seat to ease the use of this controller. The conventional collective lever is present on the left. Even though pedals are not required for yaw control in flight, pedals are provided for steering the landing gears for ground maneuvers. In addition, a mouse-like trackball controller is provided on the central console within comfortable reach for each pilot/operator. Using this controller, the pilot/operator can interact with the different displays, change the display modes, open menus and make selections in the screen. This controller is fixed, and the cursor is moved by rotating the ball with the thumb in order to avoid unwanted motion due to the vibration and other sources. This type of controller already exists, but needs additional development and special software added to the standard avionics suite.

5.1.6 Alternative Avionics Packages

The design team is aware that some of the elements in the avionics package, like the inertial sensors or the proximity radar sensors, are expensive and increase the cost of the vehicle. They are all necessary to perform the missions successfully. However, some restrictions could be imposed by a particular Fire Department on the different vehicles in the fleet if they want to reduce the cost of acquisition. For example, the cost of the Command and Control Module could be reduced by restricting its operations to be always outside of the urban canyon. With this restriction, the proximity sensors are not necessary, and a less costly inertial/GPS unit can be used without the performance outside of the urban canyon being affected. The overall mission would be limited with this restrictions, but can still be successfully achieved. Unnecessary but helpful elements can be also removed, like the trackball controller, which is not indispensable to perform the mission but would make the task much easier for the untrained operator.

The elements of the avionics package are installed in accessible areas, like in front of the engines in the cowling, the nose of the fuselage or the space underneath the cabin, and can be removed or changed easily to fit the client's needs.

5.2 Autopilot/Flight Control System

5.2.1 Stability and Control Analysis

Developing a comprehensive nonlinear model of the helicopter for stability analysis is beyond the scope of this project. Instead, a linear model was developed based on the methods described by Padfield (Ref. 46) and Prouty (Ref. 37). Both these methods, however, implicitly assume that the helicopter is a conventional main rotor/tail rotor configuration. To simplify the flight stability equations and use the aforementioned methods, an equivalent single rotor approach was adopted for the present co-axial configuration. The main drawback of such an approximation is that the yaw control, provided by differential collective in co-axial rotors, cannot be estimated with these methods. Furthermore, certain assumptions regarding the aerodynamic characteristics of the fuselage and the empennage were made. Despite these shortcomings, these methods are a suitable approximation during preliminary stages of design and were, therefore, adopted for estimation of the key stability and control derivatives.

Table 5.1: Stability derivatives in hover and forward flight speed of 60 knots.

Derivative	Hover	Cruise	Units	Derivative	Hover	Cruise	Units
X_u	-0.18	-0.25	1/sec	L_u	0.02	0.03	rad/sec-ft
X_v	-0.02	0	1/sec	L_v	-0.22	-0.10	rad/sec-ft
X_w	0	-0.06	1/sec	L_w	0	-0.12	rad/sec-ft
X_p	-2.50	-3.01	ft/rad-sec	L_p	-7.65	4.94	1/sec
X_q	6.25	16.82	ft/rad-sec	L_q	-3.06	-3.11	1/sec
Y_u	0.02	0.04	1/sec	L_r	0	0.02	rad/sec-ft
Y_v	-0.18	-0.17	1/sec	M_u	0.06	0.07	rad/sec-ft
Y_w	0	-0.11	1/sec	M_v	0.01	0	rad/sec-ft
Y_p	-6.25	5.76	ft/rad-sec	M_w	0	-0.22	1/sec
Y_q	-2.50	-2.74	ft/rad-sec	M_p	0.89	0.97	1/sec
Y_r	0	-100.98	ft/rad-sec	M_q	-2.22	-4.09	1/sec
Z_u	0	0.07	1/sec	N_u	0	-0.03	rad/sec-ft
Z_w	-0.25	-0.42	1/sec	N_v	0	0	rad/sec-ft
Z_p	0	0.17	ft/rad-sec	N_w	-0.30	0.10	1/sec
Z_q	0	101.05	ft/rad-sec	N_p	0	0.01	1/sec
Z_r	0	-7.30	ft/rad-sec	N_r	1.30	-0.23	1/sec

A linearized model of the helicopter was obtained for trimmed states in both hover and forward flight. This model was then used to determine the horizontal tail sizing to avoid speed and phugoid instabilities, determining the poles of the system and the handling qualities of the bare airframe. Once the transfer functions of the bare airframe are estimated, one can then proceed to design the flight control system to stabilize unstable modes and achieve Level 1 handling qualities.

Estimation of Stability and Control Derivatives

The stability and control derivatives were estimated from first principle, based on the methods described by Prouty (Ref. 37). Certain assumptions were made regarding the aerodynamic characteristics of the fuselage. In reality, these details are obtained from flight test or wind tunnel data. In the present analysis, these data have been approximated from existing data for similar helicopters. In a hovering flight, only the key derivatives influenced by the rotor are important. In forward flight, the effects of the fuselage, the horizontal and vertical stabilizer need to be considered.

The stability and control derivatives for two flight conditions, hover and a cruise speed of 60 knots, are presented in Tables 5.1 and 5.2. The force and moment derivatives have been normalized with the mass and their corresponding moment of inertia, respectively. Derivatives with very little influence (almost zero magnitude) are not listed in the table.

Figure 5.2 shows the longitudinal and lateral poles for two different flight conditions, hover and cruise at 60 knots. As expected, the phugoid mode is mildly unstable in hover. It is observed that the phugoid mode becomes

Table 5.2: Control derivatives in hover and at 60 knots.

Derivative	Hover	Cruise	Units	Derivative	Hover	Cruise	Units
X_{θ_0}	-3.10	-64.04	ft/sec^2-rad	L_{θ_0}	0	0	$1/sec^2$
$X_{\theta_{1c}}$	-13.16	-18.39	ft/sec^2-rad	$L_{\theta_{1c}}$	-37.47	137.04	$1/sec^2$
$X_{\theta_{1s}}$	87.01	127.91	ft/sec^2-rad	$L_{\theta_{1s}}$	16.10	20.88	$1/sec^2$
Y_{θ_0}	0	0	ft/sec^2-rad	M_{θ_0}	-5.48	16.54	$1/sec^2$
$Y_{\theta_{1c}}$	-87.01	123.04	ft/sec^2-rad	$M_{\theta_{1c}}$	4.67	5.94	$1/sec^2$
$Y_{\theta_{1s}}$	13.16	18.75	ft/sec^2-rad	$M_{\theta_{1s}}$	-30.87	-41.31	$1/sec^2$
Z_{θ_0}	-161.78	-294.56	ft/sec^2-rad	N_{θ_0}	16.96	-16.31	$1/sec^2$

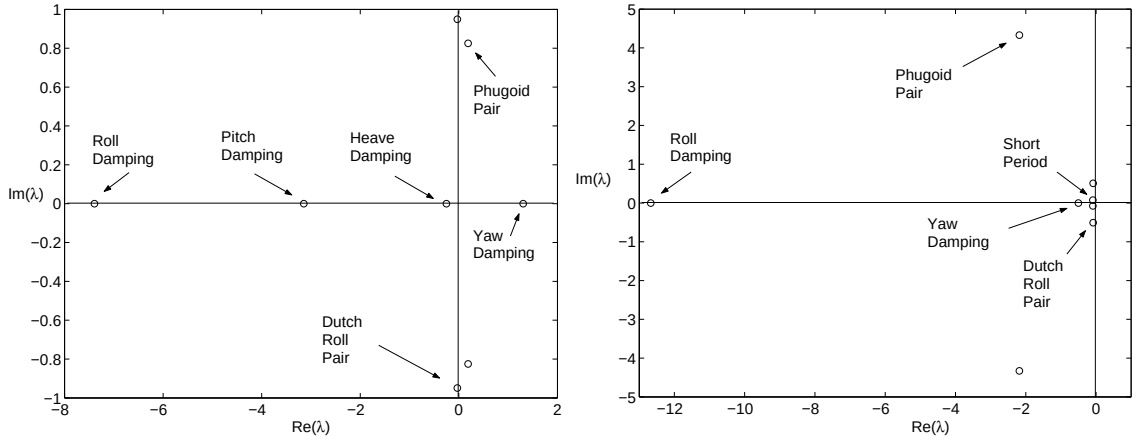

(a) Hover

(b) Cruise @ 60 knots

Figure 5.2: Poles of the linear model of helicopter.

stable with increasing forward flight speed and is, therefore, not very critical. In hover, the pitch and heave modes remain uncoupled. They are coupled through the M_w derivative in forward flight forming the short period mode. These modes are stable in both flight conditions. The dutch roll is stable for both hover and forward flight. Roll subsidence is the most stable of all the lateral modes.

Tail Sizing

The size of the horizontal stabilizer is determined by two conflicting requirements, the phugoid and speed stability. The phugoid mode becomes unstable with increasing tail size and the forward speed mode goes unstable with decreasing tail size. The speed stability criterion is given by the following equation: $M_w \times Z_u - Z_w \times M_u > 0$. This is, usually, satisfied at low speeds and is critical only at higher forward flight speeds. In the present design, a horizontal stabilizer with a surface area of 33 ft^2 is chosen. With this tail size, both the speed and phugoid modes are stable.

Handling Qualities

A linearized model of the form $\dot{x} = Ax + Bu$ can be used to study the handling qualities of the helicopter. The Aeronautical Design Standard for rotorcraft applications, known as ADS-33 (Ref. 47) establishes the criteria for acceptable handling qualities for helicopters. Preliminary analysis is done on the frequency response between the pitch attitude (for small amplitude changes) and longitudinal cyclic control at the cruise speed with the bare airframe. This analysis reveals that the short-term response achieves Level 2 handling qualities, with a bandwidth of 0.46 rad/sec and a phase delay of 0.03 secs. Overall, the handling qualities of the helicopter with the bare airframe need to be improved with the addition of a flight control system, described in Sec. 5.2.2, to decrease the workload of the pilot.

Effect of the Underslung Load on the Stability Characteristics

To account for the effect of carrying an underslung load on the stability of the helicopter, as well as for the stability of the load itself, one needs a much more sophisticated model of the system. The forces and moments on the helicopter due to the additional load on the hook need to be added, plus another set of equations to describe the motion of the subsystem has to be coupled to the helicopter equations. This nonlinear model has to be solved for trim, and then linearized about this equilibrium position to determine the stability characteristics and the response of the system.

The main effects on the stability of a helicopter with an underslung load are described by Fusato *et. al.* (Ref. 10). The underslung load is modeled as a point mass with a drag force acting on it. The main conclusions are:

- The main coupling occurs between the dutch roll and the lateral modes of the underslung load. The dutch roll damping decreases, deteriorating the handling qualities of the helicopter.
- The effect of the coupling on the phugoid is very small.
- The suspended load modifies the roll frequency response by adding a notch to the gain and a 180 degree jump to the phase curves at the pendulum frequencies.
- The changes in the bandwidth and phase delay are small. Changes to the frequency response occur at frequencies lower than those required to determine the bandwidth and phase delay.

In the present design, three ducted fans are installed on the underslung pod for providing control forces. The fans are controlled by an autonomous flight control system in the pod. This enhances the operational safety and reduces operator workload.

5.2.2 Flight Control System

The Flight Control System (FCS) of Aeneas is a full authority, triple redundant, digital, fly-by-light (FBL) system. It is partitioned into two major subsystems, the Primary Flight Control System (PFCS) and the Automatic Flight Control System (AFCS). The PFCS provides the critical flight control, equivalent to the traditional mechanical linkages. The AFCS provides the vehicle with response shaping, stability augmentation, integrated flight and engine control and other optional capabilities (Ref. 48). In addition, a Flight Director (FD) is provided as a software package to execute on the Mission Computer Clusters (MCC), which are removable hardware elements that can be added or removed to perform specific missions.

Redundancy is offered in all elements and levels of the FCS, including the autopilot and flight director, because there is very little margin for error while operating in urban canyons. It is critical to provide a safe and reliable vehicle to perform this mission.

The RFP requirements specify a hover position hold within one foot in all directions. Aeneas achieves this by combining the speed and responsiveness of the fast, accurate inertial and position sensors with high resolution, fast computers to process the commands from the pilot or flight director and a FBL system with high speed of information transmission between the pilot or flight control computers.

A FBL system was chosen for the advantages it provides over both mechanical and fly-by-wire (FBW) systems. The combination of FBW or FBL and digital computers present several advantages over traditional mechanical linkage systems, such as weight savings, reduced maintenance times, faster gust load alleviation and improved handling. Other advantages include automatic maneuver envelope protection, as the computer can limit maneuvers that are outside the normal range of operation of the vehicle, and fuel saving, as the vehicle has lower weight than one with mechanical linkages and can be flown at center of gravity positions which normally make the helicopter unstable, but that consume less fuel (Ref. 49). Moreover, the FBL is better than FBW because of its optical components instead of electrical components, the FCS is, therefore, unaffected by electromagnetic interference. As data can be transmitted faster through fiber optic systems than wire systems, FBL offer improved flight controls and handling qualities.

Figure 5.3 shows the FCS architecture for Aeneas. This architecture allows the helicopter to be flown both by an untrained pilot operator and by a professional experienced helicopter pilot. For these purposes, three options are offered: one, the pilot can control Aeneas manually, by using the control sticks, through the PFCS; second, the pilot/operator can fly the helicopter manually, but with the assistance of the stability augmentation system or any of the other AFCS modes; and third, a mission can be pre-programmed in the Flight Management Unit in the form of routes or way-points that are controlled by the Flight Director, and that the pilot/operator can load at the start of the operation or modify to adapt to changes in the mission.

A form of auto-navigation is necessary to assist the untrained operator to flight Aeneas to the disaster area. GPS auto-navigation is provided in a similar fashion as it is implemented in unmanned air vehicles, with the addition that the operator can modify flight plans during the mission. The auto-navigation system is designed to fly the vehicle by following predetermined way-points. The aircraft measures its position and compares it with the destination point at sampling times. When the distance between the vehicle's location and the desired way-point destination is less than a predefined radius, the way-point is said to have been met and the system proceeds to the next way-point (Ref. 50).

The Aeneas AFCS is comprised of four modes: rate damping (RD), rate-command attitude-hold (RCAH), attitude-command attitude-hold (ACAH) and translational rate command (TRC). The controller inputs (pitch, roll, yaw and heave) are continuously fed to each of the modes. Additionally, turn coordination and sideslip suppression can be provided to reduce the pilot workload, particularly with yaw RCAH (Ref. 51). The RD mode is a stability augmentation system (SAS) that provides damping to any unwanted oscillation that the rate sensors measure. The other three modes are stability and control augmentation systems (SCAS). The RCAH allows the pilot to establish precise, uncoupled rates of helicopter motion proportional to stick displacements. When the stick is released, the motion stops and the attitude/altitude achieved is conserved. ACAH allows the pilot to establish a hands-off stabilized attitude that can be adjusted proportionally to the stick displacement and recovered by releasing the stick. The highest level of automatic control is provided in the form of a TRC, a mode suitable for complicated tasks, such as precision hover in the ur-

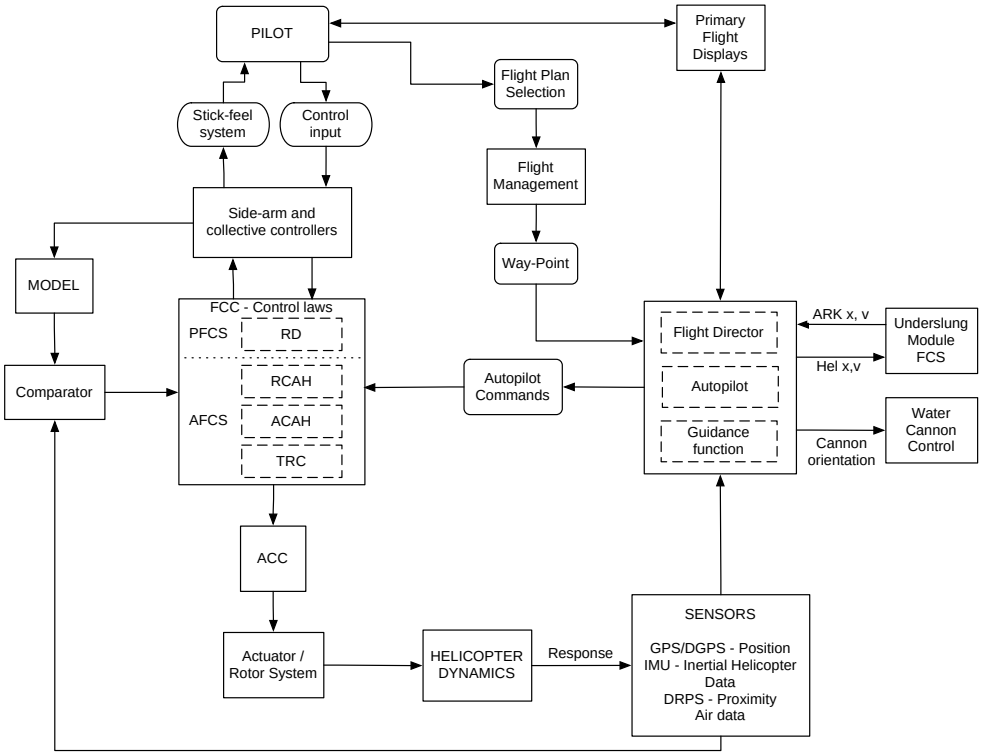

Figure 5.3: Qualitative description of the Flight Control System (FCS) showing interconnections between the helicopter FCS and the mission specific commands.

ban canyon. It is applied only to the longitudinal and lateral motion and allows the pilot to apply precise, uncoupled translational speeds proportional to the stick displacement, that return to the original speeds when the stick is released, while keeping the attained position (Ref. 52).

The Aeneas FCS should use robust model following control laws to minimize sensor noise and the effects of rotor lag. Robust controllers account for the uncertainties in the internal parameters or the presence of nonlinear functions, and uncertainties resulting from unmodeled dynamics of the system or the environment (Ref. 53). Robust control methods provide a response to inputs and disturbances that is always close to the nominal performance. The state-of-the-art in Robust Controllers are H_∞ and Structured Singular-Value (μ) Analyses.

Adaptive Neural Network (ANN) Controller for Fixed Point Hover

Current control systems are capable of ensuring hover stability in the presence of gusts. However, they cannot ensure fixed point hover, which is crucial to window rescue operations. The current design proposes to use a neural network based real time adaptive controller which provides additional control authority during these missions. This system ensures that there are no velocity and position excursions during hover. Further, with sufficient training, the ANN based real-time controller can achieve fixed point hover even in the presence of gusts and varying thrust conditions during rescue operations.

5.2.3 Mission specific additions to the FCS

To minimize pilot workload and enchance operational safety in urban canyons, the basic helicopter flight control system is integrated with certain mission specific additions. These are described in brief detail:

Firefighting — During aerial firefighting operations, the orientation of the water cannon has to be controlled by the automatic control system. In addition, the flight control system has to compensate for the reaction from the water cannon. When lifting ground based water systems, the helicopter has to maintian vertical position and also compensate for additional reactions arising from tilting of the water hose.

Window rescue using ARK — The most critical aspect of this mission is loading people into the underslung pod. The FCS has to stabilize the helicopter such that it stays directly above the underslung pod, minimizing the angle of the cable. It has to compensate for the increasing weight from loading passengers into the pod. Finally, it has to coordinate with the FCS of the underslung module to maintain exact position of the underslung pod with respect to the window of the building.

Underslung pod operations — While landing on the rooftops of urban high rise buildings, the autopilot should know the exact vertical distance between the underslung pod and the ground/landing pad to provide a safe and smooth landing.

5.3 Suggested Operator Interface

A key requirement in the RFP specifies that Aeneas has to be operated by an untrained pilot, i.e. any person, possibly a firefighter, who receives a 3 to 5 day training to operate Aeneas. To meet the RFP requirement, the following possibilities are offered. On one hand, the flight control system can be operated manually with a basic PFCS, through the AFCS with various modes available and with a way-point navigation system. On the other hand, the cockpit displays present two possible interfaces, thanks to the flexibility of MFDs: the professional pilot interface (PPI) with all the instruments to manually fly the helicopter, and an untrained pilot operator interface (UPOI), with the information needed to help the operator handle the helicopter. Both conceptual interfaces are described in this section, although emphasis is given to the UPOI.

5.3.1 Untrained Pilot Operator Interface (UPOI)

The glass cockpit panel includes three large multi-function displays for both the pilot/operator and the copilot, plus a large central display for maps, tactical displays, trajectories, navigation, etc.

The central map display requires a city/terrain database, with details on building heights and location, window levels, etc. Superimposed on the horizontal tactical display, one can have the trajectory followed, accurate directions to street addresses, and more importantly, danger zones and “no-fly zones” determined by the temperature profile around the building on fire. A vertical tactical display shows front and side views of the disaster building, at any window level. These virtual views need to be preprogrammed to great detail and accuracy to allow the pilot to ”see” the surroundings regardless of the visibility. Using the high precision location information, the helicopter’s position can also be shown in the virtual environment.

The other three displays provided to each pilot/operator can show multiple modes that can be suited to the needs of the pilot. The operator can select different MFD modes by depressing the bezel key associated with the desired function or by using the cursor controller. Of the several pages/modes available, some are designed with the untrained operator in mind, and will be described now, while others are the more conventional modes for professional pilots and will be described in the next section.

The main pages for the UPOI include a simplified flight instrument display, a mission specific display, a FLIR video page, a warning/instruction mode, an automatic flight control system selector display, Flight Director Display, Communications/Radio mode, in addition to all the regular displays offered for trained pilots.

Flight Instrument Display: The flight instrument display for the untrained operator is based on the one for professional pilots (described in the next section) with a de-clutter option. The de-clutter option removes some of the instrument information from the display, leaving only the relevant values. For instance, it would remove the altimeter, showing only a single value for the current altitude. The untrained operator can choose this mode if the regular instrument display is too difficult to interpret.

Warning/Instructions Display: The warning display will show the usual warnings about the helicopter, including engine warnings, fuel warnings, etc, plus a set of warnings directed towards the inexperienced pilot that might not be capable of maintaining awareness of all the events and displays on the helicopter. For instance, if the operator does not notice that the altitude has decreased considerably, or if the "no-fly zone" is being approached, warnings are displayed. Other warnings can be mission-related, like the indication that the distance to a nearby vertical surface is decreasing, or the underslung module is close to the ground. Simultaneously, the display can be used to give the operator instructions if he/she is trying to fly manually with the aid of the autopilot. In this case, messages that will instruct the operator to do something different, change an autopilot mode, etc, will be displayed. To simplify recognition, warnings will be shown in red, while instructions will appear in green.

FLIR Video Display: If the vehicle is requested by the Command and Control to obtain thermal maps of the building, the infrared images can be shown in the display to aid the operator point the IR camera in the right direction. Moreover, the infrared vision is also necessary to direct the water cannons in the Firefighting mission.

AFCS Display: This display will show the different AFCS modes available and allow the operator to choose one either through the bezel keys or with the cursor controller. Additional information about the selected mode can be displayed to aid the operator.

Flight Director Display: The operator can enter stored way-point, route or mission information via memory cards, via the alphanumeric keyboard of the Flight Management Unit or on the Map with the cursor. The Flight Director display can be used to aid this process, and provide additional options to the operator to set up the operational autopilot to perform certain mission.

Communications Display: Communications can be handled via the Flight Management Unit or more visually through the Communications Display. Through the display, the operator can choose who he or she wants to communicate with, which radio channel to use, etc.

The flexibility of MFDs allows for all these possibilities and is open for the inclusion of additional modes should the need arise.

Of all these modes, we recommend that the map, the warning display and the mission display (except perhaps in the Command and Control Mission) are shown at all times. The other modes can be display as needed by the operator.

5.3.2 Professional Pilot Interface (PPI)

The PPI must show the map display with all its variants at all times. Of the three pilot displays, one is almost always be dedicated to the mission specific information. In addition to the displays described in the previous sections, the following are included for the professional pilot:

Flight Instrument Display: The flight instrument display for the professional pilots shows an electronic artificial horizon, electronic attitude director indicator, airspeed indicator, altitude, vertical speed, turn and bank angle coordinator, autopilot mode and instrument landing system with heading scale.

Engine Instrument Display: The Full Authority Digital Engine Control (FADEC) allows the engine information to be shown in the Engine Instrument Display for the pilot to monitor.

Navigation Display: The navigation display shows radio navigation sources, automatic bearing, route data, etc.

5.3.3 The Mission Specific Display

The mission specific display shows a different set of information depending on the mission that Aeneas is performing. In this section, we describe the four possible modes.

Command and Control: The Command and Control Mission Specific Display is perhaps the less necessary of the four, and will not need to be shown at all times. The information shown in this display should include communications sent by the Commander in the back, FLIR thermal maps or heat emission information if the vehicle is flying around the building collecting information through the sensors, or distances to nearby walls if traveling within the urban canyon in a recognition mission.

Firefighting: In the firefighting mode, there is a lot of information that needs to be shown in mission display to help the pilot/operator perform the mission successfully. The display allows the operator to choose the cannon tilt mode between automatic (detecting region of maximum heat intensity with IR sensor) or manual (pointing with a controller to the area selected by the operator from the IR camera). It also offers different cannon choices (left, right or both), frequency of firing, and recharge option. When using a self-contained water tank, one can also monitor the water level in the tank, the mixing of water and additives and the operation of the hover snorkel to refill the tank. When using a ground pump, the display shows the control of the continuous nozzle spray geometry (fog spray/straight stream) and the distance from the ground (to prevent yanking of hose and to maintain helicopter within limitations of hose angle).

Rooftop Rescue: For the rooftop rescue mission, the display shows the height of the ARK from the ground, using proximity sensors installed on it. The moment the ARK touches the rooftop or ground, the pilot in the helicopter

is alerted about it. The display also shows the relative position of the ARK with respect to the helicopter. The pilot also has a display of the flight path that he must follow to reach the rescue spot or the designated landing point. During flight, the pilot also has a display of the weight that is acting on the cargo hook.

Window Rescue: In the window rescue mode, it is necessary to include the position of the underslung kit with respect to the window, where people should be rescued from. Also the position of the underslung box with respect to the helicopter should be shown in the display. The weight of the underslung box as people enter should also be displayed, to avoid excessive payload.

6 Weight Analysis for the Vehicle Subsystem

A preliminary weight estimation of different components in the helicopter was conducted using two methods: Prouty's (Ref. 37) method based upon multiple linear regression techniques, and Tischenko's method (Ref. 54) based on the equations developed at the Mil Design Bureau. The use of two different methods, provides a check on the weight estimates made. Both these methods rely on data from existing rotorcraft to estimate weights of various components. Therefore, these methods do not account for the recent improvements in material technologies which provide significant weight reductions for many components. To enable a more representative estimate of the empty weight, the initial estimates had to be corrected using technology advancement correction factors. The correction factors were based upon the recommendations made by Shinn (Ref. 55) and Unsworth et. al. (Ref. 56). These correction factors are discussed in greater detail in later sections.

6.1 Component Weight Breakdown

The rotorcraft empty weight was divided into groups conforming to MIL-STD-1374 and is presented in Table 6.1. Only the design weight breakdown of the helicopter is shown in this table. The payload, fuel weight, additional mission equipment weight and gross take-off weight for individual missions are shown in Table 6.2. The empty weight is defined as the dry empty weight plus the unusable fuel and trapped transmission and engine oil. An additional 5% is added to the empty weight to account for weight growth.

6.1.1 Details of the Weight Breakdown

The details of the weight breakdown for the helicopter are presented below. The corrections factors used in the preliminary weight estimation to account for technology advancements are also discussed in the relevant sections.

Main Rotor System — The weight of all the six blades was estimated to be 650 lb, and the weight of the titanium/composite bearingless rotor hub was estimated to be 468 lb. It must be mentioned that the weight of the rotor blades does not include the embedded swashplateless controls, which are included in the control system weight.

Fuselage — It has been demonstrated that using composite materials can reduce the airframe weight by approximately 22%, and without sacrificing strength and crashworthiness (Ref. 57). Further, the preliminary weight estimation

Table 6.1: Component weight breakdown for the helicopter subsystem.

Component	Weight (lb)	% Empty Weight
Main rotor	1118.8	12.48
Empennage	117.0	1.31
Fuselage	1106.2	12.35
Landing gear	526.3	5.87
Nacelles	68.5	0.76
Propulsion system	1940.0	21.64
Main transmission	1240	13.00
Control system	344.1	3.84
Auxiliary power unit	135.4	1.51
Avionics	650.0	7.26
Electrical systems	371.7	4.14
Instruments	98.5	1.10
Hydraulics	95.3	1.06
Furnishings	168.8	1.88
Air conditioning and anti-icing	177.6	1.98
Trapped fuel and oil	80.8	0.90
Ground handling	132.2	1.48
Manufacturing variation	88.8	0.99
Empty weight	**9034**	—
Max. External load	9925	—
Crew (2 @ 200 lb each)	400	—
Max. Fuel	2870	—
GTOW	**22229**	—

procedure assumes a conventional main rotor/tail rotor configuration. Weight savings can be expected in a co-axial configuration because of the absence of tail rotor and a shorter tail boom. The fuselage weight was 1106 lb.

Landing gear — Shinn (Ref. 55) suggests a landing gear weight reduction of 13% with structural optimizations. The landing gear was designed assuming the main landing gears support 70% of the weight. The final landing gear weight was estimated to be 526 lb.

Propulsion system — The propulsion system weight includes the weight of three engine, engine installation, propulsion subsystems and fuel systems. The engine weights were determined by the manufacturer specifications. Recent advancements in powerplant technology from the IHPTET initiative (Ref. 36), project improvements of about 120% in the power-to-weight ratio of turboshaft engines.

Main rotor transmission — The co-axial configuration requires only one gear box for the main rotor. The weight of

the main gear box was estimated to be 1,165 lb. The transmission weight was reduced by approximately 15% to account for composite applications, new tooth forms, higher speed input sections, and improved material characteristics and processing (Ref. 56).

Control system — The control systems include the weight of the flight control system, the cockpit controls, and the swashplateless control system (trailing edge flaps, actuators and the piezo pumps). The flight control system has digital Fly-By-Wire (FBW) controls. A 60% reduction in the lower control system weight was assumed for a FBW system (Ref. 54). The swashplateless control system was estimated to weigh approximately 120 lb. This weight includes the weight of on-blade actuators, cables, balance weights, additional blade stiffening structures, and springs at the hub, which were added to replace the conventional swashplate.

Instruments and avionics — In order to simplify the operator interface for an untrained pilot, an advanced glass cockpit was selected. The multi-function displays and other digital equipment are 50% lighter than the traditional analog gauges. The final weight of the instruments and avionics was estimated at 750 lb.

Electrical system and hydraulics — The electrical system comprises of the batteries, electrical cables, and the two generators. On board APU eliminates the cold start requirements for the batteries and allows the use of lighter batteries. Additional weight reductions were achieved by using fiber optic cables for wiring. After applying a 15% weight reduction factor, the electrical system weight was estimated at 372 lb.

Mission payload and crew — The system was designed to carry a maximum external load of 9,925 lb. The payload was determined by the rooftop occupant extraction mission. Two crew members operate the vehicle. The total weight of the two crew members and the maximum payload is 10,325 lb.

Fuel and oil — The maximum fuel requirement was estimated to be 2,870 lb. This is approximately 430 US gallons of JP4 fuel. The estimate includes the unusable fuel trapped in the fuel tanks. The fuel is stored in two main tanks which are connected by a supply tank. The engine derives its fuel supply from the supply tank.

Maximum take-off weight — The design never-exceed load for the helicopter was 23,260 lb. This is approximately 1000 lb greater than the design gross weight (22,229 lb). The helicopter was primarily designed with rescue operations in mind. In such emergency situations, the mission might require the helicopter to transport more than the 40 passenger payload for which it was designed. Anticipating the need for additional lifting capacity the helicopter was designed with an increased gross take-off weight. The additional lifting capability is also beneficial if the underslung rescue module were redesigned with enhanced features resulting in heavier mission equipments. 1,000 lb was deemed sufficient for future underslung rescue module expansion programs. The maximum gross take off weight varies for each mission. The complete details of the of payload, fuel weight and takeoff weights for the RFP missions are presented in Table 6.2

6.2 Weight Balance and Determination of CG Location

The longitudinal CG locations of the primary weight components are shown in Fig. 6.1. It was assumed that both the starboard and port sides of the helicopter are loaded symmetrically and that the CG lies in the plane of symmetry. The

Table 6.2: Complete weight details for the different missions.

Mission	**Max. Payload**[a] (lb)	**Fuel Weight** (lb)	**Max. GTOW**[b] (lb)
Rooftop rescue	9872	2597	21503
Window rescue	9930	2539	21503
Self contained firefighting	8696	2367	20097
Ground based pump firefighting	2860	2171	14065
Command and control	2953	2482	14469
Max. Payload (hover for 1 hour)	10325	2692	22229

[a] Maximum payload over a mission cycle.
[b] Computed at the maximum payload condition.

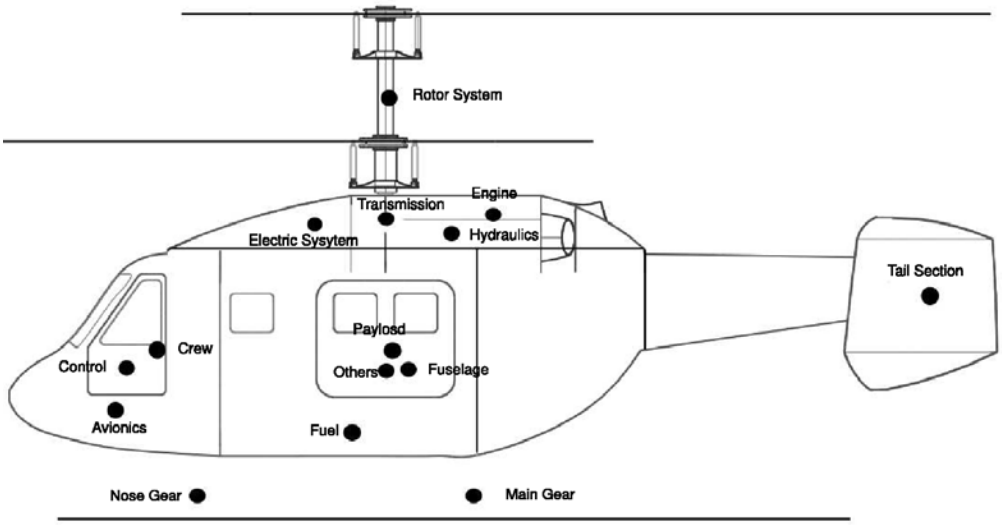

Figure 6.1: Longitudinal CG locations of the individual components.

locations of components were measured aft from the nose of the fuselage. The longitudinal CG location of the fuel tanks were kept close to the helicopter CG to minimize the CG travel during flight. Figure 6.2 shows the maximum CG travel for the rotorcraft under various loading conditions.

7 Performance Analysis

Performance analysis was conducted to determine the power requirements of the helicopter in various operating conditions and in different missions. The RFP requirements stated that the helicopter should be able to perform all the specified missions on a 95-th percentile hot summer day in Denver operating conditions. This translates, approximately, to an ISA+30 atmospheric conditions and an altitude of around 6000 ft. A summary of the vehicle performance capabilities are listed in Table 7.1.

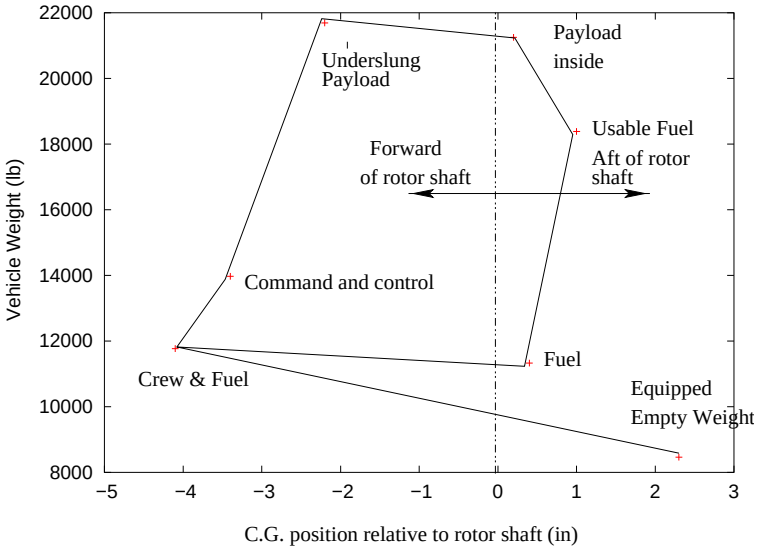

Figure 6.2: Longitudinal CG travel for the helicopter for various loading conditions.

7.1 Drag Estimation

Drag estimation is an important process in the performance analysis and requires a careful consideration to ensure optimum performance. Accurate estimates of drag can be obtained only through detailed experiments and/or numerical methods. Such advanced tools are not available during the process of preliminary design. Therefore, empirical methods suggested by Prouty (Ref. 37) and Stepniewski & Keys (Ref. 58) are used in the present design. Such methods estimate the component drags based on experimental results. Table 7.2 shows the drag breakdown for individual components of the helicopter in forward flight. The vertical drag was also estimated using a similar procedure and was found to be approximately 4.3% of the gross weight of the helicopter.

7.2 Hover Performance

The hovering capabilities of the helicopter is critical for all the missions specified by the RFP, particularly the window extraction and the aerial firefighting missions. Unlike existing helicopters, the present design was expected to hover for sustained periods of time (longer than the intermediate and takeoff periods of the engine). Therefore, it was necessary to design the helicopter such that it could hover with the engines running at maximum continuous power. The decision to choose a three engine configuration was also dictated by the OEI hover requirements. As mentioned earlier, the helicopter operates in urban canyons, close to buildings. In the event of an engine failure, the helicopter must still be capable of hovering in and ascending out of the urban canyon. Further, the helicopter operating envelope was limited to low-speed forward flight. The conditions, then, that determined the maximum power requirements were the hover ceiling requirements.

The hover performance was estimated from the main rotor model and includes empirical corrections to account for power losses from the rotation of the wake, tip vortex interference and ground effect on induced velocity. The

Table 7.1: Performance Summary (DGW, ISA+30, 6000 ft conditions unless specified).

Parameter	**Estimate**
Design gross weight	22229 lb
Nominal cruise speed	60 kts
Maximum cruise speed	100 kts
HOGE ceiling (takeoff power)	13000 ft
HIGE ceiling (takeoff power)	16000 ft
VROC, maximum (takeoff power)	2800 ft/min
Climb rate, maximum (max. cont. power)	1100 ft/min
Range, maximum	340 nm
Endurance, maximum	2 hours

Table 7.2: Equivalent flat plate area of the helicopter in forward flight.

Component	**Flat Plate Area (ft^2)**	**% of Total**
Fuselage	3.22	21.67
Nacelles	1.49	10.03
Main rotor hub and shaft	4.60	30.97
Horizontal stabilizer	0.40	2.66
Vertical stabilizer	0.57	3.82
Main landing gear	1.25	8.43
Front landing gear	0.79	5.34
Interference drag	1.29	8.67
Engine exhaust drag	0.5	3.36
Miscellaneous drag	0.75	5.04
Equivalent flat plate area	14.87	

present helicopter is designed to operate with OEI at an altitude of 6,000 ft under ISA+30 atmospheric conditions. Figure 7.1 shows the available excess power as a function of altitude for two different operating conditions, ISA and ISA+30 (Denver conditions). It can be noticed that the stringent OEI conditions at an altitude of 6,000 ft results in large excess power available at ISA conditions. On a standard day, the hover and climb performance of Aeneas is significantly better than most existing helicopters. The significantly high hover ceiling can be extremely advantageous when operating at higher density altitudes, for e.g., in mountainous terrains.

Figure 7.2 shows the available power at different altitudes when the engines are operating at maximum continuous power. This is the normal operating condition for the helicopter while hovering or maneuvering within an urban canyon. Sufficient excess power is available even at Denver conditions, which ensures a high vertical rate of climb essential for the rescue operations. The use of three engines gives Aeneas excellent hover and vertical climb performance.

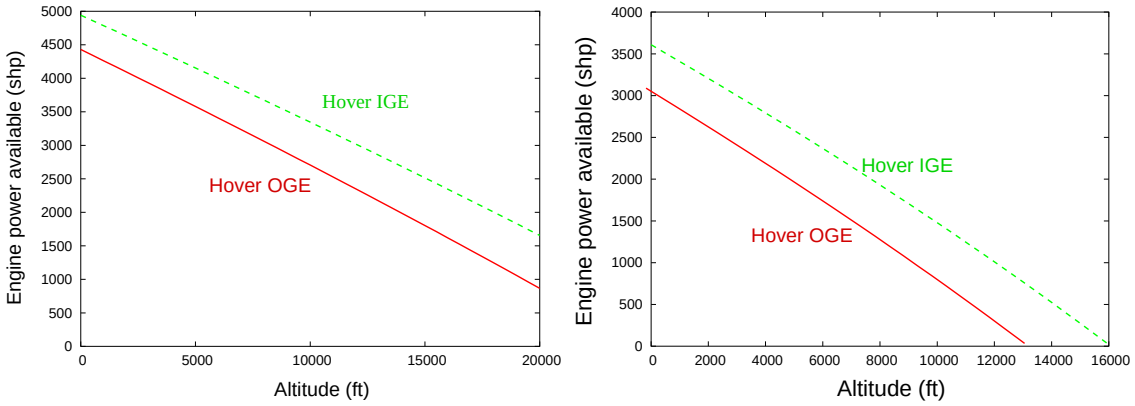

(a) ISA conditions

(b) Denver conditions

Figure 7.1: OGE and IGE hover ceiling at maximum design gross weight and maximum takeoff power rating.

7.3 Forward Flight Performance

A trim model of the helicopter was developed to analyze the forward flight performance of the helicopter. In this model, the rotor blades were assumed to be rigid, with only pitch and flap degrees of freedom. Figure 7.3 shows the power required for the main rotors as a function of the forward flight speed, when the vehicle is configured for the Disaster Command & Control mission. The helicopter design was optimized for hover and low speed forward flight. The design forward flight speed was taken as 60 knots, which is also the best endurance speed, as seen from Fig. 7.3. Figure 7.4 shows the maximum rate of climb as a function of the flight speed.

Figure 7.5 shows the payload capability of the helicopter as a function of range. The maximum range with the on board fuel tank was found to be approximately 340 nm. The payload capability as a function of endurance is shown in Fig. 7.6. A maximum endurance of 2 hours was determined for the Command & Control mission with the on board maximum fuel capacity. It must be noticed that the endurance is estimated for one hour in hover and one hour in forward flight at 60 knots. The power required in hovering flight is significantly larger than in forward flight. Therefore, endurance in forward flight conditions will be significantly greater, because of the large excess power from the three engines.

8 Cost Analysis

The price of the final product is an important factor in determining its commercial success. Considerable efforts were taken to minimize the acquisition and operating costs. However, it must be remembered that the helicopter has been designed for a very specific, critical rescue mission and has to operate in very demanding situations. Certain costly features were essential to accomplish all the missions specified in the RFP. A brief summary of the methods adopted to reduce costs will be presented first. This will be followed by a preliminary estimation of the initial acquisition costs and the direct operating costs.

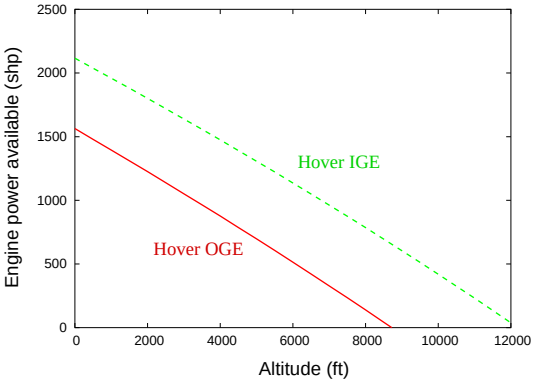

Figure 7.2: Available excess power at maximum design gross weight and maximum continuous power rating (Denver conditions).

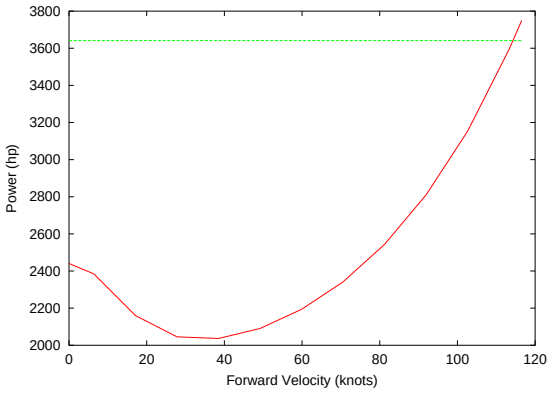

Figure 7.3: Power required in forward flight for Command & Control mission (Denver conditions).

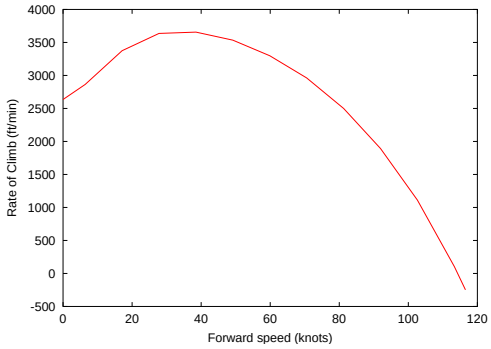

Figure 7.4: Maximum rate of climb as a function of the forward flight speed (Denver conditions).

8.1 Cost Reduction Methods

Simplified structure – Both the helicopter and the subsystems are designed in a modular manner, which is easier to manufacture and minimizes the manufacturing costs.

Low risk technology – A good balance of the proven, existing technology and reliable cutting edge technology is maintained throughout the design process, to prevent cost escalation. Incorporation of new technologies (e.g., swashplateless technology) ensures that the helicopter is a commercially attractive option for the next decade.

Easy accessibility – Special considerations were given while designing the various components to provide easy accessibility, in order to the ease the maintenance process.

Reliable systems – Highly reliable components were included in the helicopter to reduce the maintenance costs, though this increased the acquisition cost slightly. For example, the fly by wire controls are much more reliable as compared to fly by stick.

Easy and efficient maintenance – Aircraft maintenance is streamlined with the use of an integrated diagnostic and

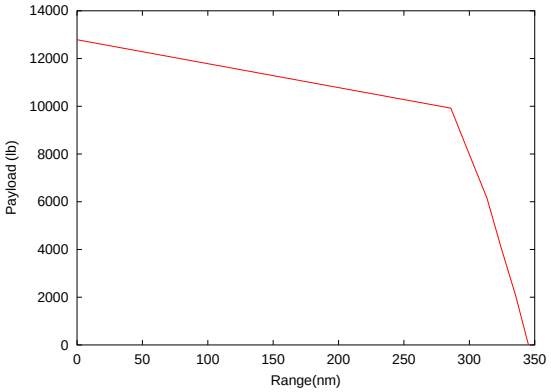

Figure 7.5: Payload-range diagram.

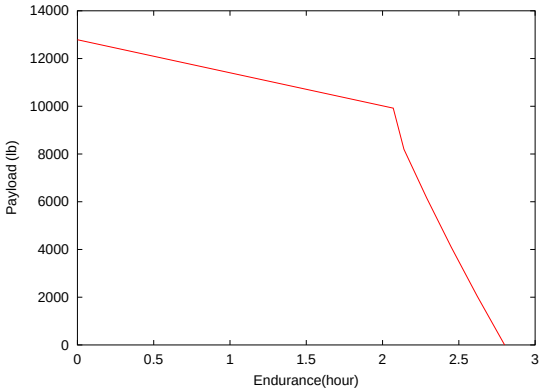

Figure 7.6: Payload-endurance diagram.

prognostic system, combined with capability of removable modular avionics. A Health and Usage Monitoring System (HUMS) is integrated into the design, enhancing maintenance predictability.

Other applications – Special attention has been paid, throughout the design process, to ensure that the helicopter that is is designed is truly a multi-task helicopter. The high payload capability makes it an ideal candidate for heavy-lift applications. The three-engine configuration gives a very high hover ceiling unmatched by existing helicopters.

8.2 Acquisition Cost

An initial estimate of the cost of the helicopter, along with the component breakup, was obtained using two methods, Bell's Cost Analysis method (Ref. 59) and Harris and Scully (Ref. 60). The breakup is shown in Table 8.1. This break up was obtained by assuming 300 helicopters are built over a span of 5 years. An inflation rate of 2.2% is added to the cost to get estimates over the present cost. Harris and Scully's method is a statistical formula, which estimates the cost based on the empty weight and the total power available. The total acquisition cost of the present helicopter is estimated at around 10 million US dollars.

The use of two different approaches to estimate the costs provides a check on the results obtained. Furthermore, the estimated acquisition costs compare well with the existing Eurocopter Super Puma (AS–332L-2). The base price for Eurocopter is 10.5 million US dollars (Ref. 61). When accounted for inflation, the price of the Eurocopter is estimated to be about 11.2 million US dollars. This agreement with the existing helicopter gives additional confidence in the predictions.

8.3 Operating Costs

The operating costs can be divided into two categories, direct operating cost (DOC) and indirect operating cost (IOC). Direct Operating costs can be further divided in to Cash DOC and Ownership DOC and Indirect operating cost can be divided into passenger related and aircraft related. The estimates for the operating costs were obtained using the

Table 8.1: Acquisition Cost Break up

Component	Cost (US $) 1998	Cost (US $) 2003
Rotor System	903,726	1,003,136
Fuselage	726,431	806,338
Installed Engines	2,133,895	2,368,624
Drive System	1,185,654	1,316,076
Avionics	336524	373,542
Others	306,382	339,973
Total Cost	8,641,843	9,581,346

Table 8.2: Operating Costs

Category	Cost
Fuel and oil	403 $/hr
Flight crew	172 $/hr
Maintenance	576 $/hr
Cash DOC	**696.9 $/hr**
Depreciation	1,152 $/hr
Insurance	1,843 $/hr
Finance	1,198 $/hr
Ownership DOC	**2787.6 $/hr**
Aircraft related	206,262 $/yr
Passenger related	13,165 $/yr
DOC	**5,760 $/hr**
IOC	**219,428 $/yr**
Total Operating Cost	**1,371,429 $/yr**

procedure presented at the NASA Aircraft Economic Workshop (Ref. 62). The estimated operating costs associated with the current design are listed in Table 8.2. The operating cost is obtained with an assumption of 200 flight hours in a year.

The high operating cost for the present helicopter can be attributed to the following:

Higher insurance cost – Insurance cost is higher because of the operation of the helicopter in such adverse operating conditions.

Higher maintenance costs – Maintenance costs are also slightly higher than usual because of the small number of flight hours, even though they have been significantly reduced by using more reliable components.

Higher fuel cost – Use of three engines to power the rotors enabling it to lift a heavy payload increases the fuel requirements.

9 Risk Identification and Risk Reduction

As has been mentioned previously, the present mission requires Aeneas to operate in adverse environments. Thus, the reliability of all of the systems is very critical for the success of the mission. Careful investigation of the possible failure modes, their effect and criticality have been conducted at all stages of the design process. Multiple redundancies have been introduced in components susceptible to failure to ensure mission capability in the event of any malfunction. The various risks identified and the steps taken to eliminate them in the design or make the system tolerant to these risks are presented in this section.

A preliminary risk identification and risk reduction study was conducted using the guidelines specified in MIL-STD-882 (Ref. 63). Marginal hazards were identified in the rotor, transmission, engine, and flight control systems for

the co-axial helicopter. The primary failure modes for the rotor were the actuated trailing edge flaps. The flaps or the pumps were susceptible to failure. Two flaps per blade and two actuators for each flap provides complete redundancy against any failure of the actuated flap mechanism. The transmission has been designed for a full takeoff power from each engine to ensure proper functioning at one engine inoperative conditions. Furthermore, the transmission has a 30 minute dry run capability, in the event of oil leakages. The IMD HUMS is designed to detect and alert the pilot of such failures. Aeneas is designed to hover with one engine inoperative. It can, therefore, continue to perform the mission in the event of engine failure. Aeneas is also designed with a triple redundant flight control system to ensure mission capability at all times.

10 Future Urban Fire Stations

During the design of Aeneas, the possible complications associated with an aerial disaster response operation were identified. It was shown that a carefully designed system can, indeed, overcome most of these obstacles and successfully perform both occupant evacuation and firefighting missions. Aeneas was designed to overcome all the challenges faced during a typical response operation and is envisaged to be the future of urban firefighting missions. Based on the disaster scenarios developed during the design process, it was estimated that a minimum of ten fully equipped systems were necessary for a typical fire on a high-rise building of 100 floors. The calculations took into consideration the average density of people in high-rise buildings, and assumed that the fire occurred on the lower floors, trapping more than two thousand occupants on the upper levels. It was shown in Chapter 3 that resource utilization diminishes with increasing number of systems. The optimum configuration was found to be a ten system package. In this configuration, four systems were required to perform both rooftop evacuation and firefighter deployment simultaneously on the rooftop. Three systems were required for window penetration and evacuation. Two systems would fight the fires, either with an on board water tank or with water supplied by ground based pumps. Finally, an aerial command and control platform would monitor the situation and co-ordinate the rescue efforts.

Figure 10.1 shows an artist's impression of the future fire stations with a mix of both ground based vehicles (fire trucks) and the proposed Aeneas systems. The compact size and the blade folding features of Aeneas minimize the hangar space required to house both the helicopters and the systems. For the proposed ten system package, the hangar size is estimated to be 165 ft $\times$ 130 ft.

11 Conclusions

The detailed design of Aeneas, The Urban Disaster Response System, has been presented. Aeneas is a multi-role, co-axial helicopter, with a gross takeoff weight of 22,229 lbs, specially designed to address the unique requirements of an emergency situation. It has a payload capability of 10,000 lbs and can evacuate up to 40 persons at a given time. Aeneas was designed for efficient hover and low-speed forward flight conditions. A three engine configuration was chosen to enable Aeneas to hover at high altitudes and safely maneuver in urban canyons, even with one engine inoperative (OEI).

A swashplateless main rotor design was chosen to eliminate the complexities associated with mechanical linkages. Primary control is provided by a state-of-the-art actuated trailing edge flaps. A fully autonomous flight control system

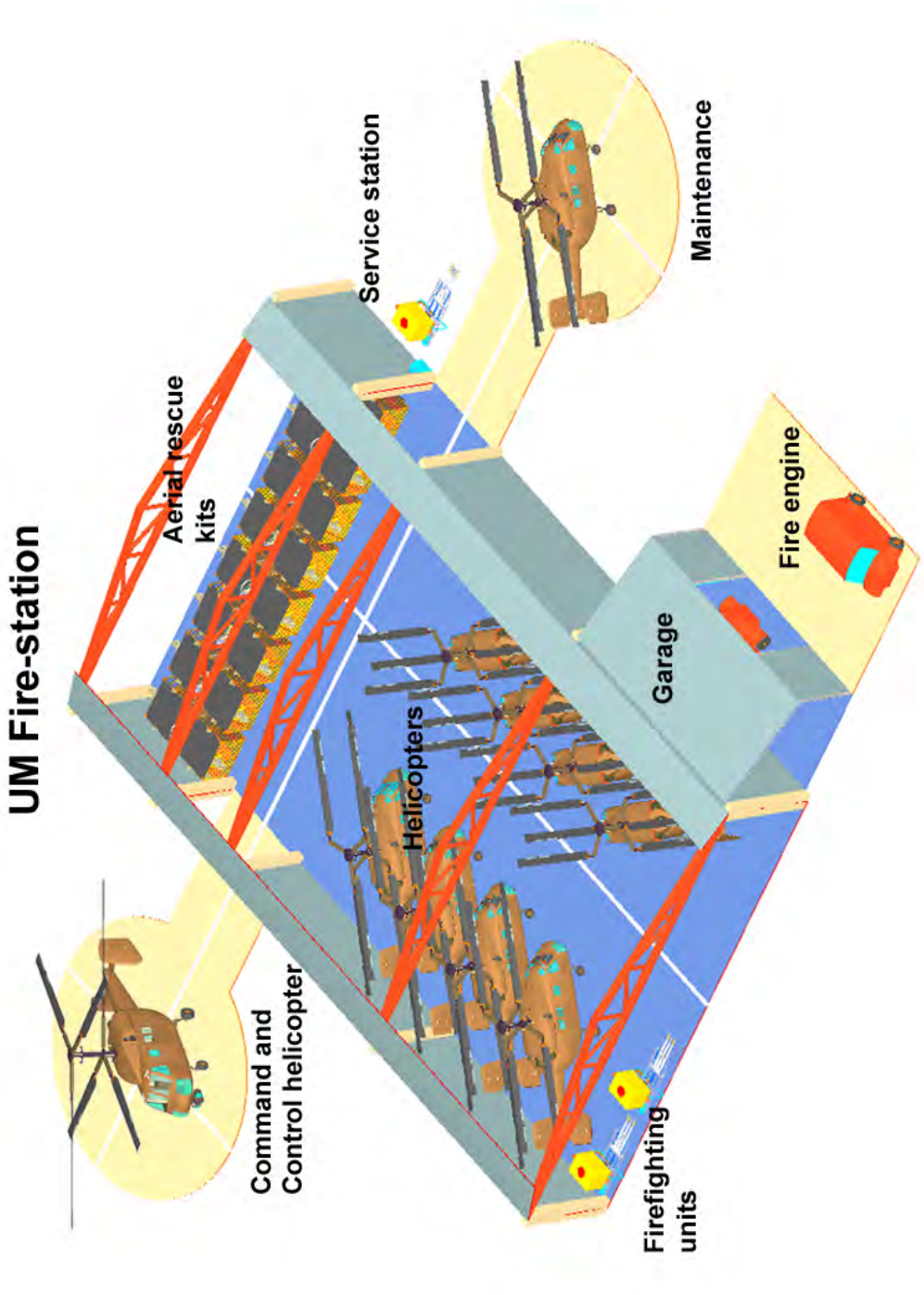

Figure 10.1: Artist's impression of a conceptual urban fire station showing Aeneas systems along with ground based systems.

ensures safe operation in urban canyons and the ease of operation for a non-professional pilot.

The rescue missions are carried out using an underslung pod. The design of the pod was driven by operational safety and controllability considerations. To enhance safety of the passengers, crash-worthy seats are provided in the pod. Three bidirectional thrust fans, along with an autonomous flight control system, provide complete control of the pod. The design is highly modular, enabling quick installation of mission specific modules and rapid reconfiguration between missions. Aeneas can engage fires at any floor, either with an on-board water tank capable of carrying 800 gallons of water, or using ground based water pumps. A well equipped command and control module, comprised of five crew members, monitors the disaster response operations.

Extensive trade-off studies were conducted to design the optimum configuration as well as the mission strategy of Aeneas. The final system package is a synergy of proven, existing technology with a feasible, more efficient, cutting edge technology. The net effect is an overall improvement in performance and reliability, along with decreased operating and maintenance costs, making it the most effective firefighting machine available. Aeneas is our answer to all the future urban disasters.

References

[1] Sirohi, J., Cadou, C., and Chopra, I., "Frequency Domain Modeling of a Piezohydraulic Actuator," Proceedings of the 11^{th} AIAA/ASME/AHS Adaptive Structures Conference, Norfolk, VA, April 2003.

[2] Klote, J. H., *SFPE Handbook of Fire Protection Engineering*, 2^{nd} ed., 1995, Ch. Smoke Control.

[3] Heskestad, G., *SFPE Handbook of Fire Protection Engineering*, 2^{nd} ed., 1995, Ch. Fire Plumes.

[4] Purser, D. A., *SFPE Handbook of Fire Protection Engineering*, 2^{nd} ed., 1995, Ch. Toxicity Assessment of Combustion Products.

[5] "Versatile Computer Unit Workstation," *http://www.x20.org/thermal/new.htm*.

[6] "DM Aerosafe – Eagle Flying Platform," *http://dmaerosafe.freeservers.com/*.

[7] Armstrong, P. J., "Emergency Technologies for Rescue Operations in Tall Buildings and structures," *CTBUH Review*, Vol. 1, No. 3, 2001.

[8] Szustak, L., and Jenney, D., "Control of Large Crane Helicopters," *Journal of the American Helicopter Society*, Vol. 16, No. 3, 1971, pp. 11–22.

[9] Gabel, R., and Wilson, G. J., "Test Approaches to External Sling Load Instabilities," *Journal of the American Helicopter Society*, Vol. 13, No. 3, 1968.

[10] Fusato, D., Guglieri, G., and Celi, R., "Flight Dynamics of an Articulated Rotor Helicopter with an External Slung Load," *Journal of the American Helicopter Society*, January 2001.

[11] "AC Propulsions Inc.," http://www.acpropulsions.com.

[12] Gage, T. B., "Living with an EV: 30,000 Miles in One Year," EVS-13 Symposium Proceedings, 1996.

[13] Unknown "Crossbow - Inertial and Gyro Systems," *http://www.xbow.com/Products/Inertial_Systems.htm*.

[14] Unknown "High performance, GRAM compliant PPS module for embedded airborne applications," *http://www.trimble.com/force5.html*.

[15] Steur, R., "IFEX Technologies Impulse Fire Extinguishing Installed on Helicopters," AHS International Meeting on "Advanced Rotorcraft Technology and Life Saving Activities, 2002.

[16] "Monsoon Nozzles," *http://www.tft.com*.

[17] Coleman, C. P., "A Survey of Theoretical and Experimental Coaxial Rotor Aerodynamic Research," NASA TN-3675, March 1997.

[18] Shen, J., Chopra, I., and Johnson, W., "Performance of Swashplateless Ultralight Helicopter with Trailing-Edge Flaps for Primary Control," Proceedings of the 59^{th} Annual Forum of the American Helicopter Society International, Pheonix, AZ, May 2003.

[19] Chopra, I., "Review of the State-of-Art of Smart Structures and Integrated Systems," *AIAA Journal*, Vol. 40, No. 11, November 2002.

[20] Koratkar, N. A., and Chopra, I., "Wind Tunnel Testing of a Mach-Scaled Rotor Model with Trailing Edge Flaps," *Smart Materials and Structures*, 2001.

[21] Bernhard, A., *Smart Helicopter Rotor with Active Blade Tips (SABT),* PhD thesis, University of Maryland, College Park, MD, March 2000.

[22] Wei, F. S., "Design of an Integrated Servo-Flap Main Rotor," Proceedings of the 59^{th} Annual Forum of the American Society International, Pheonix, AZ, May 2003.

[23] Shen, J., and Chopra, I., "A Parametric Design Study for a Swashplateless Helicopter Rotor with Trailing-Edge Flaps," Proceedings of the 58^{th} Annual Forum of the American Helicopter Society International, Montréal, Canada, 2002.

[24] Bir, G., and Chopra, I., *University of Maryland Advanced Rotorcraft Code (UMARC),* Center for Rotorcraft Education and Research, University of Maryland, College Park, MD, July 1994.

[25] Sirohi, J., and Chopra, I., "Development of a Compact Piezoelectric-Hydraulic Hybrid Actuator," Proceedings of SPIE symposium on Smart Structures and Integrated Systems, San Diego, CA, Mar. 2002.

[26] *http://www.mcmaster.com/*.

[27] *http://www.uea-inc.com/slip/work_SR.html*.

[28] Rauch, P., and Quillien, C., "Advanced Technologies for High Performance NH90 Blades," Proceedings of the 59^{th} Annual Forum of the American Society International, Pheonix, AZ, May 2003.

[29] Alex, F. W., and McCoubrey, G. A., "Design and Structural Evaluation of the SH-2F Composite Main Rotor Blade," *Journal of the American Helicopter Society*, April 1986, pp. 345–359.

[30] Prouty, R. W., *Military Helicopter Design Technology* Janes Information Group Limited, 1989.

[31] *http://www.lord.com*.

[32] Leishman, J. G., *Principles of Helicopter Aerodynamics* Cambridge University Press, 2001.

[33] Abbe, J. T. L., Blackwell, R. H., and Jenney, D. S., "Advancing Blade Concept (ABC) Dynamics"," Proceedings of the 33^{rd} Annual National Forum of the American Helicopter Society, Washington, D. C., May 1997.

[34] Roget, B., and Chopra, I., "Robust Individual Blade Control Algorithm for a Dissimilar Rotor," *Journal of Guidance, Control and Dynamics*, Vol. 25, No. 4, July-Aug. 2002.

[35] Currey, N. S., *Aircraft Landing Gear Design: Principles and Practices* AIAA Educational Series, Reston, VA 1988.

[36] Hirschberg, M., "On the Vertical Horizon: IHPTET – Power for the Future," *http://www.vtol.org/IHPTET.HTM*, June 2001.

[37] Prouty, R. W., *Helicopter Performance, Stability, and Control*, PWS Engineering, Boston, 1986.

[38] Dudley, D. W., "Handbook of Practical Gear Design," General Electric Company, 1954.

[39] Lewicki, D. G., and Coy, J. J., "Vibration Characteristics of OH-58A Helicopter Main Rotor Transmission," NASA TN-2705, 1987.

[40] Unknown "Northrop Grumman Navigation Systems," *http://www.ngnavsys.com*.

[41] Unknown "Automotive OE — Adaptive Cruise Control," *http://www.visteon.com/technology/automotive/ adaptive_cruise.shtml*.

[42] Nalezinski, M., Vossiek, M., and Heide, P., "Novel 24 GHz FMCW Front-End with 2.45 GHz Saw Reference Path for High-Precision Distance Measurements," *IEEE*, 1997.

[43] Klotz, M., and Rohling, H., "A 24 GHz Short Range Radar Network for Automotive Applications," *IEEE*, July 2001.

[44] Unknown "Infrared Thermal Cameras," *http://www.x20.org/thermal/new.htm*.

[45] Unknown "Thales Avionics Flight Management System," *http://www.thalesgroup.com/avionics/ products/flight_systems.shtml*.

[46] Padfield, G. D., *Helicopter Flight Dynamics: The Theory and Application of Flying Qualities and Simulation Modeling*, 1^{st} ed., AIAA Educational Series, 1996.

[47] "ADS33," *http://www.redstone.army.mil/amrdec/sepd/tdmd/Documents/ads33front.pdf*.

[48] Bozcar, B., Borgstrom, D., and Everett, P., "Key Aspects and Attributes of the RAH-66 Comanche Flight Contr ol System," Proceedings of the 55^{th} Annual Forum of the American Helicopter Society International, May 1999.

[49] Pallett, E., and Coyle, S., *Automatic Flight Control*, 4^{th} ed., Blackwell Scientific Publications, 1993.

[50] Nilsson, C., C. Hall, S. H., and Chokani, N., "GPS Auto-Navigation Design for Unmanned Air Vehicles," *AIAA Journal*, 2002.

[51] Sattler, D., and Reid, L., "Automatic Flight Control for Helicopter Enhanced/Synthetic Vis ion," *AIAA Journal*, 2001.

[52] Taghizad, A., and Bouwer, G., "Evaluation of Helicopter Handling Qualities Improvements Durin g a Steep Approach Using New Piloting Modes," 55^{th} Annual Forum of the American Helicopter Society, May 1999.

[53] Gili, P., and Battipede, M., "Adaptive Features of a MIMO Full-Authority Controller," AIAA Guidance, Navigation and Control Conference and Exhibit, August 2000.

[54] Tischenko, M. N., Nagaraj, V. T., and Chopra, I., "Preliminary Design of Transport Helicopters," *Journal of the American Helicopter Society*, 2003.

[55] Shinn, R. A., "Impact of Emerging Technology on the Weight of the Future Rotorcraft," Proceedings of the 40^{th} Annual Forum of the American Helicopter Society International, 1984.

[56] Unsworth, D. K., and Sutton, J. G., "An Assessment of the Impact of Technology on VTOL Weight Prediction," Proceedings of the 40^{th} Annual Forum of the American Helicopter Society International, 1984.

[57] Reisdorfer, D., and Thomas, M. L., "Static Test and Flight Test of the Army/Bell ACAP Helicopter," Proceedings of the 42^{nd} Annual Forum of the American Helicopter Society International, 1986.

[58] Stepniewski, W. Z., and Keys, C. N., *Rotary-Wing Aerodynamics* Dover Publications Inc., New York, 1984.

[59] "16^{th} Annual Student Design Competition Request for Proposal," American Helicopter Society International & Bell Helicopter Textron.

[60] Harris, F. D., and Scully, M. P., "Helicopters Cost Too Much," Proceedings of the 53^{rd} Annual Forum of the American Society International, April 29 – May 1 1997, pp. 1575 – 1608.

[61] *The Official Helicopter Bluebook*, 1^{st} ed.,, Vol. XXIII HeliValue$, Inc., 2001.

[62] Leslie, P., "Short Haul Civil Tiltrotor and Bell Model 412 Cost Drivers," Rotorcraft Economics Workshop, Moffet Field, CA, 1996, NASA Ames Research Center.

[63] U.S. ARMY MATERIAL COMMAND *Engineering Design Handbook Helicopter Engineering. Part Three. Qualification Assurance*.